Universitat Autònoma de Barcelona

Virtualization and real-time analysis of pharmaceutical and food products by near infrared spectroscopy

Dong Sun

Universitat Autònoma de Barcelona

Virtualization and real-time analysis of pharmaceutical and food products by near infrared spectroscopy

Dong Sun

Tesi doctoral

Programa de Doctorat de Química

Directores: Dr. Manel Alcalà Bernàrdez

Prof. Dr. Marcelo Blanco Romia

Departament de Química

Facultat de Ciències

2017

Memòria presentada per aspirar al Grau de Doctor per **Dong Sun**

Dong Sun

Vist-i-plau,

Dr. Manel Alcalà Bernàrdez **Prof. Dr. Marcelo Blanco Romia**

Bellaterra, de 2017

Acknowledgements

This thesis has been developed with the assistance of the following institutions:

Universitat Autònoma de Barcelona

Personal investigador en formació (PIF)

Applied Chemometrics Research Group

Departament de química, Universitat Autònoma de Barcelona

Bellatera, Spain

Laboratorios Menarini S.A

Badalona, Spain

Viavi Solutions Inc.

California, United States

Semillas Fitó S.A.U.

Barcelona, Spain

Acknowledgements

During these 4 years, many stories have been written in to my life. They are sweet, bitter cheerful and memorable. All of them are treasures which will be kept in my collection. Time flies, 4 years has pasted just like in one second. At the beginning, everything here was new for me and I didn´t know what would happen in the future. But now, I have a deep affection for here and I feel I´m a part of here already sometimes.

It is lucky that Barcelona is the city where I have lived. The buildings, sea, mountains and people here are so beautiful and friendly. It is honorable that UAB is the university where I have studied. It is a great pleasure that I have enjoyed a wonderful time in the applied chemometrics research group during my doctoral study. And I am grateful to each person who I met here during this 4 years. There are many people who have helped me a lot not only with my academic career but also my daily life. It is so important that you have encouraged and supported me when the difficulties run to me.

Therefore, I want to say thank you very much to all of you! First of all, I would like to extend my sincere gratitude to my dear directors Prof. Marcelo Blanco and Prof. Manel Alcalà whose dedicated attitudes in the academic career and kind-hearted manners in daily life have helped me a lot! You offered me the great opportunity to join our research group and taught me how to become a qualified doctoral student. Thank you very much to Prof. Santiago Maspoch, Prof. Jordi Coello and Dr. Jordi Cruz who have given me so many professional supports and a feel like home! Thank you for my perfect colleagues in UAB, Ana, Vanessa, Diego, Maria, Julen, Judit Brassier, Aira, Gloria, Laia, Judit Puig, Elia and Xavi! You guys are the most amazing friends in my life. And thanks to bo, xi yue who have offered me their best supports when I need help!

At the end, I wish my doctoral research would provide some energy which drives our world to be a more peaceful, beautiful and civilized place.

Thank you very much for all of you!

Yours sincerely,

Dong Sun

Barcelona, 2017

Contents

Abbreviations

ANOVA	Analysis Of Variance
API	Active Pharmaceutical Ingredient
CQAs	Critical Quality Attributes
EMA	European Medicines Agency
FDA	Food and Drug Administration
GMP	Good Manufacturing Practices
ICH	The International Council for Harmonisation of Technical Requirements for Pharmaceuticals for Human Use
LVF	Linear Variable Filter
LVs	Latent Variables
NIRS	Near Infrared Spectroscopy
PAT	Process Analytical Technology
PCA	Principal Component Analysis
PCs	Principal Components
PLS	Partial Least Squares
PLSR	Partial Least Square Regression
PRESS	Predicted Residual Sum of Squares
QA	Quality Assurance
QbD	Quality by Design
QC	Quality Control
RMSE	Root Mean Square Error
RTA	Real Time Assurance
RTM	Real Time Monitoring
RTR	Real Time Release
SG smoothing	Savitzky-Golay smoothing
SNV	Standard Normal Variate transformation

Abstract

Abstract

The realization of the smart factory has been investigated in this Thesis. The smart factory is a trend of development in the information age. Human beings could receive a lot of assistance from the smart tools which make works be done in a high quality way. Technology-intensive industries, such as pharmaceutical and modern food industries, are pioneers who have the advantages to enjoy the smart factory. Nowadays, the product quality is a key factor that determines the market share. In order to assure a high quality both in the process and final product, several institutions have published some guidelines. Quality by Design (QbD) and Process analytical technology (PAT) were two guidelines used in this thesis for the pharmaceutical methods. Near infrared spectroscopy (NIRS) could virtualize the physical and chemical information of the process product in real time. Therefore, it was taken as the smart tool to realize these concepts in the pharmaceutical industry and study about the food quality improvement.

A portable MicroNIR spectrometer was used to determine critical quality attributes in different stages of the pharmaceutical process for the manufacturing of solid formulations. Quantitative partial least-squares regression models were calculated and validated. The MicroNIR has a miniaturized size, low energy consumption and rugged optical system. So it has shown a good robustness in the operation process. The experiment design has offered a simple way to calculate the models without a complex reference method. The good results of validation reveal that the MicroNIR is an excellent PAT tool in the pharmaceutical industry. The MicroNIR was also adopted to calculate and validate a spectral library to identify 223 pharmaceutical formulations. The internal and external validations have shown that all the formulations can be uniquely identified. This simple and nondestructive method has offered the customer a simple tool to qualify the pharmaceutical product in the retail stores. Besides, the benchtop NIR spectrometer was also adopted to analyze several chemical and sensory parameters of tomato. The analysis was operated in real time mode without any sample pretreatment. The quantitative models were calculated by PLS. The predictive ability was good and it was demonstrated that NIRS is a robust, accurate and safe method to improve the quality of tomato product.

Based on the discussion above, this Thesis has studied the application of NIRS as a tool to virtualize and real time analyze pharmaceutical and food industries. All these studies have indicated that the NIRS is a suitable technology for the realization of the smart factory.

Resumen

La realización de la fábrica inteligente ha sido investigada en esta Tesis. La fábrica inteligente es una tendencia de desarrollo en la era de la información. Los seres humanos pueden recibir mucha ayuda de las herramientas inteligentes que permiten realizar los trabajos de un modo de alta calidad. Las industrias con elevada carga en tecnología, como las farmacéuticas y las industrias alimentarias modernas, son pioneras en el uso de los conceptos de fábrica inteligente. Hoy en día, la calidad del producto es un factor clave que determina la cuota de mercado. Con el fin de asegurar una alta calidad tanto en el proceso como en el producto final, varias instituciones han publicado algunas pautas. La Calidad por Diseño (QbD) y la Tecnología Analítica de Procesos (PAT) fueron dos pautas utilizadas en esta tesis para los métodos farmacéuticos. La espectroscopía de infrarrojo cercano (NIRS) puede virtualizar la información física y química del producto de proceso en tiempo real. Por lo tanto, se tomó como la herramienta inteligente para realizar estos conceptos en la industria farmacéutica y estudiar la mejora de la calidad de los alimentos.

Se utilizó un espectrofotómetro portátil MicroNIR para determinar atributos críticos de calidad en diferentes etapas del proceso farmacéutico para la fabricación de formulaciones sólidas. Se calcularon y validaron modelos cuantitativos de regresión por mínimos cuadrados parciales. El MicroNIR tiene un tamaño miniaturizado, bajo consumo de energía y un sistema óptico resistente. Por lo tanto, ha demostrado una buena robustez en el proceso de operación. El diseño del experimento ha ofrecido una forma sencilla de calcular los modelos sin un método de referencia complejo. Los buenos resultados de validación revelan que el MicroNIR es una excelente herramienta PAT en la industria farmacéutica. El MicroNIR también se adoptó para calcular y validar una biblioteca espectral para identificar 223 formulaciones farmacéuticas. Las validaciones internas y externas han demostrado que todas las formulaciones pueden identificarse de forma única. Este método simple y no destructivo ha ofrecido al cliente una herramienta sencilla para calificar el producto farmacéutico en las tiendas minoristas. Además, se utilizó un espectrofotómetro NIR de sobremesa para analizar diversos parámetros químicos y sensoriales del tomate. El análisis se realizó en modo de tiempo real sin pretratamiento de muestras. Los modelos cuantitativos fueron calculados por PLS. La capacidad predictiva fue buena y se demostró que NIRS es un método robusto, preciso y seguro para mejorar la calidad del producto de tomate.

Con base en la discusión anterior, esta Tesis ha estudiado la aplicación de NIRS como una herramienta para virtualizar y analizar en tiempo real las industrias farmacéutica y alimentaria. Todos estos estudios han indicado que el NIRS es una tecnología adecuada para la realización de la fábrica inteligente.

Chapter 1

Pharmaceutical and food industry

1. Pharmaceutical and food industry

1.1 Pharmaceutical industry

A drug is defined as an agent intended for use in the diagnosis, mitigation, cure, or prevention of disease in humans or in other animals[1]. In 1550 BCE, Ebers Papyrus, the earliest textbook on medicine was written in Egypt. It included some basic dosage forms such as powder, plaster, pill and ointment. In 1843, Mr. William Brockedon invented the first tableting machine for sodium carbonate and potassium carbonate. Claudius Galenus (131-201A.D.) is a prominent Greek physician who is the inventor of theriac. The use and manufacturing of theriac continued until the late 19th Century. In 1847, Mr. James Murdock created the capsule to enclose medicines. And in 1886, Stanislas Limousin invented the ampoule which improved the application of injection. During 19th Century, the second industrial revolution brought the rapid development of pharmaceutical Machines. And in 20th Century, the digital revolution prompted the machinery automation of pharmaceutical industry.

Nowadays, the pharmaceutical industry becomes a technology-intensive industry where new theories, new techniques and new equipment continue to emerge.
Generally, the development of modern medicine has experienced four ages[2]–[4],

a) Traditional tablets, capsules, injections and so on, before 1960.
b) Sustained-release preparations and enteric preparations whose aim is to control the release rate. It is the first generation of Drug Delivery System (DDS).
c) Controlled release formulations and targeting preparations which are carried by liposome, microspheres or monoclonal antibody. It is the second generation of DDS.
d) Drug delivery systems which response to the feedback of vivo information and release at the cellular level. It is the third generation of DDS.

The modern drug dose forms could be classified by different ways, such as the route of administration, the decentralized system and the physical form. In this thesis, the drug dose forms were classified by their physical form.

Normally, there are four forms:

- Liquid (solutions, injections…)[5]
- Gas (aerosols, sprays…)[6]
- Solid (pills, tablets…)[7]
- Semisolid (ointments, suppositories…)[8]

The solid preparations, because of their unique advantages, have been chosen as the preferred dosage forms in the pharmaceutical industry and have occupied around 70% of all the products. Our researches discussed in following chapters were also carried out with solid preparations.

1.1.1 Solid pharmaceutical formulations

As mentioned above, there are four physical forms of drug generally. In this thesis, the solid form is the item which has been studied. Thus, some solid preparations are introduced here.

The main preparation process of solid drugs is explained in Fig. 1.1

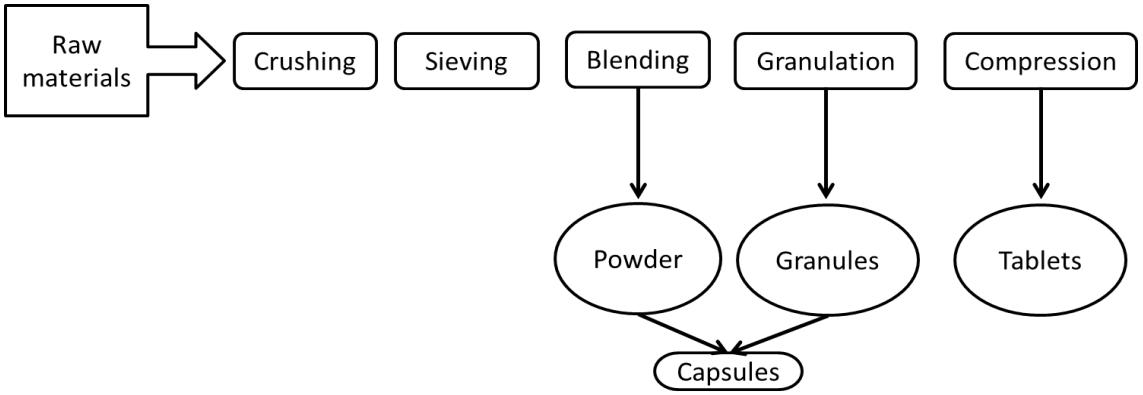

Fig. 1.1 Main process of solid drug preparation

The raw materials have to be eventually crushed and sieved before been processed into different types. The powder preparation could be done when all the ingredients are well blended. The granule preparation would be done when well mixed powder is granulated and dried. The tablet preparation would be done when granules are compressed properly. And the capsule preparation could be done when the powder or the granules are enclosed in the capsule. In terms of the solid preparation, the uniformity, fluidity and filling property of the material are key points for the manufacturing process.

1.1.1.1 Powder

Powder is a collection of numerous solid particles. In the pharmaceutical industry the range of particle size is around 1μm to 3 mm. Table 1.1 shows the classification of different particles,

Table 1.1 Classification of different particles by their size

Geometric diameter	Name
3mm-100μm	granular material
100-0.1μm	powder
100-10μm	granular powder
10-1μm	super fine powder
1-0.1μm	ultrafine powder
<0.1μm(100-1nm)	nanometer particle

As we know the solid materials do not have fluidity, but the solid powder has it[9]. When the bulk solids are crushed into medium size powders, they own the fluidity which is similar with liquid, the compressibility which is similar with gas and the deformation resistance which is similar with solid. Therefore the powder is a kind of the fourth physical state.

There are six main steps in the powder preparation process, see Fig. 1.2

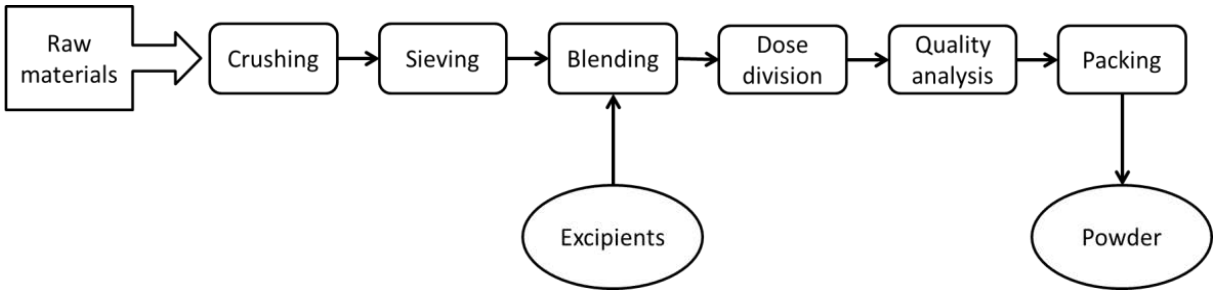

Fig. 1.2 Production process of powder preparation

Generally, before crushing, the pretreatments of raw materials are necessary, for example drying.

1.1.1.1.1 Crushing

The bulk solids are broken into particles by the mechanical force. The aim of crushing is to decrease the geometric diameter and increase the specific surface area[10].

The specific surface area has two expressions which are the specific surface area by volume and the specific surface area by weight.

The equations are:

$$S_V = \frac{s}{v} = \frac{\pi d^2 n}{\pi d^3 n/6} = \frac{6}{d} \qquad \text{Equation 1.1}$$

$$S_W = \frac{s}{w} = \frac{\pi d^2 n}{\pi d^3 \rho n/6} = \frac{6}{d\rho}$$ Equation 1.2

Where S_V is the specific surface area by volume, S_W is the specific surface area by weight, s is the total surface area, v is the volume, d is the volume surface mean diameter, n is the particles number, w is the total weight and ρ is the density.

The degree of crushing is defined as:

$$n = \frac{D_1}{D_2}$$ Equation 1.3

Where D_1 is the original geometric diameter and D_2 is the geometric diameter after crushing.

The total particles number is correlated with the specific surface area and the degree of crushing. The crushing process could be operated by several instruments,

- ✓ Mortar
- ✓ Ball mill
- ✓ Impact crusher
- ✓ Fluid-energy mill

The mortar [11] is suitable for the lab usage. The ball mill is made of a cylindrical barrel which has some steel balls inside.

These balls move freely when the barrel rolls and bulk solids are hit and grinded by these metal or ceramic balls. Fig. 1.3 is the ball mill

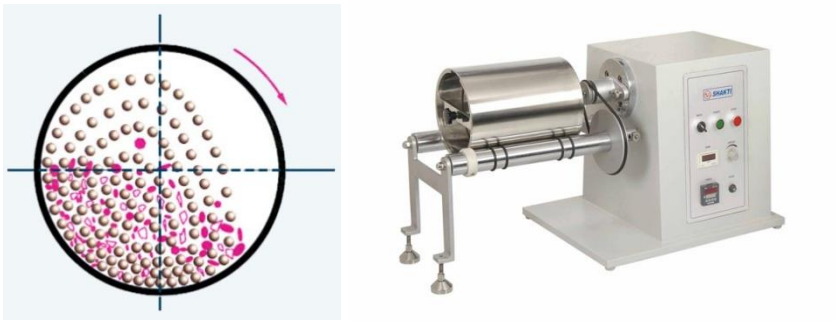

Fig. 1.3 The schematic diagram and object picture of the ball mill

The ball mill has a history which is more 100 years. It´s structure is simple but the working efficiency is low. The operation is closed, so it is suitable for the precious materials, sterile smashing, dry crushing, wet crushing or intermittent crushing, and the inert gas could be added in order to protect materials.

The impact crusher[12] uses the impact force to smash the bulk solids. It is suitable for the brittle or ductile materials, and could produce super fine or ultrafine powder. There two structures in impact crusher, the hammer mill, see Fig. 1.4, and the impact column mill, see Fig. 1.5. The hammer mill has several hammers on the rotary shaft, and the bulk solids are smashed by these high speed rotating hammers. There is a sieve on the wall of the operation room, and particles which are smaller than the sieve aperture come out of the mill. The impact column mill has a high-speed turntable which is fixed with some metal columns. When the turntable rotates, the bulk solids run from the center to the edge of the turntable and the metal columns crushed them into powder. Also, there is a sieve on the wall of operation room which controls the particle size.

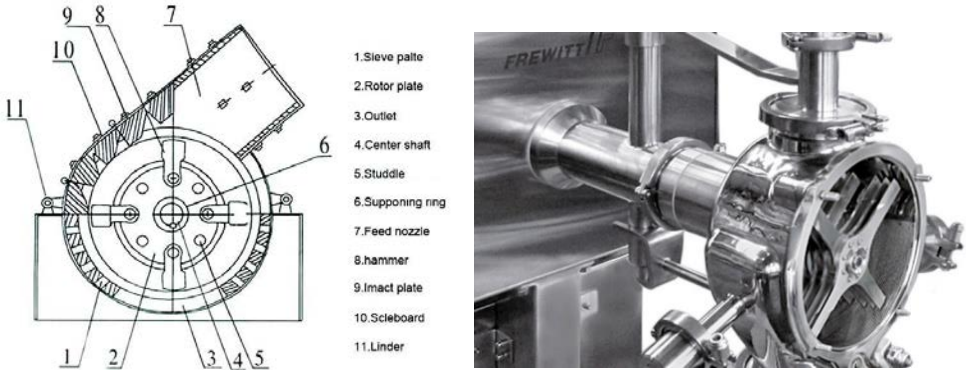

Fig. 1.4 The schematic diagram and object picture of the Hammer mill

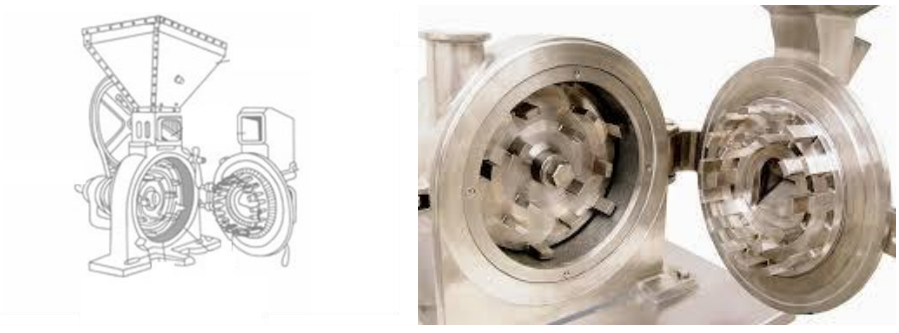

Fig. 1.5 The schematic diagram and object picture of the impact column mill

The fluid-energy mill [13]–[15], Fig. 1.6, also called jet mill, uses the compressed gas to push the materials. The materials are impacted with each other and the mill. The compressed gas pressure may

be more than 7-10 times of the normal barometric pressure. It is suitable for the super fine powder, sterile smashing and thermosensitive materials.

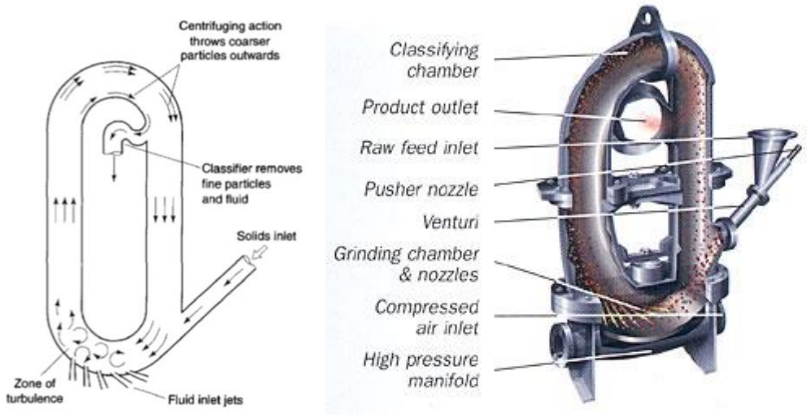

Fig. 1.6 The schematic diagram and object picture of the fluid-energy mill

The key parameters which have to be monitored in crushing are the particle size and humidity.

1.1.1.1.2 Sieving

The crushed particles are sieved by the vibrating sieve, see Fig. 1.7. The sieves with different mesh size are equipped with an oscillation motor, and particles are separated by these sieves depending on their size.

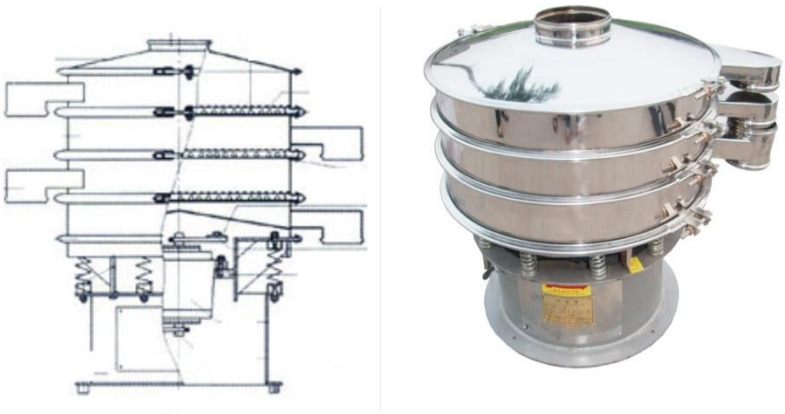

Fig. 1.7 The schematic diagram and object picture of vibrating sieve

In this process the key parameters are similar with the crushing, the particle size and humidity.

1.1.1.1.3 Blending

The operation which mixes two or more kinds of materials uniformly is called blending. The blending of solid is different from liquid, because the solid is consisted of particles which can´t be blended totally. There is a way to express the degree of mix,

$$M = \frac{\delta_0^2 - \delta_t^2}{\delta_0^2 - \delta_\infty^2} \qquad \text{Equation 1.4}$$

Where M is the degree of mixing, δ_0^2 is the variance of totally separated, δ_∞^2 is the variance of totally mixed, and δ_t^2 is the variance of t time.

$$\delta^2 = \frac{1}{n-1}\sum_{i=1}^{n}(X_I - \bar{X})^2 \qquad \text{Equation 1.5}$$

Where n is the total sample number, X_i is the percentage (weight or number) of a component in the i sample. $\bar{X}$ is the average percentage of one component and $\bar{X} = \frac{1}{n}\sum_{i=1}^{n} X_i$.

If the M is 0, this means two materials are totally separated. And if the M is 1, it means that two materials are totally mixed.

Theoretically, there are 3 moving methods during blending operation[16], [17],[18]

- ✓ Convective mixing
- ✓ Shear mixing
- ✓ Diffusive mixing

Convective mixing refers to the movement between particle groups. The shear mixing is about the movement inside the particle group which breaks the agglomeration state. And the diffusive mixing is related to the movement between particles. These three mixing methods don´t occur alone, they are correlated with each other.

The blending process can be affected by the material, the equipment and the operation. The particle size distribution, particle shape, geometric diameter, density and fluidity are critical properties which affect the blending process. If there is a significant difference between materials in the particle shape, geometric diameter or density, the segregation phenomenon will happen. The spherical particles are easy to flow which causes the instability of the products. The proportion of every material is another important property. A large difference in the proportion of each material results a low degree of mixing. The equipment influences the blending by its shape, size and material. For operation, such as the blending speed, filling amount, filling method and ending time are some key points for the blending process.

Instruments of blending operation have several models, they are [19][20][21][22]

- ✓ Cylindrical blender
- ✓ Cubic mixer
- ✓ 3D biconical blender
- ✓ V-shape blender
- ✓ Stirring tank blender
- ✓ Vertical screw mixer

The horizontal cylindrical blender, see Fig. 1.8, 3D biconical blender and cubic mixer are similar with each other. The container rotates along the fixed horizontal axis or rolls with a moving axis. Materials run up and down when the container rotates, and the convective and shear mixings are their main moving methods.

1. Cylindrical blender 2. Cubic mixer 3. 3D biconical blender

Fig.1.8 Object picture of different blenders

The V-shape blender, see Fig. 1.9, is consisted by two cylinders which are connected with an 80^0 angle. When the blender rolls with the fixed horizontal axis, materials are divided into two parts firstly and then mixed together again. The convective mixing is the main moving method. This process continues and a high degree of mixing would be achieved in a shorter time than the cylindrical blender.

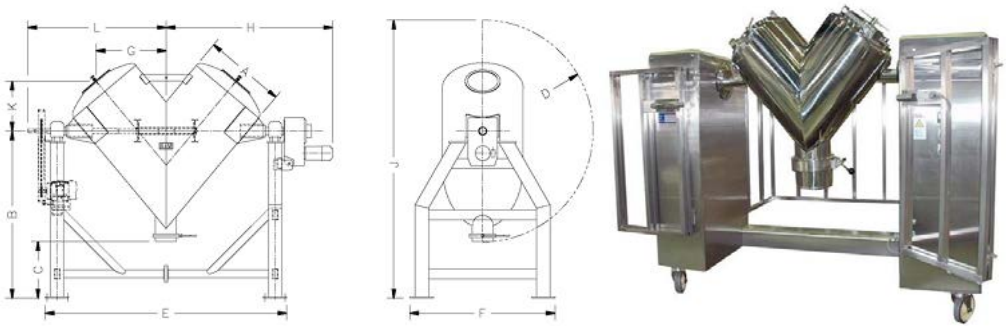

Fig. 1.9 The schematic diagram and object picture of V-shape blender

The stirring tank blender, see Fig. 1.10, has some paddles inside a U-tank. These paddles rotate along the horizontal axis, so materials are mixed by the shear mixing mainly.

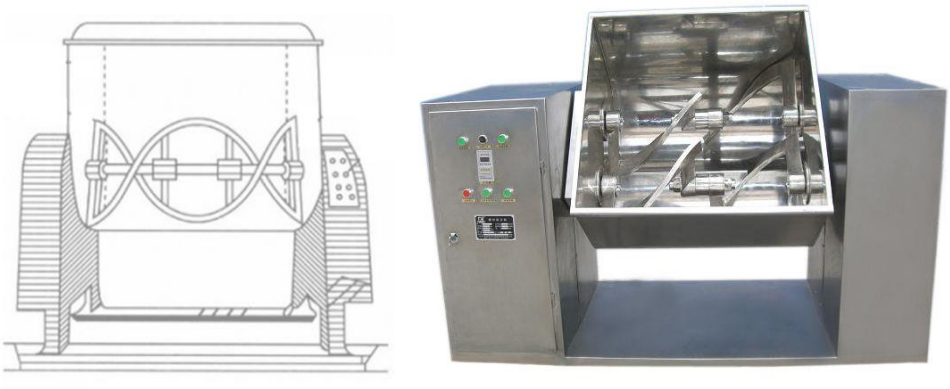

Fig. 1.10 The schematic diagram and object picture of stirring tank blender

The vertical screw mixer, see Fig. 1.11, is a conical container with one or two screw propellers inside. Materials are pushed up from the bottom by the propellers, then fall down when they reach the top of the propellers. The conical container usually has a 35^0 angle. Materials which own a large different in weight proportion could be well mixed too by the vertical screw mixer.

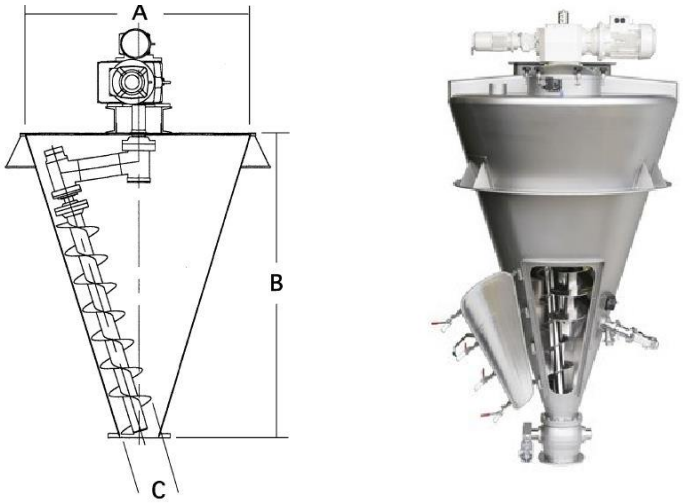

Fig. 1.11 The schematic diagram and object picture of vertical screw mixer

In the blending process, the key factors include the content uniformity and the humidity.

1.1.1.2 Granules

Preparation process of granule which is named the granulation has two types, the wet granulation and dry granulation. The granulation step improves the fluidity, compressibility and the content

uniformity of the solid drugs, so it is wildly used in the pharmaceutical industries. Besides the tablet, the capsule and pellet are preparations which need the granulation process.

1.1.1.2.1 Wet granulation

The traditional wet granulation process is the more popular method in the pharmaceutical industry[23]. The crushing, sieving and blending processes are the same with powder preparation, so only other operation units are discussed here.

The wet granulation process is shown in Fig. 1.12

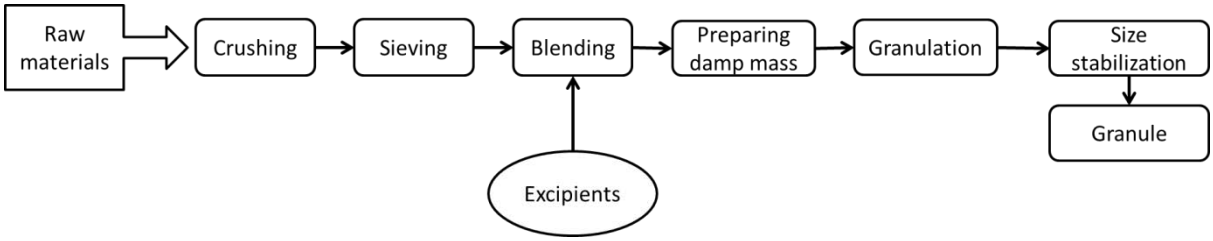

Fig. 1.12 Flowchart of wet granulation process

- Preparing damp mass

  This process mixes the Active Pharmaceutical Ingredient (API), excipients and liquid together. The damp mass could be neither too hard nor too soft. It depends on the properties of the drug.

- Granulation

  The granulation process, see Fig. 1.13, is very complex. The attraction between solid particles, the binding force of liquid bridge or solid bridge, and the mechanical interlocking are the inter-particle bonds which connect solid particles.[24], [25]

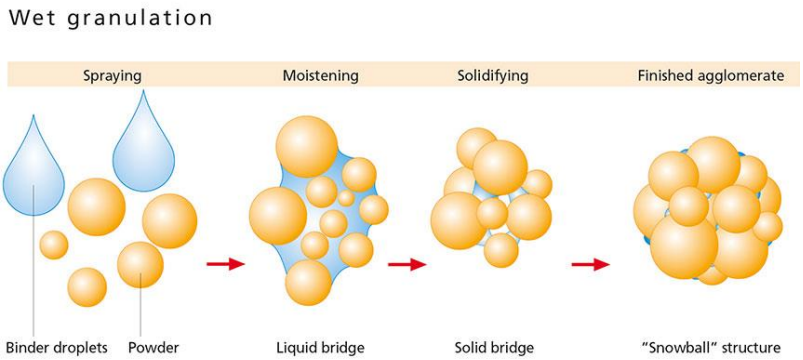

Fig. 1.13 Physical theory of wet granulation

The wet granulation has six processes in general, they are [26]–[32]

- ✓ Extrusion granulation
- ✓ Rotating granulation
- ✓ High speed stirring granulation
- ✓ Fluid bed granulation
- ✓ Spray granulation
- ✓ Spherical crystallization granulation

The extrusion granulation, see Fig. 1.14, method pushes the damp mass through a sieve and the particle size is controlled by the mesh of the sieve. The humidity of damp mass and extrusion speed are key factors of this operation. There are three ways for extrusion which are spiral extrusion[33], rotary extrusion and swing extrusion[34].

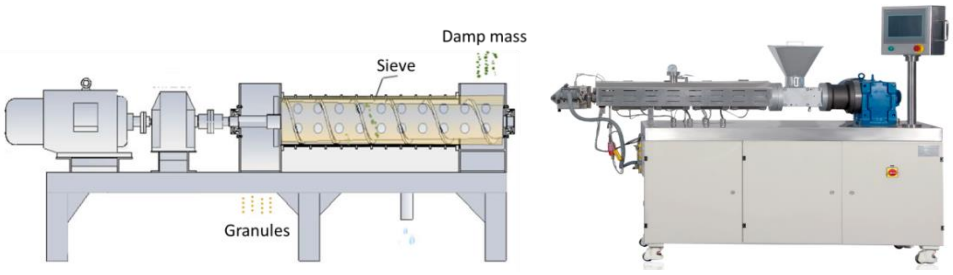

a) Spiral extrusion

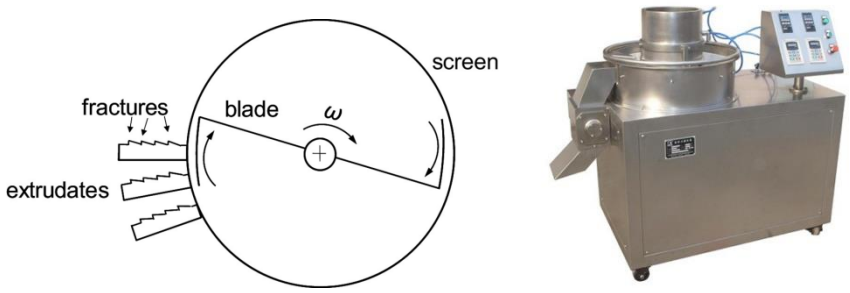

b) Rotary extrusion

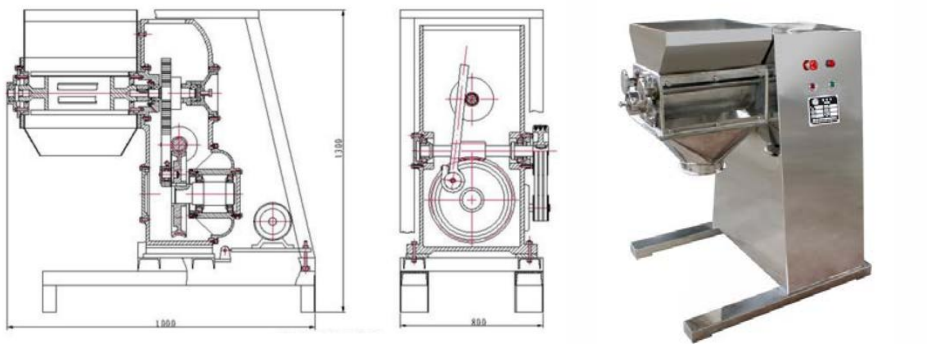

c) Swing extrusion

Fig. 1.14 The schematic diagram and object picture of three typical extrusion methods

The rotating granulation, see Fig. 1.15, produces round particles which are made by the rolling movement inside a rotating plate. There are three steps in this process, the formation of nucleus, the growth of nucleus and the compaction. The particle distribution of rotating granulation is larger than the extrusion method.

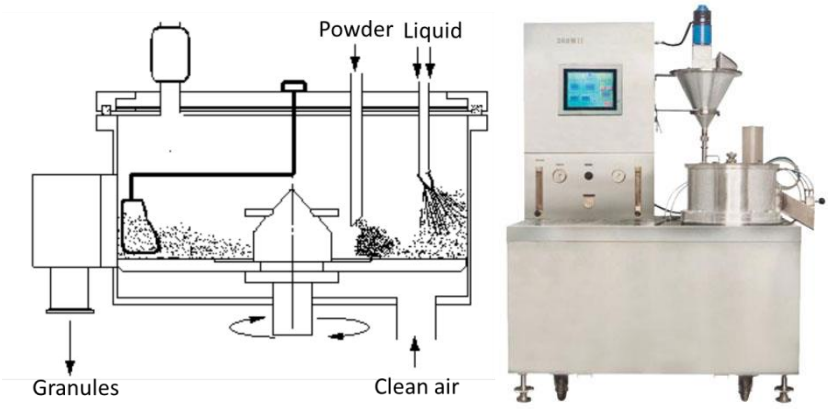

Fig. 1.15 The schematic diagram and object picture of rotating granulation

The high speed stirring granulation, see Fig. 1.16, could produce both the dense particles for capsule and soft particles for tablet. The damp mass is made inside a closed container by the stirring blades and cut into particles by the high speed cutter. The speed of stirring, the amount of liquid, the particle size of dry powder and the shape of the cutter are the key factors.

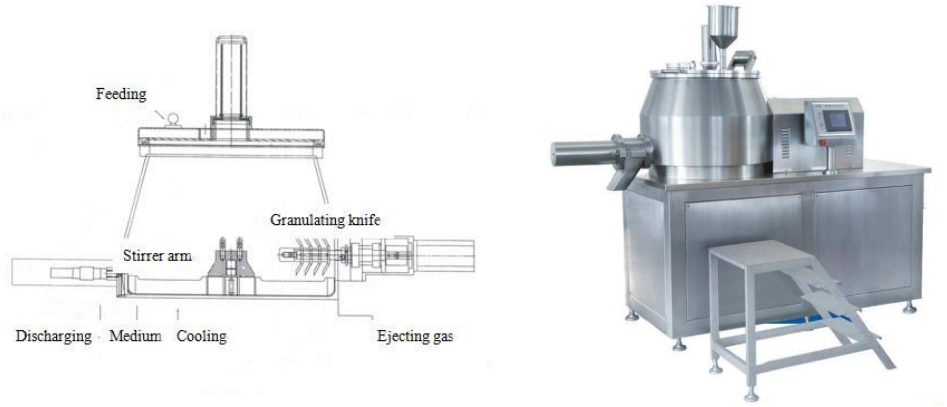

Fig. 1.16 The schematic diagram and object picture of high speed stirring granulation

The fluid bed granulation, see Fig. 1.17, use warm air to make the powders suspended and mixed, then the liquid binder is sprayed from the top of the instrument to combine powders into particles. Meanwhile, these wet particles are dried by the warm air. The mixing, granulation and drying

processes are carried out at the same time in the fluid bed, so it is also called one step granulation. The speed and temperature of warm air, the speed and drop size of the spray, the position of the spray head and the amount of the powder are key factor of this operation. The particles produced by the fluid bed are soft and have a high fluidity.

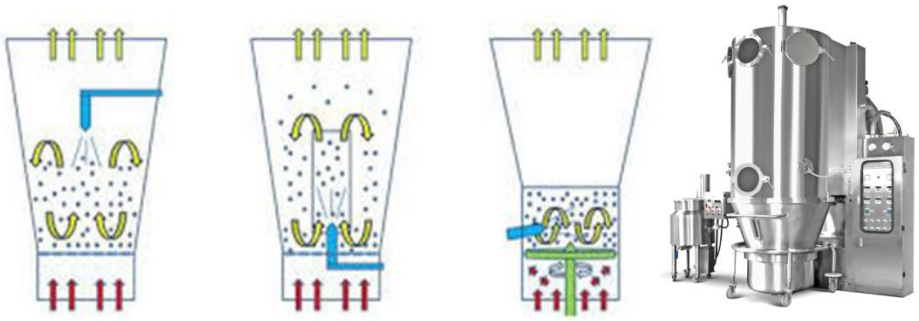

Fig. 1.17 The schematic diagram and object picture of fluid bed granulation

The spray granulation, see Fig. 1.18, takes the drug solution or suspension as the raw material. This liquid is sprayed into the container which has warm air flowing inside. The liquid is dried in just several seconds and the particles are produced. The spray granulation could produce solid particles from the drug solution or suspension directly and is suitable for the heat sensitive materials. The speed and temperature of warm air and the speed and drop size of the spray are the key factors.

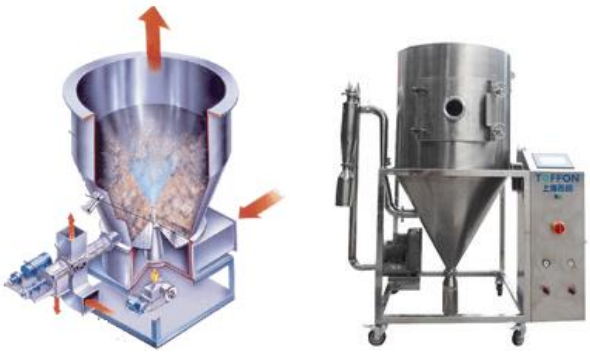

Fig. 1.18 The schematic diagram and object picture of spray granulation

The spherical crystallization granulation, see Fig. 1.19, combines the crystallization and stirring operation to produce particles. It needs three basic liquids, the solvent which could dissolve the drug, the solvent which make the drug crystallize and the bridge solvent which combines the drug crystals. The granules are round balls and their size could be controlled by the solvent system, the temperature and the stirring speed.

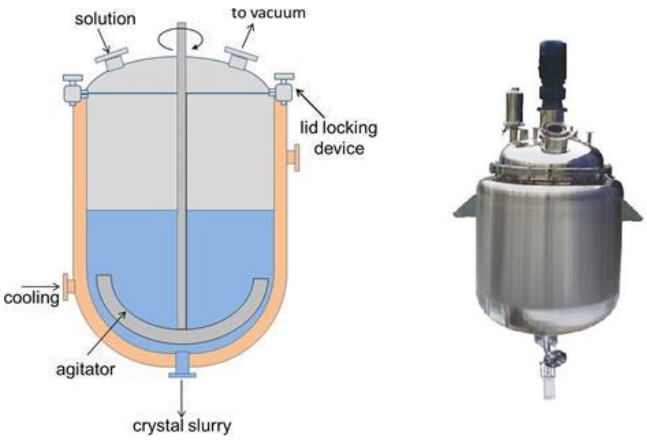

Fig. 1.19 The schematic diagram and object picture of spherical crystallization granulation

1.1.1.2.2 Dry granulation

The dry granulation process, Fig. 1.20, compresses the powder of all materials into bulk solid and then crushes it into granules. [35]–[37]

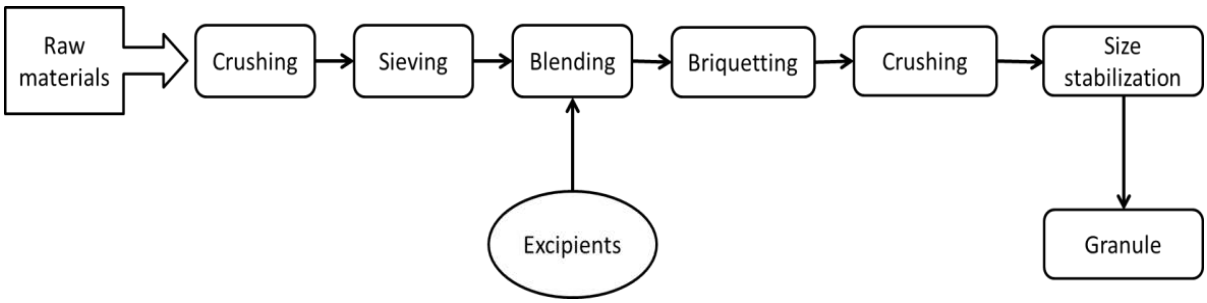

Fig. 1.20 the flowchart of dry granulation process

The most popular method which carries out the briquetting operation is the roller compaction method, see Fig. 1.21. This method uses two rolling cylinders to compress the powder mixer into bulk solids. And the bulk solids are crushed into particles whose size is suitable for the next operation.

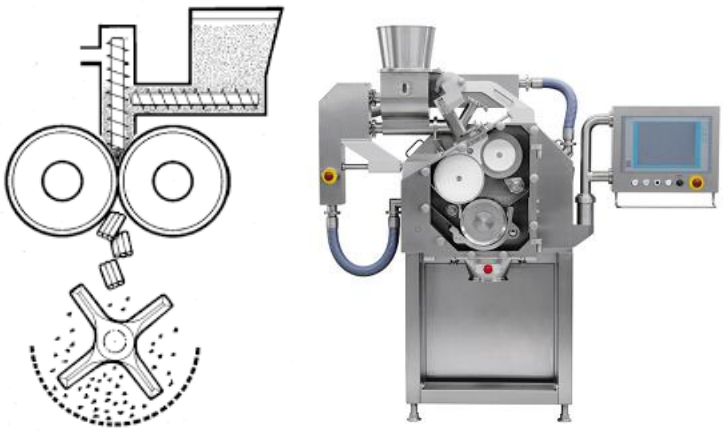

Fig. 1.21 The schematic diagram and object picture of dry granulation

There are several key factors in granulation process, such as particle size, content uniformity and humidity.

1.1.1.3 Tablets

The tablet preparation is produced by compressing the API and the excipients into a tablet. Tablets can be round shape or other shapes. It is most common preparation in the daily life. The tablet has accurate ingredients concentration, stable chemical properties, mechanized production, high production, low cost, various types, convenient transportation and storage,

1.1.1.3.1 Compression

There two types of compression, the compression with granules and the direct compression method.[38]–[43]

The compression with granules is shown in Fig. 1.22, the granules are lubricated and blended first, and then this mixture is compressed by the tableting machine.

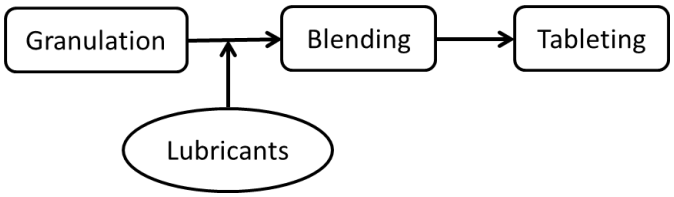

Fig. 1.22 The tableting process with granules

The direct compression is shown in Fig. 1.23, the raw materials are crushed into powder, and then the powder is compressed directly after blending

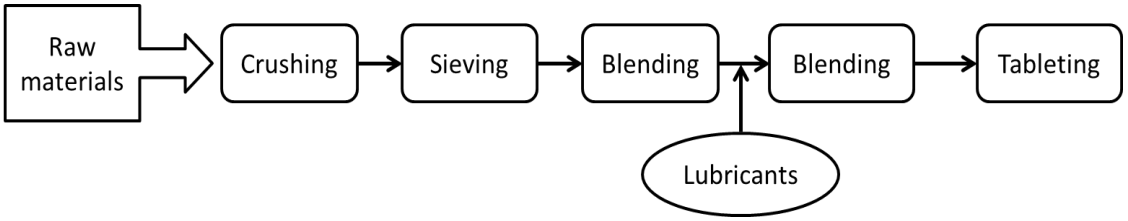

Fig. 1.23 The tableting process with the direct compression

Before compression, the weight of a tablet should be calculated.

$$Weight = \frac{Labeled\ amount\ of\ API\ in\ a\ tablet(g)}{Mesured\ content\ of\ API\ in\ the\ granules\ (mg/g)} \qquad \text{Equation 1.6}$$

The instruments for the compression have two types, Fig. 1.24, the single punch tableting machine and the rotating tableting machine. The single punch machine has simple structure but Low productivity, and is suitable for the development of new drug. The rotating tableting machine is more complex. It has several components such as machine table, pressure wheel, tablet weight regulator, pressure regulator, powder feeding system, vacuum cleaner and protective device. The machine table has three levels, the upper level is the upper punch, the middle level is the mold and the lower level is the lower punch. There are three steps in the manufacturing process, the filling, compression and pushing tablet. Firstly, granules are fed into the mode and the spatulas scratch the extra powder. And then, two punches compress the powder into tablet. Finally, the tablet is raised by the lower punch and collected by the spatula.

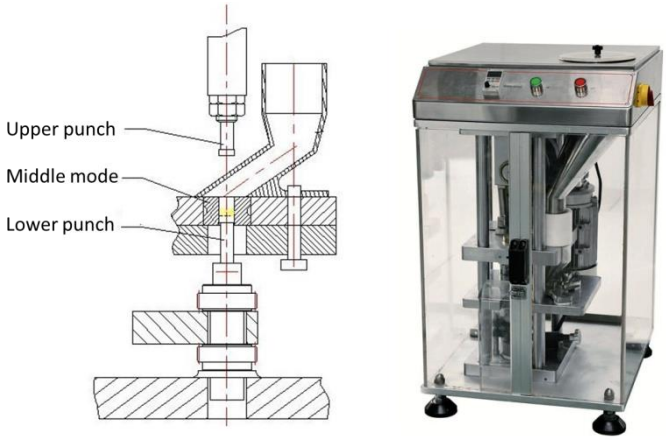

a) Single punch tableting machine

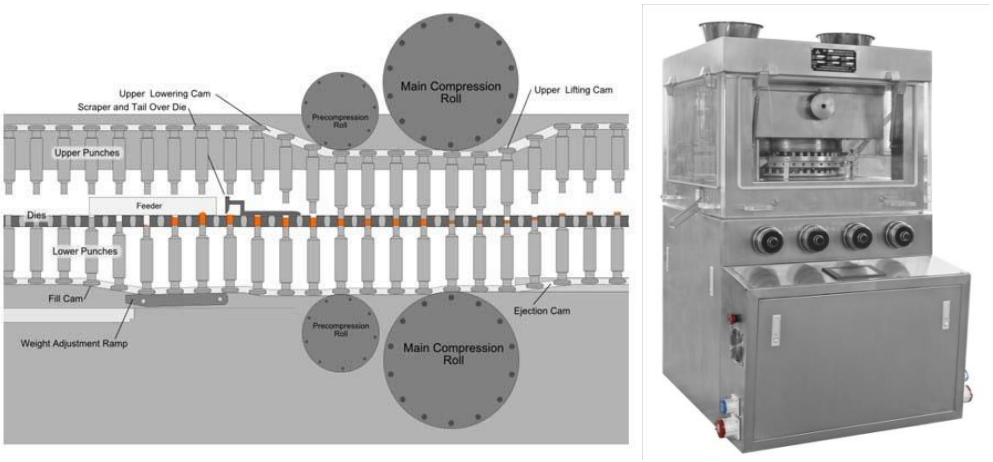

b) The rotating tableting machine

Fig. 1.24 Two typical tableting methods

The key factors for tableting include tablet density, tablet size, content uniformity and humidity.

1.1.2 Process Analytical Technology (PAT)

The drug quality consistency is one of the key factors in the manufacturing process. In order to maintain the high quality of pharmaceutical products and reduce identified manufacturing risks, some important regulations were issued by different organizations. Food and Drug Administration (FDA), drug regulatory agencies are national authorities. The International Council for Harmonisation of Technical Requirements for Pharmaceuticals for Human Use (ICH) and European Medicines Agency (EMA) are international bodies.

The pharmaceutical Quality Assurance (QA) and pharmaceutical Quality Control (QC) are two items which make medicines safe, effective, and of standard quality. The QA is defined as the sum of all activities and responsibilities required to ensure that the medicine that reaches the patient is safe, effective, and acceptable to the patient[44]. And the QC is the process concerned with medicine sampling, specifications, and testing, and with the organization's release procedures that ensure the necessary tests are carried out and the materials are not released for use, nor products released for sale or supply, until their quality has been judged satisfactory.

Good Manufacturing Practices (GMP) is a performance standard which are part of the quality assurance activities that ensure that products are consistently produced and controlled to the quality standards appropriate to their intended use and required by the drug regulatory authorities[45]. With GMP, the quality is assured by testing and inspection. The manufacturing process is fixed but variables in the products can´t be removed totally. Therefore, two new concepts in pharmaceutical industry which are Quality by Design (QbD) [46]and PAT [47]come out. Different from GMP, the

QbD assures the quality by well-designed product and process. This concept makes the manufacturing process adaptable and provides a consistent output.

The FDA defines PAT as ``a system for designing, analyzing, and controlling manufacturing through timely measurements (i.e., during processing) of critical quality and performance attributes of raw and in-process materials and processes, with the goal of ensuring final product quality.´´

Normally, the quality of pharmaceutical products is evaluated in a laboratory with the collected samples of different batches. However, the PAT could offer more innovations to benefit pharmaceutical development, manufacturing, and quality assurance. Because the challenges of new discoveries and new business requirements (e.g., individualized therapy or tailored treatment), the pharmaceutical industry needs to employ innovation, cutting edge scientific and engineering knowledge and better principles of quality management. The aim of PAT is to understand and control the process of pharmaceutical manufacturing. What´s more, PAT could help the quality to be built into pharmaceutical products which is correlated with the current drug quality system. The concept of built-in quality could be achieved, if we have fully understood the follwing 4 points[44], see Fig. 1.25

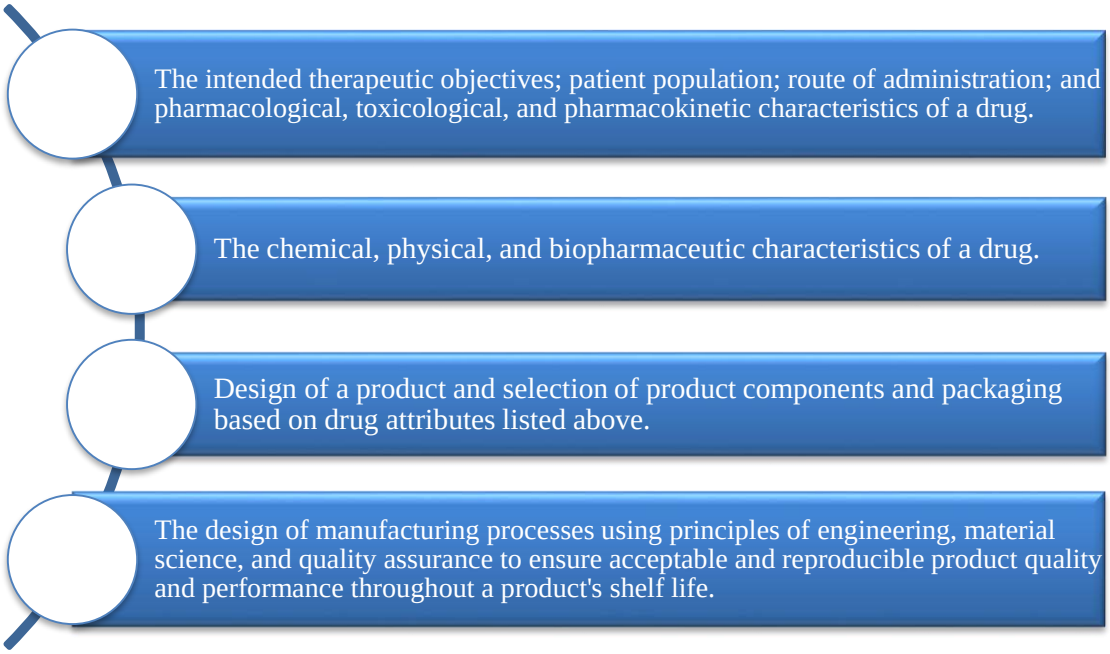

Fig. 1.25 Key points of built-in quality concept

The advantages which would be brought by PAT vary in processes and products, but typically there are five points, see Fig. 1.26

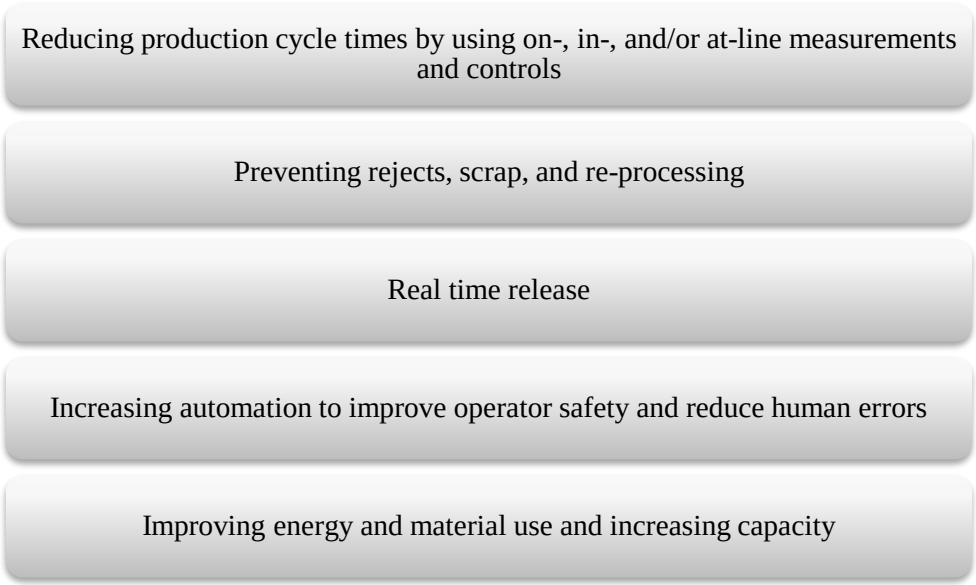

Fig. 1.26 Advantages of PAT

Pharmaceutical manufacturing processes of solids include a series of unit operations, such as blending[48], granulation[49] and compression[40]. Not only chemical attributes should be analyzed, but also the physical and mechanical attributes of pharmaceutical ingredients have to be identified. Thus, the raw and in-process materials both need a well understanding of attributes which are critical to the final product quality. There are many PAT tools which are able to provide effective and efficient means for the fundamental understanding of the pharmaceutical manufacturing processes. Several of them do not need sample preparation, could assess multiple attributes and run real time analysis on samples nondestructively. These PAT tools are[50], see Fig. 1.27

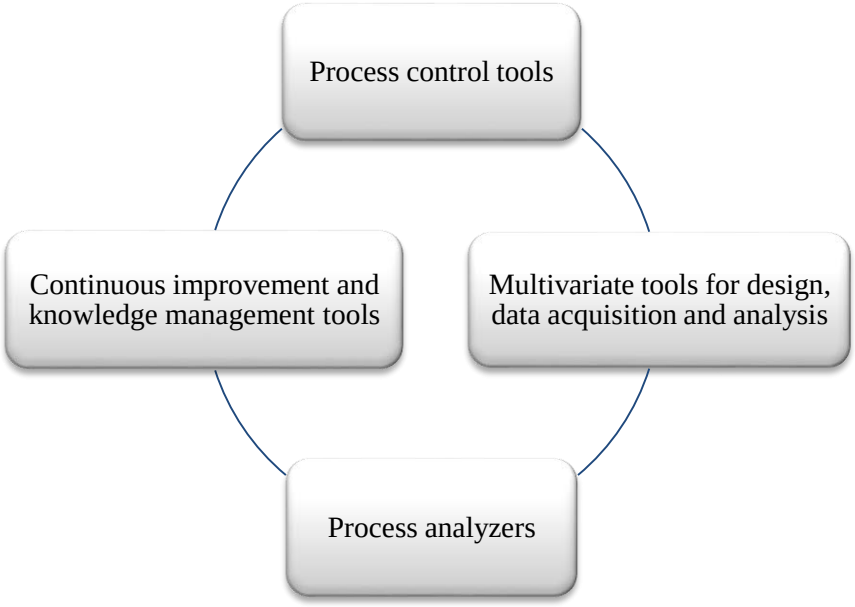

Fig. 1.27 PAT tools

These tools can be combined to serve a single-unit operation or a whole manufacturing process. For the tools of process analyzers, in detail, there are three types of measurements which provide biological, physical, and chemical attributes of the process samples. They are, see Fig. 1.28

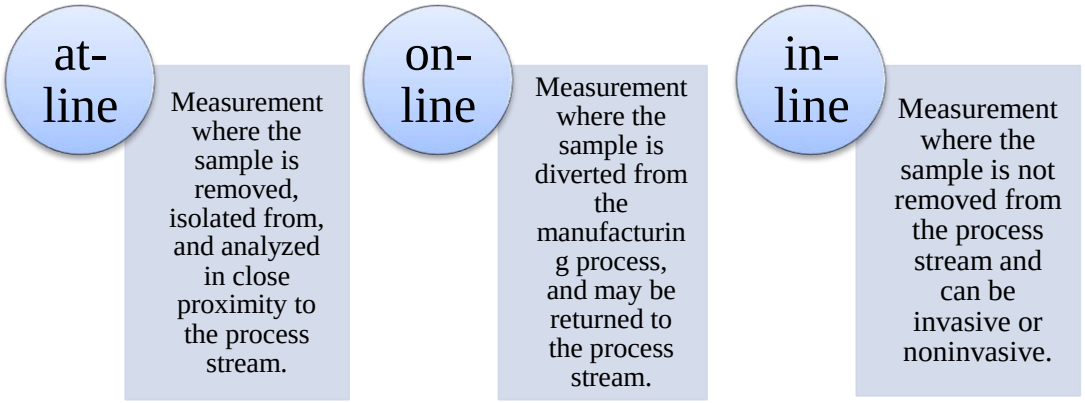

Fig. 1.28 Three types of measurements for process analyzers

These measurements do not have to collect the absolute values of the attribute of interest. The changes of materials during the process also offer us the useful information for process control. What´s more, the PAT is a risk-based and integrated systems approach. The more we understand the manufacturing process, the lower the risk of producing a poor quality product will be. And the Current Good Manufacturing Practices (CGMPs) inspections, joint training, Chemistry Manufacturing and Control (CMC) review and certification make up an integrated systems approach to the regulation of PAT. Real Time Release (RTR) is another important component of PAT, it is defined as ´´the ability to evaluate and ensure the acceptable quality of in-process and/or final product based on process data´´. PAT could provide a valid combination of assessed material attributes and process controls to achieve this goal.

QbD is defined by FDA as ´´a systematic approach to pharmaceutical development that begins with redefined objectives and emphasizes product and process understanding and process control, based on sound science and quality risk management.´´ Different from GMP, the QbD assures the quality by well-designed product and process. This concept makes the manufacturing process adaptable and provides a consistent output. The ICH Q8 [51] has discussed the QbD approach, it said that ´´quality cannot be tested into products; quality should be built in by design´´. The table explained the different between the traditional concept and the QbD concept. See Table 1.2

Table 1.2 Comparison between traditional and QbD concepts

ICH Q8	
Traditional concept	QbD concept
Empirical development	Systematic development
Data Driven	Knowledge driven
Retrospective	Prospective
"Test to document quality"	Science and Risk based assurance of Quality
Acceptance criteria based on batch data	Acceptance criteria based on patient needs
Variability not understood and avoided /Focus on reproducibility	Variability explored and understood (Design Space, **PAT**)

The goal of QbD is to design robust and efficient manufacturing processes which maintain the highest quality of pharmaceutical products at the lowest cost and PAT is a useful tool to achieve this goal.

In order to apply the PAT and QbD concepts in the manufacturing process, the chemical and physical information of products have to be acquired and virtualized. The fast spectroscopy, which includes both the chemical and physical data, is a powerful tool to make it come true.

1.2 Food industry

In the food industry, the products quality is an essential issue. A safe and nice user experience can create huge profits for the company and the society. But how can we analyze the product quality in a better way is an issue which need to be considered. Nowadays, some classic methods are not suitable for the modern manufacturing lines. The method which is simpler and more rapid is demanded. New reliable technologies which have those advantages offer us some powerful tools to analyze the product quality in the modern manufacturing lines. In order to control and improve the products quality, some basic knowledge of the food industry was introduced in the following part.

1.2.1 Food quality

The high quality products which offer a good value are popular in the market. Practically, the customer satisfaction is the main index of quality[52]. In terms of the manufacturing level, the better productivity and safety are key factors. Food quality is defined as a measure of purity, strength, flavor, color, size, maturity, workmanship and conditions, or any other distinctive attribute or characteristic of the product[53], [54].

The dimension of quality could be summarized as two parts, design and conformance. The design involves engineering decision, customer requirements, manufacturing process and stakeholder profits. The conformance is defined by David A. Garvin that connects the customer requirements with engineering design[55], [56]. In detail, it has eight items,

a) Performance, the basic characteristics of manufacturing process.

b) Features, the additional characteristics which improve the appeal of products.

c) Reliability, the likelihood that a product will be well in a period.

d) Conformance, the precision between product and the specific standards.

e) Durability, the length of time when the product stays well.

f) Serviceability, the speed of bringing a broken product back to work.

g) Aesthetics, the response of a customer owned to the product.

e) Perceived quality, the quality of product affected by indirect measures.

Food producers who follow a high standard of quality have good reputation among customers and their products are sold well. Typically, there are 4 standards [57]–[60] legal standards, company or voluntary label standards, industry standards and consumer or grade standards. The legal standards are

published by federal, state or municipal agencies which are mandatory laws or regulations. They are the minimum requirements of the food quality. The company or voluntary label standards are founded by the various segments of the food industry and they are the corner stones of brand value of each company. The industry standards refer to quality limits which are launched by specific industry associations. They are not involved in the legal standards. Consumer or grade standards include the requirements of products from consumers. They are formed by the experience of consumers, for example the military standards.

1.2.2 Analysis methods

There are many methods which could evaluate the food products[61], [62]. They can be divided into 2 parts, the subjective methods and the objective methods[63].

The subjective methods are depended on the opinions of the analysts. They involve the physiological response of the trained analysts, the influence of personal preference and the individual perception. These methods which qualify or quantify the characteristics have to be operated by the analysts with their individual opinions. And the opinion is related to the various senses of organs such as the color, flavor and touch.

The objective methods are carried out with recognized standard scientific tests which exclude the sensory of analysts. The objective methods, what´s more, could be classified as three types: physical methods, chemical methods and microscopy method. For physical methods, they are fast and do not need too much training. Such as the size, texture, consistency, imperfection, filling weight, head space and vacuum can be analyzed by physical methods. The chemical methods used in food industry are belonging to wet chemistry normally, such as titration, chromatography and ashing, they are time consuming and tedious. Nowadays, researchers are developing quick test methods to determine the material content in products such as soluble solid concentration, pH and moisture content. In the microscopy method, there are two common groups: a) adulteration and contamination which analyze the bacteria, yeast, mold and so on, and b) differentiation between cell types, tissue types and microorganisms of various stored food which include tissue testing for deficiency of fertilizer materials, stored food in the tissues of plant materials and undesirable fermentation changes.

Traditional analysis methods are off-line measurements which cost hours or days for analysis in a quality control, but there are many requirements for faster methods and the idea of real-time, at-line or on-line analysis has come out.

- The customs ask for a consistent and high quality, which needs much quicker measurements of process variables or product attributes.

- The column and rate of production are large, so the traditional method could not meet the increasing workloads.
- The competitive pressure of longer shelf-life makes the off-line analysis less acceptable.
- The trend of industrial 4.0 boosts the development of continuous automatic production which is based on the real-time process control.

There are also some requirements for instruments,

- Appropriate accuracy and sensitive for the specific product
- Hygienic design and construction
- Non-destructive analysis
- Suitable robustness to stand hostile operation environment
- Automatic and simple operation steps which could be used by non-skilled operator
- Low maintenance level
- Total cost is lower than the benefits gained

It is important that the traditional and off-line analysis methods are transferred to the rapid and real-time process control methods.

1.2.3 Process control in the food industry

In order to achieve a consistent high quality in the finished food, the process control program has to be carried out. The traditional QC focuses on the finished products, but the process analysis becomes more and more important for the manufacturing. A change in strategy has come out: from detection to prevention of substandard quality[64]–[67]. The aim of the process control is to

- Achieve a high quality specification consistently
- Release only the acceptable middle product to the following operation
- Favor improved stability
- Reduce variation in the manufacturing process

The basic of the process control is a full understanding of the manufacturing process, the equipment and the establishment of the specifications.

Besides, there are some other key points in the process control in the food industry. Fig. 1.29 is the flowchart of the process control management.

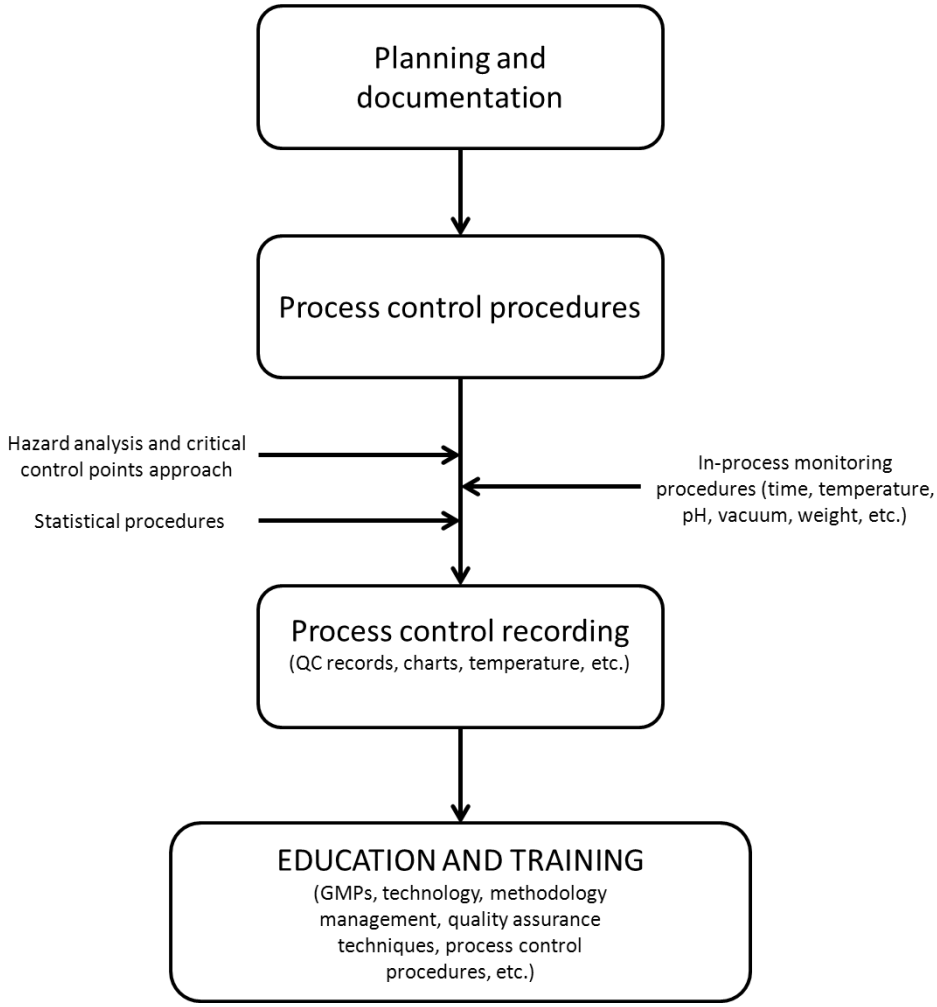

Fig. 1.29 Process control management in food industry

The food processing procedures, according to their functions, can be combined into unit operations[68], such as batching, heating, cooling, blending, pasteurization, sterilization, freezing, evaporation, dehydration, fermentation, distillation, extraction, separation and so on. Every unit operation has its specific, identifiable and predictable effect on a food. In order to achieve the function, each unit operation may have several activities. And the total food manufacturing process is accomplished by the selection and combination of unit operations. In the following part some typical unit operations are introduced.

Materials handling is the very first step in the process, the harvesting on a farm is an example. It´s quality is controlled by maintaining the raw material quality and sanitary conditions, minimizing product losses, bacterial growth and holdup time. Cleaning has a large range which includes operations from removing the dirt on the egg shells to the bacteria in the liquid food. Depending on the food type, brushes, high velocity air, steam, water, vacuum, magnetic attraction of metal contaminants could be the tools for cleaning. Separation procedure could be operated among the solid, liquid and gas, such as compressing juice, centrifuging oil and vacuuming air from food.

Disintegration means the operations which divide the large size food into smaller units. The pulping cutting, homogenizing and grinding could be the methods to provide disintegration. Pumping is very common in the food unit operation. The liquid or solid foods are moved from one processing step to another step by pumping unit operation. The types of pump instruments are chosen according to the food state. Mixing operation is carried out among liquid, solid and gas in food manufacturing. The blenders used in this process are selected by the properties of food materials. Heating could destroy microorganisms and preserve the food, drive off moisture, develop flavors, inactivate enzymes and destroy natural toxic substances. The most used methods heating are conduction, convection and radiation. Cooling is used to preserve a food-keeping quality, which reduces the loss of food. Evaporating could remove the water so that the product concentration would be improved. Another function is to recover desirable food volatile compounds. Drying also removes the water from food, but almost makes the weight to the total dryness. The dried milk powder and instant coffee are examples after drying. Packaging procedure is to protect the food from contamination, destroying, loss of flavor and give a better outlook.

These unit operations have to be monitored so that the product quality could be controlled. The multivariate data analysis is an ideal method to help us realize this aim. It could measure the content of ingredients, deal with sensory studies, make the detection of adulteration and carry out image analysis. By analyzing variables during the manufacturing process, the most influential factors can be determined. And a further understanding of the products would offer the factories consistent quality food and lower the waste in the process.

1.2.4 Tomato quality improvement

Tomato is one of the most important plants in the world. It´s quality can be improved both at the genetic level and the manufacturing level. The evaluation of the quality depends on not only the content of ingredients but also the sensory characteristics.

In terms of genetic level[69], [70], some breeding programs have been carried out to find out the tomato which keeps the typical shape, has a good agronomic behavior and meets the organoleptic requirements from consumers.

The ingredients and sensory traits of tomato could be modified by the diallel crossing. The best genotype is selected from the second or more generations later. Thus, a better score of sweetness, soluble solid, skin perception, pericarp mealiness, intensity of aroma and intensity of taste could be achieved.

Normally, in order to analyze these sensory traits of a new genotype, a sensory panel which has several stages is needed. Panelists have to be trained before evaluation of samples. Thus, it is hard to analyze a large amount of samples by the sensory panel. Only some representatives can be tested and the procedure is complex. For the ingredients analysis, sucrose, fructose, glucose and acids are quantified by several classic methods. As the same problems as panel test, these methods are complex and should destroy the structure of tomatoes. It is necessary to have a simple method which could analyze the sensory and ingredients without destructing the fruits. In terms of the manufacturing level, the processed tomato products are manufactured by unit operations. These unit operations have a strong influence on the sensory traits and the ingredients content of final product. The quality of processed food could be improved, if unit operations are monitored in real-time, because important variables could be found and well controlled during the manufacturing process. A further understanding of the manufacturing process of tomato products would improve the skills in operation so that products with the desired sensory traits and ingredients content can be obtained. Fig. 1.30 is a manufacturing flowchart of tomato product. Each unit operation can be operated by various types of machines and systems and also could make a wide range of different food products. The traditional analysis methods only provide information in a delayed way. Products can´t be check one by one, so the consistent quality can´t be guaranteed. Besides, the traditional methods also cost a lot of money and labor.

The rapid spectroscopy is a tool has been applied in the food industry to deal with problem mention above in some other food products. Tomato products, as one of the most important food, should use this powerful tool to improve their quality. By this way, high profits would be gained by the companies and better products would be offered to consumers.

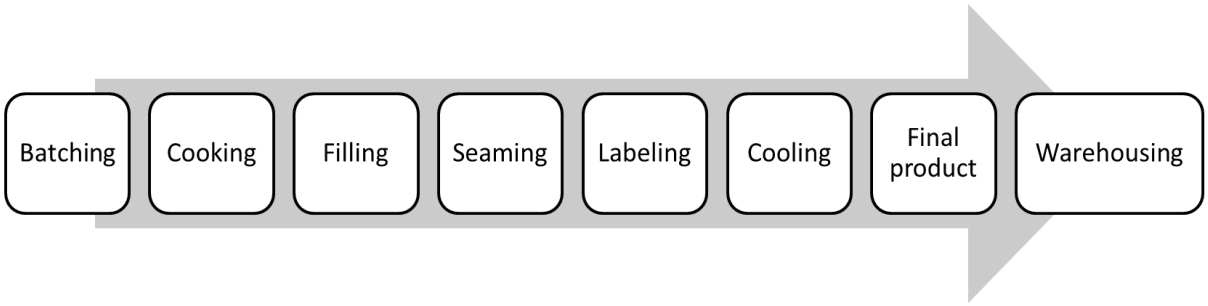

Fig. 1.30 Tomato sauce manufacturing flowchart

In this thesis, a study which focuses on the analysis of sensory and the chemical ingredients in tomato products is done. The chemometrics combined with Near Infrared Spectroscopy (NIRS) was used to lead the upgrading in the food industry.

1.3 NIRS in industry 4.0

The innovation of a technology is always following the development of human modernization process. Technologies which could meet the current needs of the modernization process would be created and optimized by researchers, engineer or some genius.

From the perspective of industrial sector, there are three remarkable items in the history of human modernization process, the first industrial revolution, the second industrial revolution and the digital revolution. The first industrial revolution started from 1760s and its character was the transition from hand production methods to machines powered by water and steam. The second industrial revolution began at 1870s and the sign of this period was mass production and the invention of the internal combustion engine and electricity. The digital revolution (also called the third industrial revolution) originated in 1950s, and its symbol was the change from mechanical and electronic technology to digital technology, which aroused the development of digital cellular phone, computer and internet.

Right now, the 4^{th} industrial revolution is growing up. From 2010s, industry 4.0 was firstly raised by the high-tech strategy of the German government[71]–[74]. Then the European Commission carried out the international Horizon 2020 CREMA project to encourage the concept of industry 4.0[75]. In USA, there is a national strategic plan for advanced manufacturing which focuses on industrial internet and reindustrialization[76]. In Japan, 30 Japanese companies launched the industrial value chain initiative which aims at creating standards for technology to connect factories and to combine efforts to internationalize industrial standards from Japan. Therefore, it is important for us to understand and follow this trend in the world.

The realization of 4^{th} industrial revolution needs the support from many aspects, such as economy, public policy and new business style. Besides them, the technical Innovation is the fundamental workhorse of 4^{th} industrial revolution.

There are several key points for the design of industry 4.0 scenarios. Virtualization and real time capability are two of them. Virtualization means that Cyber-Physical Systems (CPS) are able to monitor physical processes. These sensor data are linked to virtual plant models and simulation models. Thus, a virtual copy of the physical world is created. Real time capability means that data is collected and analyzed in real time.

NIRS is a technology which could transfer the chemical and physical information of an object into digital information without destructing the object. With the help of chemometrics, all the digital information could be analyzed and a final quantitative/qualitative decision could be made by the simulative model. It could help the virtualization of the product. What´s more, the real time capability

is a main advantage for NIRS. Instead of hours or days, the NIRS only needs seconds or minutes to analyze samples in the whole process. Therefore, the Real-Time Monitoring (RTM) of products Critical Quality Attributes (CQAs) could be provided. At a higher level, these data acquired would be further understood. The relationship among instrument data, engineering variables and analytical laboratory reference could be analyzed by models. These models offer a more specific control space definition which help manage the Real-Time Assurance (RTA) of product quality. At the highest level, the process analysis results are precise and accurate enough to replace the traditional laboratory analysis, which fulfills the RTR goal.

In this thesis, the pharmaceutical and food industries are taken as examples of the application of NIRS. Especially, the MicroNIR was chosen as the spectrometer to analyze all the pharmaceutical samples. Miniaturization is the development trend of the NIR spectrometers. The instrument components are designed into microstructures so the spectrometers will be portable and easy for the application in a complicated environment. Pharmaceutical industry has to produce safe, effective and acceptable medicines for patients. The concept of industry 4.0 could help the pharmaceutical factories to manage the QC and QA in a way which is real time, intelligent and customized. The QC and QA management could be improved, so the medicine would be safer, more effective and more acceptable. Besides, the pharmaceutical manufacturing is a technology-intensive process which already has a good foundation for the evolution of the industry 4.0. The economic and technology investments for this change are undergoing now. The food industry needs to produce products which could be in great demand in the market. In order to reach its aim, the products have to be safer, tastier and meet the consumer preferences. The concept of industry 4.0 could help the food factory monitor and control the manufacturing process so that the food quality can be guaranteed and the products can be selected automatically to meet the customized requirements.

Chapter 2

Near-infrared spectroscopy (NIRS)

2. Near-infrared spectroscopy

The near infrared region is the electromagnetic wave whose λ is located in 780-2500nm according to the American Society for Testing and Materials (ASTM)[77]. It is the earliest non-visible light region discovered by human.

NIRS is a spectroscopy which investigates the sample spectra with the absorption range from 780 to 2500nm (12820 to 4000 cm^{-1}). This range is usually divided into two parts, shortwave (780-1100nm) and longwave (1100-2500nm)[78]. In order to commemorate Mr. William Herschel, who discovered the NIR shortwave range in year 1800 firstly, the shortwave range is also called Herschel wavelength range.

The NIR absorption is mainly caused by overtones and combinations of the lower-energy fundamental molecular vibrations and resonances[79]. The absorption intensity of the functional groups is correlated with the change in the dipole moment that occurs during the molecular vibration and on the anharmonicity of the transition. Thus, the NIR absorption intensity is 10-1000 times weaker than the absorption intensity of MIR. Non-polar molecule skeleton(C-C, C=C, etc.) or functional groups containing heavier atoms (C-Cl, C-N, etc.) are too weak to contribute significantly in the NIRS[80]. There is a practically useful exception which is the weak second overtone absorption of C=O bands.

Some molecular groups, mainly the hydrogen-containing group X-H (C-H, N-H, O-H), are the active NIR absorption structure. The local electronic environment has a particularly strong influence on the X-H bond force constants, and this influence generates high signals in NIR spectra.

NIRS has a history more than 210 years but its development progress was quite slow before 1970s when the research group of Norris started to apply it on agriculture samples[81]. The main reason is that, comparing to IR, the NIR spectrum contains very little sharp peak and its peaks are always overlapped with each other or by the baseline. The overtones and combination of fundamental frequencies is strongly affected by both intermolecular and intramolecular H-bonding effects. So, it is hard to use the traditional spectral method to identify the molecular structure, also difficult to apply the Beer-Lambert Law to quantify concentration. Besides, the NIR absorbance is much weaker than IR so the NIR instrument needs a high S/N. Thus, Wetzel in 1983 said that NIRS was a sleeper among spectroscopic techniques[82].

Until 1980s, the application of chemometrics, new spectral instrument and the computer technology had made a great favor to the development of NIR. The CNIRS was founded in 1988, Journal of Near Infrared Spectroscopy and NIR news were two professional journals on NIRS. The numbers of publications about NIR went up dramatically.

Recently, NIRS becomes one of the hottest topics in agriculture, pharmaceutical Industry, petrochemical industry and Bio-industry. The reason why NIRS could have such a rapid growth in a lot of fields is that it has several advantages as following[80], [83]–[90],

a) Non-destructive analysis

   The spectrum could be acquired without sample preparation. Both transmission and diffuse reflectance are suitable for NIRS, so the physical state of sample could be gas, liquid or solid. There is no need to use any reagent to change the sample state. By this way, sample could be sent back to the production line after analyzing and the environment pollution is avoided.

b) Real-time analysis

   The acquisition time of a NIR spectrum costs only some seconds normally and then all the data would be calculated by a computer automatically. Products could be analyzed at real time, so it is possible for the operator to know what is happening to the product within less than 1 minute.

c) Same spectrum for qualitative and quantitative analysis

   NIR spectrum is a cross- sensitive technique which includes not only the chemical information but also the physical properties of the substance or chemical mixture. The same spectrum used for a quantitative measurement may also be used to identify the substance or mixture.

d) Low cost and Low labor-intensive analysis

   The NIRS instrument has a simple physical structure, and the accessories could be made by both quartz and glass. So the instrument cost may keep in a low level compared to some classical instruments.

   NIRS is controlled by standard software installed in a computer and the spectrum may be acquired by an on-line sensor. Operators do not need a labor-intensive work and the application of fiber transition has separated the operators from the dangerous production environment.

e) Miniaturization

   The design of the NIRS instrument has a trend in miniaturization. They are portable and have a smaller size which is suitable for the real time analysis. The application of the miniaturized NIRS does not ask for a complex adjustment of the production line and could be controlled by one operator.

2.1 Fundamental theory

Spectroscopy is an explanation of energy transfer between light and matter. In 1924, Mr. Louis de Broglie found the light had both particle properties and wave properties. This is called wave-particle duality. According to his theory, the energy of a photon is defined as[91]:

$$E_t = h\nu = hc/\lambda \qquad \text{Equation 2.1}$$

In which h is Planck´s constant, ν is the frequency of the light wave, c is the speed of light and λ is the wavelength of the light wave.

The NIR absorption range is between 780 and 2500nm. In wavenumbers, it is from 12820 to 4000 cm^{-1}. The function to convert from nanometers to wavenumbers is:

$$\text{Wavenumbers} = 10^7/\text{nanometers} \qquad \text{Equation 2.2}$$

Chemical bonds vibration in a molecule occurs when photons or energy are absorbed by the molecule. The way of vibration is similar with a diatomic oscillator. Thus, the vibrational modes of diatomic molecules were introduced firstly and then this theory was expanded to the normal modes of vibration of polyatomic molecules.

2.1.1 Diatomic molecule

2.1.1.1 Harmonic oscillator

According to the classical mechanics[92], a diatomic molecule consists two atoms, whose mass are m1 and m2, could be recognized as a spring oscillation of two balls. If the vibration follows the Hooke's Law perfectly, it is called simple harmonic motion. And the oscillator is called harmonic oscillator. The potential energy function is:

$$V(x) = \frac{1}{2}k(r - r_e)^2 = \frac{1}{2}kx^2 \qquad \text{Equation 2.3}$$

Where V is the potential energy function, k is bond force constant, r is internuclear distance, r_e is equilibrium internuclear distance, and $x=r-r_e$.

Fig. 2.1 is the potential energy shows the harmonic and anharmonic oscillator.

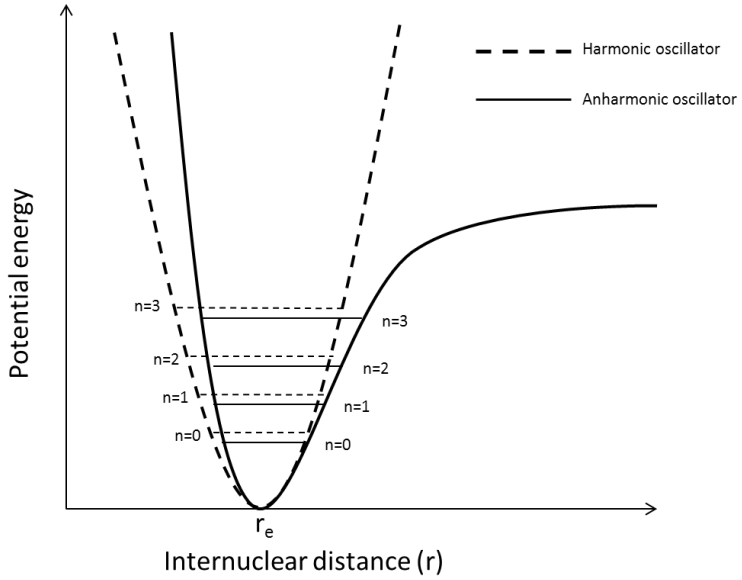

Fig. 2.1 Harmonic oscillator superimposed on the anharmonic oscillator (solid line) in a potential energy plot.

Assuming that the vibration of diatomic molecule is simple harmonic motion, we can get the vibration frequency ν is:

$$\nu = \frac{1}{2\pi}\sqrt{\frac{k}{\mu}} \qquad \text{Equation 2.4}$$

Where k is the bond force constant, μ is reduced mass, $\mu = m_1 * m_2 / (m_1+m_2)$, m_1 and m_2 are the mass of two atoms.

Defined by quantum mechanics, the solution to the Schrödinger equation for a particle confined within a simple harmonic potential well is a set of discrete allowed energy levels with equal intervals of energy between them, and the equation is:

$$E\Psi(x) = \frac{1}{2}kx^2\Psi(x) - \frac{\boldsymbol{h}^2}{2m}\frac{\partial^2\Psi}{\partial x^2} \qquad \text{Equation 2.5}$$

Where $\boldsymbol{h}$ = h /2 π, h is Planck's constant, ψ (x) is the vibrational wavefunction.

If taking the vibration of diatomic molecule as a simple harmonic motion, we could get:

$$E_n = h\,\nu(\mathrm{n} + \tfrac{1}{2}) \qquad \text{Equation 2.6}$$

Where h is Planck's constant, ν is the vibration frequency, n=0, 1, 2, 3…

The first important conclusion from this solution of a simple harmonic potential well is that the gap between adjacent energy levels is exactly the same:

$$\Delta E = E_{(n+1)} - E_n = h\nu \qquad \text{Equation 2.7}$$

And only one unit change in quantum number could be allowed for the particle in energy level.

$$\Delta n = \pm 1 \qquad \text{Equation 2.8}$$

What´s more, transition energy of the molecule is:

$$P_{n''\to n'} = \int \Psi^*_{n'} \varepsilon \Psi_{n''} d\tau \qquad \text{Equation 2.9}$$

Where $\Psi_{n'}$ and $\Psi_{n''}$ are two vibrational wavefunctions whose states are n´ and n´´, ε is dipole moment and it can be expressed as a linear function:

$$\varepsilon = \varepsilon_0 + (\frac{d\varepsilon}{dx})_e x \qquad \text{Equation 2.10}$$

Where x is the vibration displacement, ε_0 is the dipole moment of the equilibrium separation.

Therefore, transition will be allowed if P is not 0. This also means the ε can´t be 0. The dipole moment should change so that the transition could occur. At room temperature, the Boltzmann factor (kT) is around 200 cm^{-1}, so almost molecules are in the their vibrational ground state (n = 0). So only n=0→n=1 transition is allowed. This will cause MIR absorption but NIR spectroscopy would not exist.

2.1.1.2 Anharmonic oscillator

In fact, molecules are not ideal harmonic oscillator. First, the gap between adjacent energy levels is not the same. Secondly, overtone transition, such as n=0→n=2, 3, 4… are allowed. Thus the anharmonic oscillator is needed to explain this situation. Anharmonicity are generated by two reasons, one is mechanical anharmonicity and the other one is electrical anharmonicity. In the mechanical anharmonicity, there is a function to explain the potential energy well called Morse potential energy function:

$$V(r) = D_e(1 - e^{-\alpha(r-r_e)})^2 \qquad \text{Equation 2.11}$$

Where r is the distance between the atoms, r_e is the equilibrium bond distance, D_e is the well depth, and α controls the 'width' of the potential (the smaller α is, the larger the well).

The different between harmonic oscillator and anharmonic oscillator is that the gap between adjacent energy levels is no longer the same. The higher the energy level is, the lower the gap. In the electrical anharmonicity, the squared term and higher order terms are added into the dipole moment equation:

$$\varepsilon = \varepsilon_0 + (\frac{d\varepsilon}{dx})_e x + \frac{1}{2}\left(\frac{d^2\varepsilon}{dx^2}\right)x^2 + \cdots \qquad \text{Equation 2.12}$$

So the overtones transition energy of the molecule ($P_{n''\to n'}$) is not the integer multiples of the fundamental frequency, and it is lower than this. Above all, the overtone absorptions are the key absorptions of NIR spectrum. And they are caused by the anharmonicity of the chemical bonds[91].

2.1.2 Polyatomic molecules

One molecule which includes N atoms has 3N-6 degrees of freedom. In the case of the linear molecule, it has 3N-5 degrees of freedom. The degree of freedom determines the number of fundamental frequency vibrations. Supposing that the molecular vibrations of polyatomic molecules are harmonic oscillators, we can point out:

$$E_{(n_1+n_2+n_3\cdots+n_{(3n-6)})} = E_{(n_1)} + E_{(n_2)} + E_{(n_3)} \cdots + E_{(n_{(3n-6)})} \qquad \text{Equation 2.13}$$

However, if taking anharmonicity into account, we can find overtones and combinations of the fundamental molecular vibrations in the polyatomic molecules. But their absorptions are much weaker than the absorption of fundamental frequency. For polyatomic molecules, frequency of combination bands is possible. It is caused by exciting two or more different vibrations simultaneously, for example, the combination of fundamental and overtones. But, not any two vibrations in a molecule can produce a combination band. The vibrations must have the same symmetry. There are two more issues which affect the NIR spectra a lot, the Fermi resonance and Darling-Dennison resonance.

Fermi resonance can happen when the energy of a fundamental transition is similar with the energy of an overtone or combination transition in the same molecule. If Fermi resonance occurs, the intensities of the two bands will become very similar. Their frequencies will be more separated from each other which will result in two absorption peaks in the NIR spectrum. In fact, the intensity of overtone or combination mode will increase and the intensity of fundamental mode will decrease. Therefore, the Fermi resonance makes two bands have a more close intensity.

The effect of Darling-Dennison resonance is similar to Fermi resonance. But instead of fundamental transition, its interactions are between different overtone transitions in a same molecule. The interacting levels tend to stay at similar separation at each level of excitation. Thus, if the level of excitation increases, the vibrational levels will be more far away from their expected position. And the description of the levels becomes less accurate. As a result of these two resonances, there is a possibility of the presence of two peaks where only one is expected.

Above all, the characteristics of NIR spectra are[91], [92]:

a) The absorption of overtones, combination of fundamental and resonances are the main sources of NIR spectra. For the same molecule, the NIR absorption is much weaker than the MIR absorption.

b) The mostly observed absorption bands in NIR spectra are bands of X-H, such as C-H, N-H and O-H. The anharmonicity of X-H vibration is quite high, so its overtones and combination of fundamental have intensive absorbance in the NIR spectral region.

c) Hydrogen bond affects the NIR spectra significantly. The hydrogen bond has a stronger effect in the overtones and combinations than the fundamental. So the changes of solvents or temperature can cause the displacement of the absorption peaks.

d) Comparing to the MIR or Raman spectra, there is a heavy overlap of different absorption bands in NIR spectra. So it is hard to identify the peaks clearly.

e) The diffuse reflectance of NIRS includes physical information of sample so it is possible to perform the solid state analysis.

2.2 NIR Instruments

2.2.1 Development of NIR instruments

To understand the world is not the final aim, we also want to change the world even a little bit. Instruments are the tools which could help us to apply our understandings of the world into the reality. Therefore, in the section, the NIR instruments were introduced.

The earliest NIR instrument was a spectrograph which only pointed out the existence of NIR absorption but can´t qualify or quantify compounds. Before 1950s, researches had done plenty of works with the UV and MIR instruments, but NIRS was still only an extension of UV-Vis and had not been highlighted. The first transmission NIRS instrument was created by Kay at 1950. Mr. Karl Norris was the first person who applied NIRS into the analysis of agriculture and food products. He has designed a customized NIRS instrument in order to decrease noise in the spectrum in 1960s. In 1970, Illinois department of agriculture made a call for the production of NIR instruments which could analyze soybean moisture, protein and fat content. Diekey-John was the first company who produced the commercial NIR instruments. This instrument had a tungsten–halogen light, six interferometric filters and a PbS detector. Neotec company designed a NIRS instrument which had three rotary filters.

In 1970s, Technicon company and Diekey-John company produced a NIR instrument named Infra Analyzer 2.5. Later on, Neotec company produced Neotec 31EL. These products could control the running temperature and the optical components were sealed so that the instrument stability has increased. Meanwhile, the integrating sphere was used to analyze the sample´s integrated signal.

In early 1980s, the development of microprocessor promoted the stability and accuracy of NIR instrument, new systems like self-diagnostic system and automatic error correction system were installed. The GAC Ⅲ from Dickey-John, Infra Analyzer 400 from Technicon and Neotee 101 from Neotee were the most famous products at that time.

In late 1980s, high-resolution Fourier transform infrared spectrometer had emerged and the performance of grating spectrometer improved significantly. Companies started to develop customized instruments. During this period, the NIR instruments became mature.

In 1990s, acousto-optic tunable filter NIR spectrometer appeared and multi-channel detector performance was improved which brought down the price of the spectrometer. The application of optical fiber probe has added many new advantages to NIRS, for example remote online analysis.

In 2000s, the NIR chemical imaging (NIR-CI) spectrometer has been produced by some companies. The spatial and spectral information can be obtained together. Therefore, it has a high tolerance to variations in sample geometry. The push-broom scanning and staring imager method are two approaches which create the spectral hypercube.

In 21th century, the portable and minimized spectrometers are the current development trend. The minimization of instruments provides low cost and easy operation which could facilitate the on line application in the production line. MicroNIR from Viavi Solutions Inc.and Infratec Sofia from Foss are two famous types.

2.2.2 Core technology

In general, there are four systems in a NIR instrument[93],

a) Optical system
b) Mechanical system
c) Electronic system
d) Computer system

The computer system is to record, process and store data. Besides it also is an instrument control device. The electronic system consists of the light source power supply circuit, detector power supply circuit, signal amplification power supply circuit, analog-to-digital converter and the control circuit. The mechanical system includes the prime movers, transmission and executive system.

The key component is optical system which can be divided into four parts[93]. The light source, beam-splitting system, detector and accessories for analyzing sample.

2.2.2.1 Light source

The mostly used light source is the tungsten – halogen source in a quartz bulb containing an inert gas like krypton or xenon and a trace of a halogen such as bromine or iodine. This structure is cheap and has a long duration time if operated at appropriate filament temperature and lamp wattage. Normally power supply is around range 25–100 W and operation temperature is around 2000–3000 K. It could offer a continuous light from 320 nm-2500 nm. The position and the type of the quartz bulb may cause the Instabilities of the spectrum, so it is better to use the same mode from the same factory and install it in the fixed position. There is another light source, the light-emitting diodes (LED). It´s wavelength can be selected and the linearity is good.

2.2.2.2 Beam-splitting system

Beam-splitting system is the key of optical system whose function is to transfer the polychromatic light into the monochromatic light. It´s main characteristic of evaluation is the spectral resolution. The spectral resolution is defined as the capability to discriminate between two very close wavelengths.

$$R = \frac{\lambda}{\Delta\lambda} \qquad \text{Equation 2.14}$$

Where R is the spectral resolution, Δλ is the smallest difference in wavelengths that can be distinguished at a wavelength of λ.

However, the R is not the higher the better. Researcher needs to consider the detailed application. According to the position between the sample and the beam-splitting system, the spectrometer has two types. One is the sample stay before the beam-splitting system, and the other one is the sample stay after the beam-splitting system. Fig. 2.2 shows the two types,

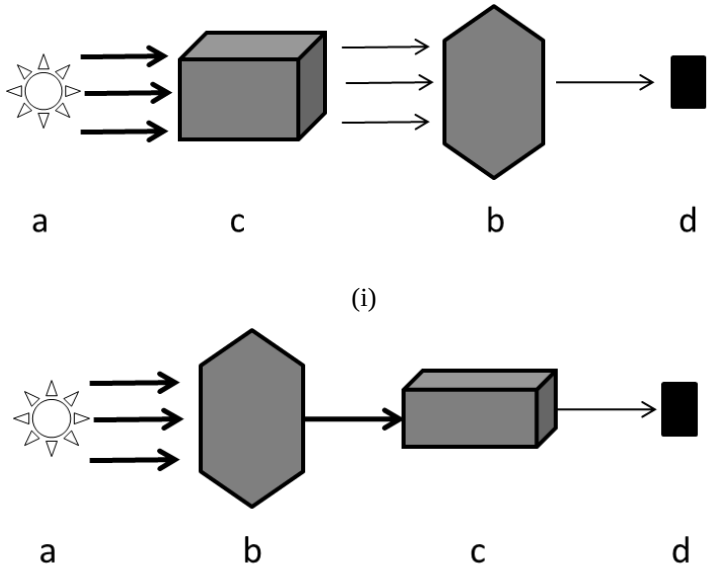

Fig. 2.2 Two types of spectrometer, a: light source, b: beam-splitting system, c: sample, d: detector

Generally, there are four typical beam-splitting systems for the commercial NIR spectrometer[94].

a) Filters
b) Dispersive grating

c) Acousto-Optic Tunable Filter (AOTF)
d) Fourier transform

The system which does not include movable component could be designed as the portable spectrometer.

2.2.2.2.1 Filters

The optical interference filter is based on the theory of thin film interference. The interference between incident and reflected light can give us the monochromatic light with a very narrow band whose half wavelength could be lower than 10 nm.

The typical filter spectrometer is rotary filter spectrometer. It contains several filters in a rotary wheel which could change the working filter according to specific case. Fig. 2.3 is the fixed filter

Fig. 2.3 Filters fixed in a rotary wheel

Besides, the Linear Variable Filter (LVF) has the same principle with the band-pass filter. The difference between LVF and ordinary band-pass filter is the film thickness of LVF varies linearly along the longitudinal direction of the substrate. So the LVF can make the center wavelength of passband vary linearly in the longitudinal direction. Fig. 2.4 shows the LVF structure[90]

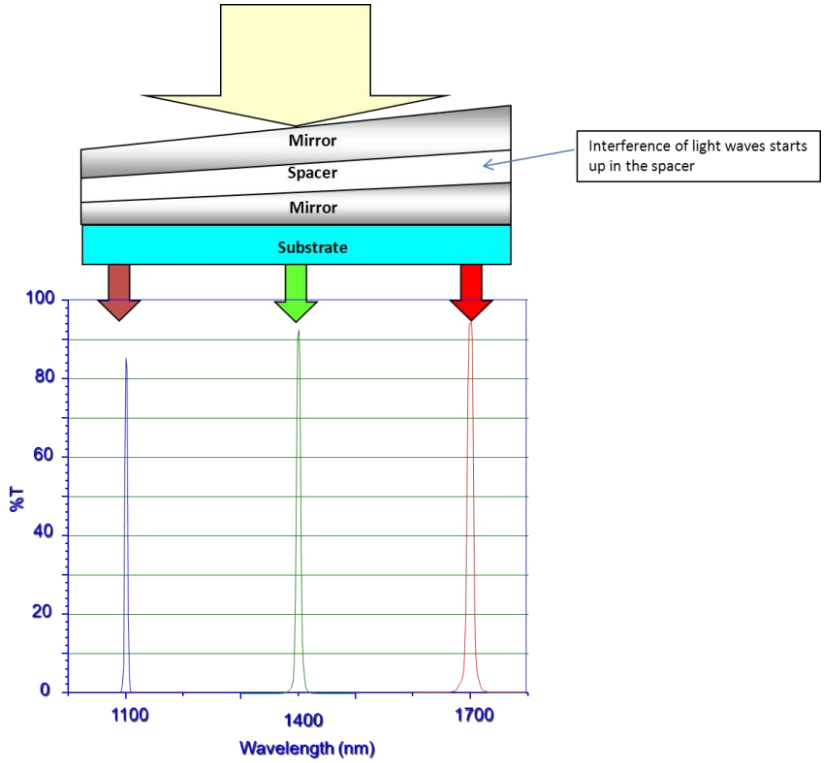

Fig. 2.4 LVF system

A single piece of substrate is separated into N*N blocks of small areas. Each small area of the surface is coated with a layer of film with different wavelength transmittance. So that a single piece of substrate is divided into an N-channel filter. If polychromatic light irradiates on the N-channel filter, N wavelengths of monochromatic light will be dispersed through the filter surface of the film. Because of the cumulative and linear change in film thickness of LVF, the film with different thickness can be transmitted selectively by different wavelengths of monochromatic light. And wavelengths of monochromatic light are proportional to the thickness of film. There are tilting filter and circular variable filter for the NIR spectrometer too. The advantages of filter spectrometer are fast, firm and suitable for portable instrument. However, the normal filters are only transparent to the short-wavelength region from 750 to 1200 nm.

2.2.2.2.2 The dispersive grating

Dispersive instruments equipped with one detector have some different types. Fig. 2.5 is the different dispersive grating types

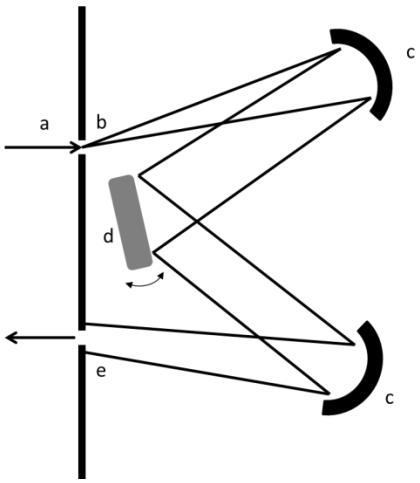

(A) Symmetric Czerny–Tuner

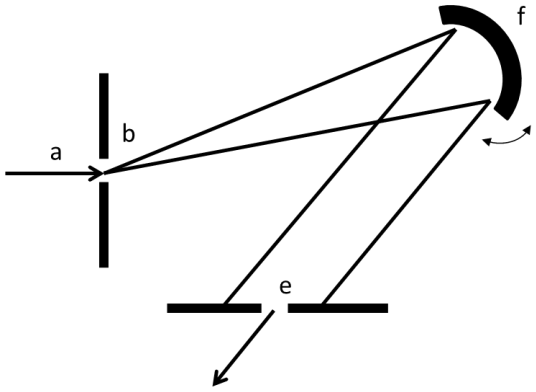

(B) System employing a concave dispersion grating

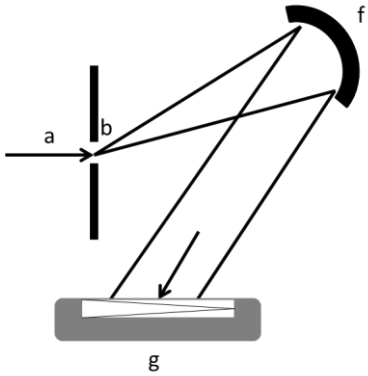

(C) System with linear detector array

Fig. 2.5 The dispersive grating, a: polychromatic NIR light source, b: entrance slit, c: concave mirror, d: planar grating, e: exit slit, f: concave grating, g: linear array of detectors

There are two dispersing elements, one is planar and the other one is concave. The planar grating could diffract reflection or transmission of radiation. And the reflection version is more conventional.

The surface of planar reflection grating, Fig (A), is carved by a high number of grooves which are covered by a thin film of aluminum or gold. The density of grooves is between 200 and 600 grooves/mm in NIR spectrometer.

The concave grating, Fig (B), is a kind of holographic grating which is made by interferometric lithographic or plasma etching technology. The density of grooves is between 150 and 3600 grooves/mm or much higher, so it is suitable for the high-resolution instruments. Actually, the concaved holographic grating is the most used grating in dispersive scanning instruments.

Linear detector array, Fig (C), is suitable for the system whose sample is placed before the grating. This means the light passes the sample first, and then goes to the fixed grating. The light which has

been dispersed focuses on the detector array finally. The detector for shortwave region is made by the Charge-Coupled Device (CCD) which is an integrated circuit etched onto a silicon surface forming light sensitive elements. And the detector for longwave light is made by PhotoDiode Array detector (PDA) with PbS or InGaAs.

What´s more, the Micro Electro Mechanical System (MEMS) scanning grating is a new technology in NIR spectrometer. It´s optical theory is similar with traditional scanning grating, but it is produced by the MEMS technology. The advantages of MEMS are millimeter scale, light, low power consumption, durable and low cost.

2.2.2.2.3 AOTF

AOTF device is based on the acousto-optical diffraction theory. It consists of birefringent crystal lattice, Radio Frequency (RF) radiation source, electroacoustic transducer and acoustic absorber. The crystal usually is tellurium oxide (TeO_2) which has a wide transparency between 370 nm and 3500 nm. The radio frequency radiation source offers the high frequency radiation which could be changed. The electroacoustic transducer could transfer the high frequency electric signal into ultrasonic vibration inside the crystal. And the acoustic absorber absorbs the acoustic waves which have gone through the crystal.

The polychromatic light goes to the crystal with a fix angle and interacts with the acoustic wave generated by RF source. Then, the incident light is diffracted into two polarized monochromatic beams and a no diffracted beams. The λ of two diffracted beams is related to the frequency of the acoustic wave. When the frequency of the ultrasonic wave changes continuously, the λ of the diffracted beam will change too. Thus the incident light could be dispersed into a monochromatic beam. Fig. 2.6 shows the AOTF principle

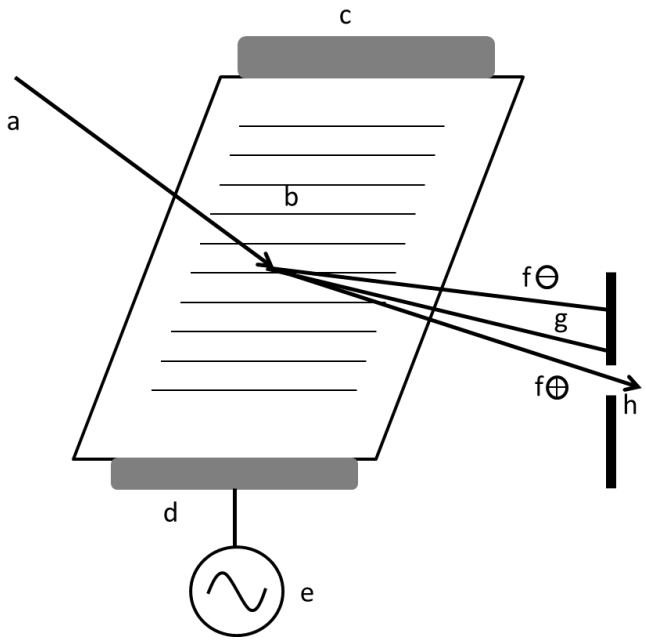

Fig. 2.6 the AOTF principle, a: polychromatic NIR radiation, b: TeO_2 crystal, c: acoustic absorber, d: electroacoustic transducer, e: rf source, f: diffracted monochromatic beams which have been orthogonally polarized, g: no diffracted beams and h: exit slit.

Practically, the AOTF devices have a tuning bandwidth from 900–1800 nm, 1000–2000 nm or 1200–2400 nm. Because the wavelength range is limited both by the detector range which is normally a thermo - electrically cooled InGaAs detector and the frequency drive range of the RF oscillator.

The scan speed of AOTF is very fast and wavelength could be selected by programming the RF driver frequency. Besides, it´s size is small and is a solid-state device without moving parts.

2.2.2.2.4 Fourier transform

Instead of wavelength selection, Fourier transform NIR spectrometers provide a method to encode wavelength. Thus, a single detector is enough to measure all transmitted wavelengths. The key component is the Michelson interferometer, it´s structure is shown in Fig. 2.7

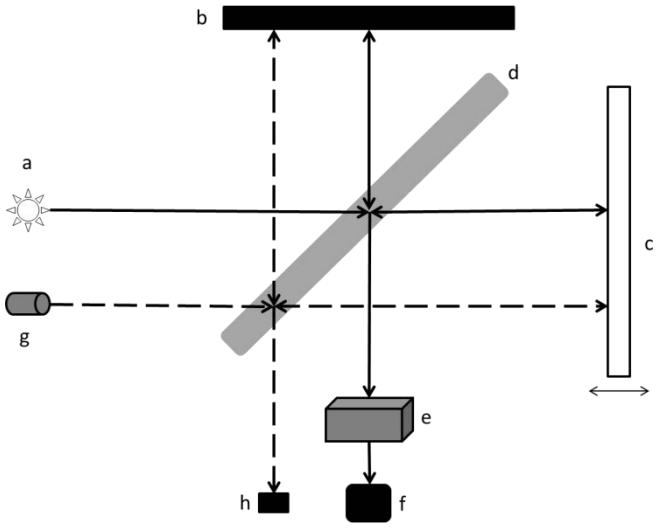

Fig. 2.7 Fourier transform principle, a: polychromatic radiation source, b: fixed mirror, c: moving mirror, d: beam splitter, e: sample, f: detector, g: laser and h: photodiode.

The polychromatic incident light is divided by the beam splitter into two beams. One goes to the fixed mirror and the other one goes to the moving mirror. After reflecting, these two beams recombine at the beam splitter position which could cause a constructive interference in all wavelengths. When the moving mirror retards, the intensity of the interference light will increase or decrease according to the relative position of peaks in these two coherent light. For example, if the incident light is a monochromatic light, we can get a cosine interferogram. In order to recover the intensities at each frequency (or wavelength), the Fourier transform is applied to the interferogram. Finally, a whole range spectrum will be plotted by the computer. The laser could offer a standard cosine interferogram which determine the time to acquire the sample interferogram. The laser signal is detected by a photodiode.

Except the classical Michelson interferometer, more types of interferometers have been designed to get better mechanical tolerance and higher robustness. The wedge polarization interferometer, Fig. 2.8, *wish-bone* version interferometer, Fig. 2.9, and encode photometric interferometer, Fig. 2.10, are two representatives[93], [94].

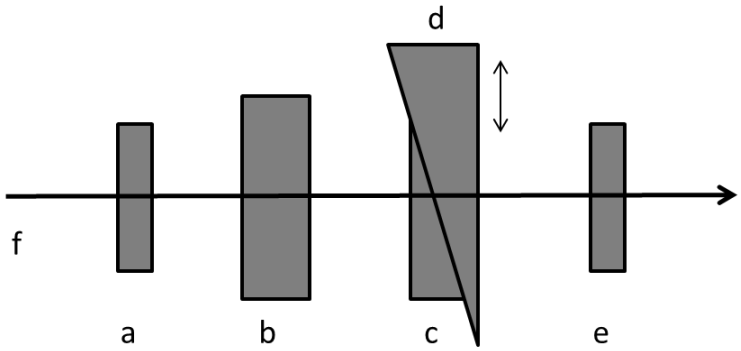

Fig. 2.8 Polarization interferometer, a: polarizer (+45°), b: compensating crystal, c: fixed crystal wedge, d: moving crystal wedge, e: analyzer (−45°), f: polychromatic light

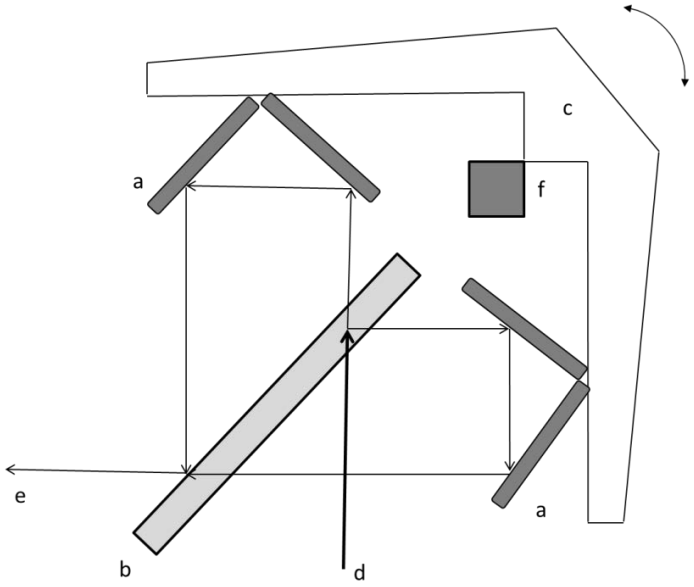

Fig. 2.9 Wish-bone interferometer, a: cube-corner reflectors, b: beam splitter, c: rotating arm, d: polychromatic light, e: interference light and f: pivot.

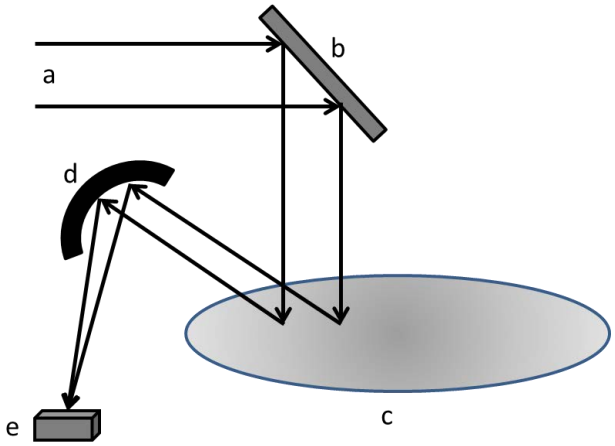

Fig. 2.10 Encode-photometric interferometer, a: polychromatic light, b: dispersion grating, c: encoding disc, d: focusing mirror and e: detector

In the polarization interferometer, polychromatic light passes a polarizer and changes into polarized light, then the distortions of the polarized beam is corrected by a compensating crystal. The corrected beam is divided into two beams in the fix crystal wedge and then the retard is caused by the continuous movement of the moving crystal wedge. Later, in the analyzer, the interference light can be formed.

In the *wish-bone* interferometer, the polychromatic light is divided be the beam splitter, and then the movement of the rotating arm causes the Optical Path Difference (OPD) between beams. Finally, the interference light comes out from another part of the beam splitter.

In the encode-photometric interferometer, a rotating disk is encoded by the lithographic way in a circumferential sinusoidal pattern. The polychromatic light is dispersed by the grating and then goes to the disc. All wavelengths are encoded with a sinusoidal amplitude modulation and they can be recovered by a FT transform.

So far, the conventional beam-splitting systems have been introduced already. Besides, there are Hadamard transform, MEMS active grating and Fabry-Perot interferometer. They are not explained in detail here.

2.2.2.3 Detectors

The function of the detector is to transfer the light signals into the electric signals, and these electric signals are output by the analog-to-digital converter.

The classical detector is made of a PbS semiconductor which is suitable for the scanning grating monochromator. A semiconductor could be sensitive to photons whose energy exceeding its bandgap. In another word, the detecting limitation will be shorter than the cutoff wavelength related to the semiconductor bandgap. It could detect the whole NIR range, even exceeding the typical NIR spectral region. But its linearity and response speed is low[94].

The InGaAs detector is a photodiode device which is very linear, fast and sensitive, so it has been widely applied in some instruments that need a rapid and precise detector. It is an alloy semiconductor and the alloy composition can be adjusted, thus the band gap can be varied for different wavelength cutoffs according the composition.

Array detector is fit for the rear splitting type. There are two parts in the detector, one is made of Silicon CCD for the shortwave region and the other one is made of PDA with PbS or InGaAs for the longwave region. Focal plane array (FPA) detector is one type of array detector applied with the NIR-

CI spectrometer. It is placed on the focal plane of the optical system and creates a hypercube. Horizontal pixels, vertical pixels, and pixel size are key parameters of the focal plane array.

2.2.3 Accessories for analyzing sample

One of the most important advantages of NIRS is that NIR spectra can be obtained without sample preparation. Therefore, accessories which could be applied directly with various types of measurement like transmittance, reflectance and transflectance, process monitoring modes like at-, on-, and in-line, physical states like solid, liquid and gas, sample properties like viscosity, homogeneity, particle size and process types like batch and continuous are designed.

In this part, the principles of accessories for measuring liquid, solid and gas were introduced. What´s more, three typical interfaces, the flow cells, the fast loop and the fiber optics probes were discussed.

2.2.3.1 Liquid and gas samples

For the liquid and gas, the measurements are normally transmittance or transflectance. So the base of their absorption spectra is the Beer-Lambert law, which can be defined as[91]:

$$A = \lg\frac{I_0}{I_t} = \lg\frac{1}{T} = \varepsilon lc \qquad \text{Equation 2.15}$$

Where A is the absorbance, I_0 is incident intensity, I_t is transmitted intensity, T is transmission coefficient, ε is molar absorptivity, l is length of the light path and c is concentration.

The light path length in the liquid sample needs to be assessed. The absorbance of liquid samples at different wavelengths varies a lot (maybe several times difference). In order to get best spectrum at the target wavelength, the best path length should be chosen. The absorbance of liquid samples is quite sensitive to the temperature. The lower temperature could suppress volatilization or degradation. But the low temperature may cause the freezing process.

Accessories for the liquid samples are normally made by BK7 glass, quartz and fused silica.

The gas samples need a large volume cell which could offer a long light path length. In some case, the length changes from 1- 100 meters. This is because the gas concentration is much lower than liquid. Besides, the gas samples are very to the temperature too.

2.2.3.2 Solid samples

For the solid, there are also transmittance, reflectance and transflectance[91], [93], [94]. But diffuse reflectance is a main interaction which provides both physical and chemical information.

The concentration of samples could be explained by the Kubelka–Munk equation:

$$F(R_\infty) = \frac{(1-R_\infty)^2}{2R_\infty} = \frac{K}{S} \qquad \text{Equation 2.16}$$

Where R_∞ means the relative diffuse reflectance when the sample is infinitely thick, K is K-M absorption coefficient and S is K-M scattering coefficient.

When the concentration is not too high, the K is proportional to the concentration (c), so the equation could be:

$$F(R_\infty) = \frac{K}{S} = \frac{bc}{S} = b'c \qquad \text{Equation 2.17}$$

The b´ is related to the K and S.

From the K-M equation, it seems the linearity of diffuse reflectance exists in a multi-component system. However, the diffuse reflectance doesn´t have additivity. This non-linear problem could be solved by the chemometrics method.

Accessories for the solid sample have several modes, one is that the incident monochromatic light irradiates onto the sample surface vertically and the detectors which are geometrically arranged receive the reflected light at the 45 degree. The best distance between sample and the instrument window should be evaluated. Another one is to use the integration sphere, see Fig. 2.11

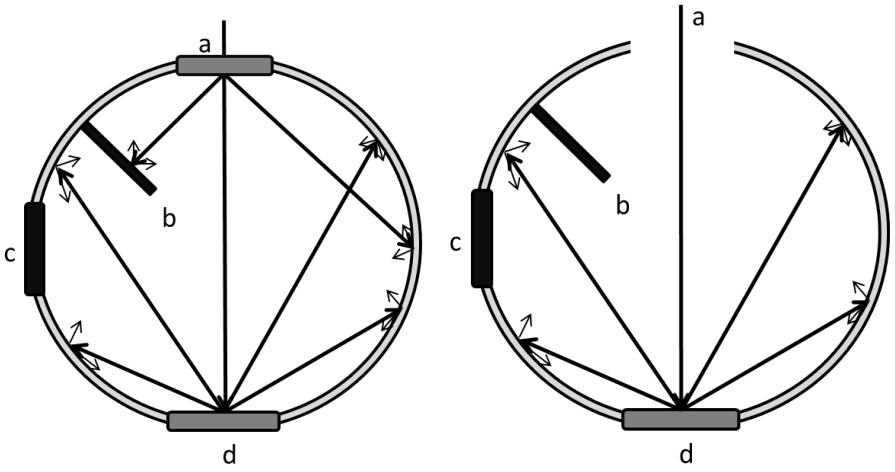

Fig. 2.11 (i) is the integration sphere for measuring transmittance, a: Sample holder, b: baffle, c: detector, d: standard reference. (ii) is the integration sphere for measuring reflectance, a: incident light, b: baffle, c: detector, d: sample holder.

The sample and the detector are placed with a 90 degree angle. The incident light firstly transmits or reflects from the solid sample which contacts the measurement window of the integration sphere. Then the diffused light is integrated by reflecting on the internal white surface of the sphere before reaching the detector. By this way, the geometrical effects of the reflectance can be removed, so the Signal to Noise Ratio (SNR) and repeatability are improved.

2.2.3.3 Typical interfaces

Flow cell, see Fig. 2.12, means that the sample could pass a cell whose optical path length is fixed successively. It cancels the noise caused by the changing of the cell and provides an opportunity of automate sampling and data acquisition. In practical, the flow cell must avoid generating air bubbles in the optical path or reacting with the sample.

Fig. 2.12 Flow cell

The fast loop interface, see Fig. 2.13, collects samples from a point of continuous production line and pumps them to a shelter at a high flow rate. A NIRS analyzer is equipped in the shelter where the analyzing environment is well controlled. Normally, the shelter is placed a few meters away from the sample collection point, in order to supply a safe space for analysis.

Samples which have been analyzed are sent back to the production line. The fast loop interface offers an independent space to carry out the analysis, thus temperature and pressure of samples could be adequately changed. Even samples ask for a chemical or physical pretreatment, it can be automatically carried out without disturbing the process.

Fig. 2.13 Fast loop interface

Fiber optics probe[94], see Fig. 2.14, is composed by two parts, the optical fiber and the probe. The optical fiber is made of two sections which are called the core and the cladding. These two sections should have different refractive indices. The core needs a higher refractive index and the cladding is lower. By this way, the total reflection can appear at the interface of these two sections when the incident light travels inside the fiber.

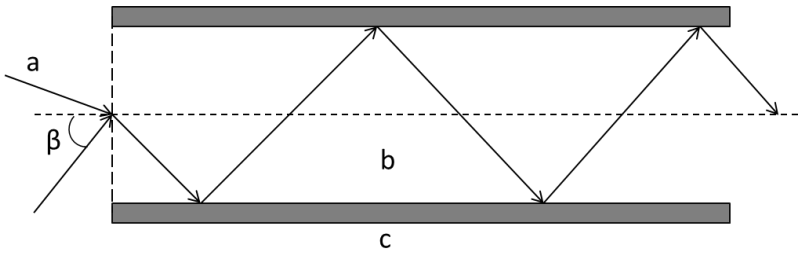

Fig. 2.14 Fiber optics probe, a: incident light, b: core with higher reflective indices, c: cladding with lower reflective indices, β: the acceptance angle of total reflection.

The composition of the optical fiber should contain low number of O-H or C-H bands, because they have a strong absorption of NIR beams. Usually, the NIR beams could travel in a nonlinear optical fiber from 10-100meters without much loss of intensity.

Most probes, see Fig. 2.15, are made of stainless steel, so that they can bear the tough environment in a process stream. The probe window needs to be often cleaned and the reference spectrum has to be renewed regularly, thus the probe should be able to be taken out from the machine easily. There are three acquisition modes for the probe, transmittance, reflectance, or transflectance. In order to collect beams efficiently, probe could be coupled with an N*M fiber bundles. N bundles of source fibers which send the incident beams to the sample. And M bundles of detector bundles which collect the beams from the sample.

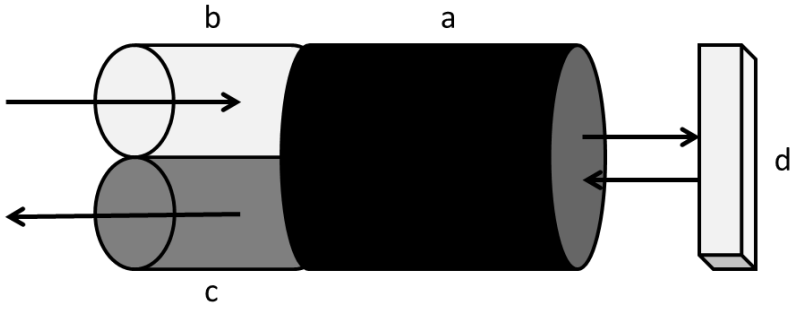

Fig. 2.15 Probe, a: probe, b: source fibers, c: detector fibers, d: sample

So far, the basic theories of NIR spectrometers have been explained except the near infrared chemical imaging (NIR-CI) type. The spectrum of the NIR-CI is an average spectrum which is acquired by scanning every spatial point of the sample with the whole wavelength range. It is a 3D data matrix which consists of a 2D space and a 1D wavelength, called hypercube. The hypercube also could be taken as a series of pixels or image planes. In this thesis, it was not discussed.

2.2.4 Commercial instruments

Right now the applications of NIRS have appeared in a lot of fields, such as agriculture, petrochemical, pharmaceutical, food and clinic. Instruments of different applications can be designed as the bench top or portable spectrometer.

2.2.4.1 Benchtop NIR spectrometers

The basic design of a NIR spectrometer is benchtop, because the optical system needs a stable running condition. All optical systems that mentioned above could be applied as bench top. The Foss, Bruker, Buchi, ThermoFisher are some companies who produce bench top instrument. They have two types, the dedicated and the universal instruments.

The universal spectrometer has wide spectral range, high resolution, high SNR and their accessories could offer the measurements of transmittance, reflectance and transflectance.

The XDS™ Rapid Content Analyzer of FOSS could analyze solid, viscous and liquid samples. It is dispersive grating and provides a full spectrum from 400 to 2500 nm. The MPA of Bruker could analyze food, feed, pharmaceutical, cosmetics and chemicals. It is a FT-NIR spectrometer whose range is from 12800-3600 cm^{-1}. The NIRFlex N-500 of Buchi could analyze powder, tablet, granule, paste, liquid and so on. It is a FT-NIR spectrometer which provides a range from 800 to 2500 nm. Antaris™ II of ThermoFisher could analyze solids, paste, gel, syrup, films, liquids and so on. It is a FT-NIR whose spectral range is from 833 to 2630nm. Fig. 2.16 is the benchtop spectrometers

Fig. 2.16 Bench top spectrometers

The dedicated spectrometer means that a shorter wavelength range is selected to address specific applications. These so-called dedicated instruments only have few wavelengths which represent the

characteristic peaks of samples. Typically, the dedicated instruments contain filters or LED, so the size can be reduced. If equipped with batteries, they will become portable. There are dedicated spectrometers now in several analytical fields, such as cereals analysis, meat analysis, milk analysis and fruit analysis. Table 2.1 shows some bench top spectrometer in the market

Table 2.1 Bench top spectrometers of different companies

Company	Name	Type	Wavelength range
Foss	XDS Rapid Content Analyzer™	Dispersive grating	400-2500nm
Bruker	MPA	FT	12800-3600cm^{-1} (781-2777 nm)
Buchi	N-500 FT-NIR	FT	800-2500nm
ThermoFisher	Antaris™ II	FT	833-2630nm
Perten	DA 7250 NIR analyzer	Diode array detector	950-1650nm
Perkinelmer	Frontier NIR Reflectance System	FT	700-2500nm
ABB	MB3600	FT	11,000-3,900cm^{-1} (909-2564nm)
ASD	LabSpec 4 Bench Benchtop Analyzer	Silicon array detector	350-2500nm
Unity Scientific	2600 XT-R	Predispersive scanning monochromator	680-2600nm

2.2.4.2 Portable NIR spectrometers

Comparing to the bench top instrument, the portable NIR spectrometer is much smaller, lighter and more robust[93].

One of the most important requirements of the portable instrument is that the optical system should be stable or robust. Because the optical structure is precise, the frequent movement of the instrument has a significant affect to its moveable parts. Optical systems like filter, AOTF, fixed grating and MEMS grating are options for portable spectrometer. Their systems are solid-state, knocking or shaking movements can´t disturb the optical structure. Besides, the size and weight of the instrument have to be designed as little as possible, so that it can be carried by one person. Taking the MEMS as an example Fig. 2.17, the MEMS chip consists of an array of micro mirrors which can be controlled by a program of the control circuit. These mirrors may change their position by installing a new program.

With the position changing, the blaze angle and grating pitch of the MEMS chip could be controlled. Therefore, the expected diffraction spectrum can be acquired by the detector. Because the displacements of mirrors are determined by the voltage, around in 500ms, a high quality spectrum could be acquired.

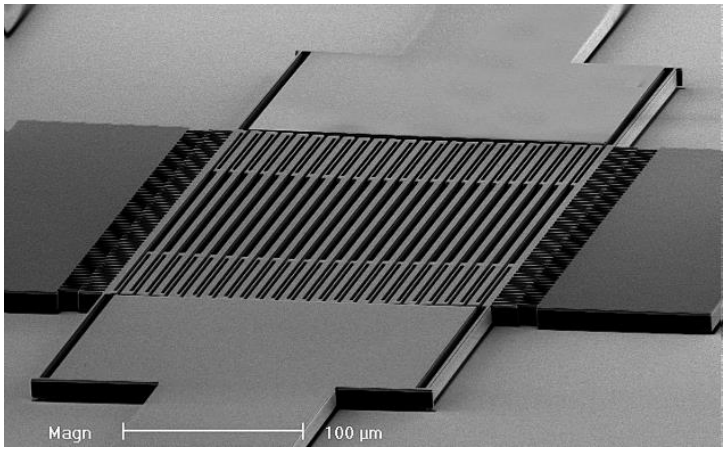

Fig. 2.17 MEMS chip

The micro NIR with a LVF Fig. 2.18 is another representative of portable NIR spectrometer. The LVF is a bandpass filter coating that intentionally wedged in one direction, the wavelength transmitted through the filter will vary in a linear fashion in the direction of the wedge. Therefore, it can provide a spectral range from 600-2200 nm. What's more, the miniaturization and portability of the NIRS instrument are very important for on line application. The LVF is tiny and does not need to work with a large laser light source, so the size of the instrument will be reduced significantly. And the spectrum generated by the LVF can be transferred to a tablet computer by USB interface, thus the instrument is portable.

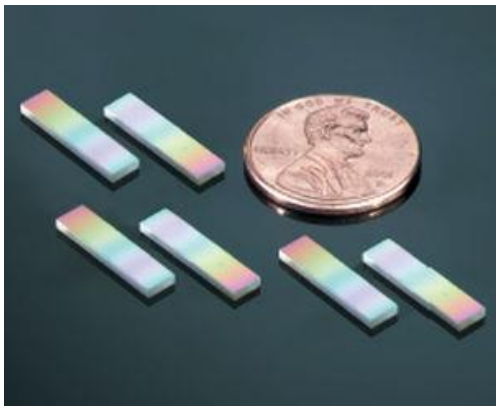

Fig. 2.18 LVF

AOTF based instruments which have been discussed above are suitable for the portable design too. Because their optical system do not have moveable component and the size of crystal is small. Its wavelength could span the whole NIRS region or just scan a specific band.

In Table 2.2 and Fig. 2.19, there are some commercial portable instruments.

Table 2.2 Portable NIR instruments

Company	Name	Wavelength range
Thermo	microPHAZIR RX	1600-2400nm
ASD	Analytik	350-2500nm
Viavisolutions	MicroNIR	950–1650nm
Ocean Optics	USB4000-VIS-NIR	350-1000nm

a) MicroPHAZIR RX b) Analytik c) MicroNIR d) USB4000-VIS-NIR

Fig. 2.19 Portable NIR instruments

In this thesis, the NIR spectrometers from FOSS and Viavisolutions were used to acquire spectra. The rapid content analyser and probe odes of FOSS were applied for the food quality improvement. And the MicroNIR of Viavisolutions was focused on the pharmaceutical products.

Chapter 3

Chemometrics in NIRS

3. Chemometrics in NIRS

3.1 History

``The art and science of extracting useful information from chemical data´´ is the most casual way to explain what is chemometrics[95]. In European pharmacopoeia, the definition of chemometrics is the chemical discipline that uses mathematical and statistical methods, a) to design or select optimal measurement procedures and experiments, and b) to provide maximum chemical information by analyzing chemical data[96].

Chemometrics was born in 1970s. Prof. S Wold named one of his projects as chemometrics in 1971. In 1974, the International Chemometrics Society (ICS) was founded by Prof. S Wold and Prof. B R Kowalski in Seattle, USA. At the beginning, the chemometrics only included some classical statistics method like Principal Component Analysis (PCA) for deconvolution of speak overlapping, Partial Least Squares (PLS) for multivariate calibration at reduced rank and derivative for increasing the spectrum resolution.

In 1980s, the development of computer science and the analysis instrument have supported the application of chemometrics. The theory and algorithm have been improved significantly which offered a firm foundation for the application of chemometrics. Journal of Chemometrics (1987, Wiley) and Chemometrics, Intelligence Laboratory Systems (1988, Elsevier) together with some classical chemometrics books were published during this period.

In 1990s, it became common that the modern analysis instruments were equipped with a computer which was installed with the chemometrics software. The chemometrics was applied in many fields such as NIRS, pharmacy and biomedical research. Chemists started to use some methods which combined modern mathematics with computer science together, such as Artificial Neural Networks (ANN), Wavelet Transform (WT) and Support Vector Machines (SVM).

Nowadays, under the concept of industry 4.0, the chemometrics has shown an advantage in virtualization and real time analysis. Since the world around us is inherently multivariate, the univariate analysis can´t extract the hidden information. It makes sense to apply multiple measurements, for example PLS, in data analysis procedure.

3.2 Pre-processing

Raw spectra include not only the useful chemical or physical information, but also some noise and irrelevant information. Before modeling, it is necessary to pre-process the raw spectra in order to improve the extraction of physical and chemical information. Pre-processing methods have five types, Offsetting, variable-wise scaling, filtering, sample-wise scaling and compression[94]. Fig. 3.1 is the plot of pre-processing methods

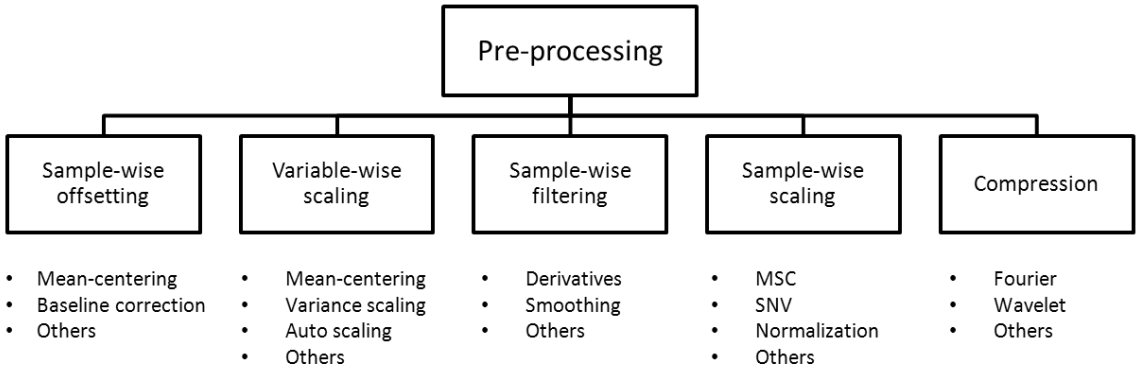

Fig. 3.1 The classification of pre-processing in chemometrics

3.2.1 Mean centering

The mean-centering pre-processing has two forms, one is variable-wise which is performed by subtracting the average spectrum from each individual sample spectrum, and the other one is sample-wise which is performed by subtracting the average absorbance value from each individual wavelength number. It is the mostly used method before modeling, because it could increase difference between samples. It can be explained as:

$$a_{ij}^{*} = a_{ij} - \frac{1}{n}\sum_{i=1}^{n} a_{ij} \qquad \text{Equation 3.1}$$

Where a_{ij}^{*} is the pre-processed data matrix, a_{ij} is the raw sample matrix, n is the total sample number (sample wise) or the total wavelength number (variable wise), and j is wavelength point. Fig.3.2 shows the difference, the variation in the preprocessed spectra has been enlarged and the signal intensity stayed in the same scale.

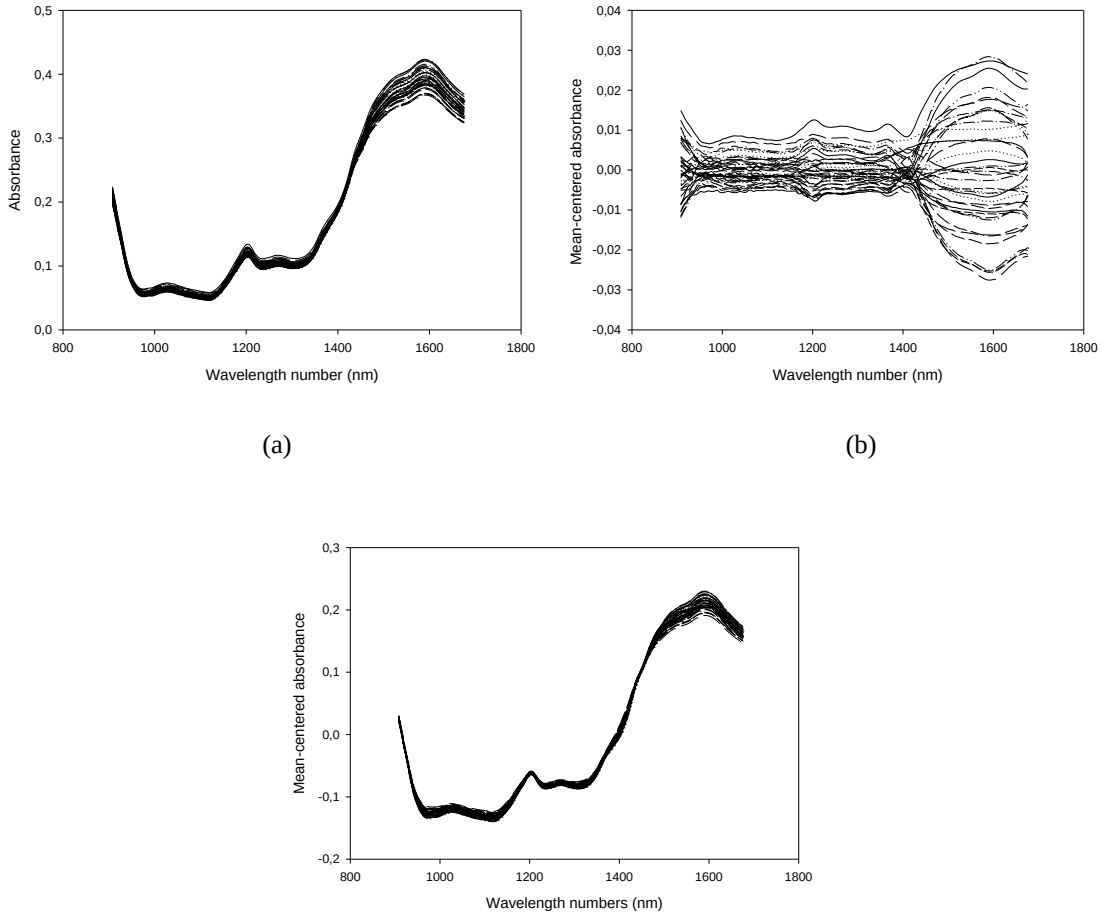

Fig. 3.2 (a is the original spectra without mean centering, (b) is the spectra after mean centering (variable-wise) and (c) is the spectra after mean centering (sample-wise)

3.2.2 Baseline correction

Baseline correction is a series of methods which subtract a baseline component from an individual sample spectrum, such as offset correction, linear, quadratic and user-defined correction. The equation is:

$$a_{ij}^{*} = a_{ij} - d_{ij} * k \qquad \text{Equation 3.2}$$

Where a_{ij}^{*} is the preprocessed spectrum, a_{ij} is the raw spectrum, d_{ij} is the baseline component and the k is a constant. Fig. 3.3 shows the difference, the lowest value of preprocessed spectra is around 0 and the signal intensity had the same scale.

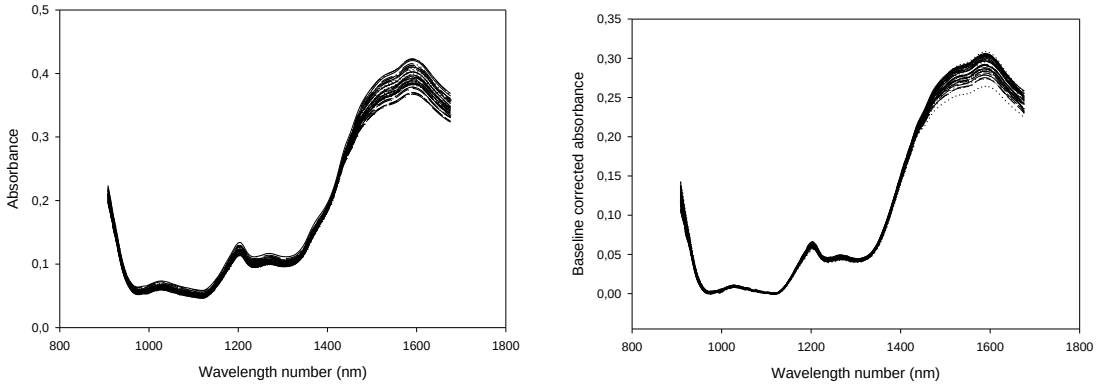

(a) (b)

Fig. 3.3 (a) is the original spectra and (b) is the spectra after offset baseline correction.

3.2.3 Variance scaling

The variable wise scaling gives equal weighting to all the spectral data vectors. The sum of the squared values for each column equals is 1 and the mean values is 0. The functions of autoscaling are:

$$\bar{a}_j = \frac{\sum_{i=1}^{n} a_{ij}}{n} \qquad \text{Equation 3.3}$$

$$s_j = \sqrt{\frac{\sum_{i=1}^{n} (a_{ij} - \bar{a}_j)^2}{n-1}} \qquad \text{Equation 3.4}$$

$$a_{ij}^{*} = \frac{a_{ij} - \bar{a}_j}{s_j} \qquad \text{Equation 3.5}$$

Where s_j is standard deviation of spectral vector, a_{ij}^{*} is the pre-processed data matrix and $\bar{a}_j$ is the average spectral vector of calibration sample.

Variance scaling is usually used when the magnitude of signals or the S/N varies considerably from each wavelength point. Fig. 3.4 shows the difference, in the preprocessed spectra, the signal intensity of each individual wavelength point has similar scale.

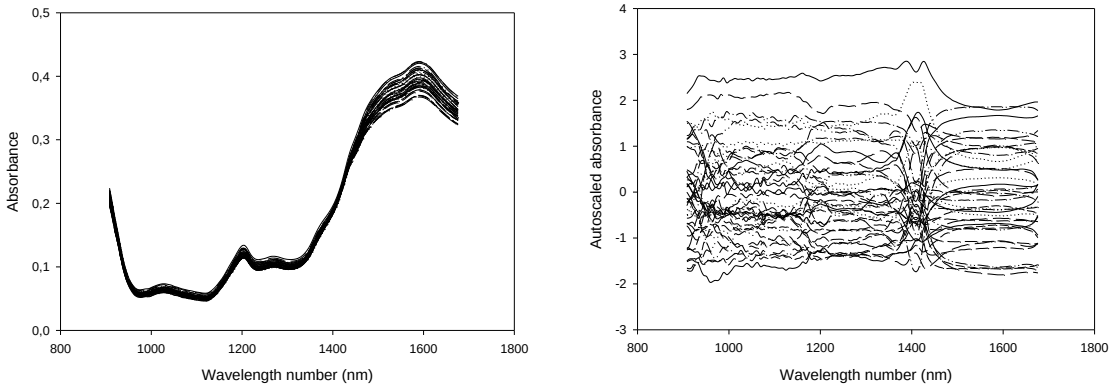

(a) (b)

Fig. 3.4 (a) is the original spectra and (b) is the spectra after autoscaling.

3.2.4 Smoothing

Noise is the information which may result in errors in the calibration and smoothing methods are able to decrease the noise and increase S/N. But strong smoothing could reduce the resolution of the spectrum too. Two smoothing methods are introduced here.

3.2.4.1 Moving average

Moving average is calculated by a running average for a narrow window of points. The average values from the window form the new spectrum. The equation is:

$$a_k = \bar{a}_k = \frac{\sum_{i=-w}^{+w} x_{k+i}}{2w+1} \qquad \text{Equation 3.6}$$

Where a_k is the pre-processed data matrix, the moving window size are 2w+1 points, k is the center point.

The size of the window is an important factor, because a large window size may low down the resolution and a small window size could not decrease the noise.

This causes problems at the endpoints of the curve, and numerous authors have described different methods for treating them.

3.2.4.2 Savitzky-Golay smoothing (SG smoothing)

The polynomial smoothing is the most commonly used method in practice, also called SG smoothing which are names of two authors of this method. The equations are:

$$a_k = \bar{a}_k = \frac{\sum_{i=-w}^{+w} x_{k+i} h_i}{H} \quad \text{Equation 3.7}$$

$$H = \sum_{i=-w}^{+w} h_i \quad \text{Equation 3.8}$$

Where a_k is the pre-processed data matrix, the sliding window size are 2w+1 points, k is the center point, H is the normalization factor and h_i is the smoothing factor. Fig. 3.5 shows the difference, the preprocessed spectra are smoother than the original spectra.

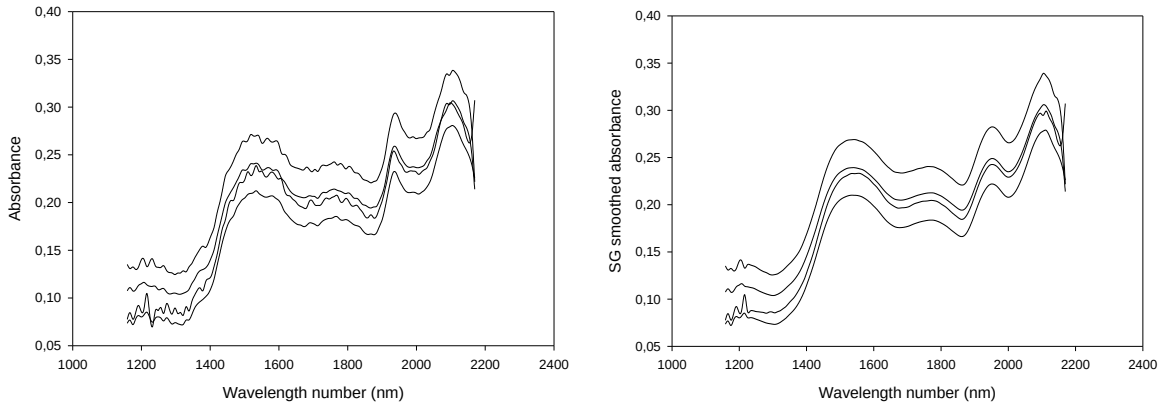

(a) (b)

Fig. 3.5 (a) is the raw spectra and (b) is the pre-processed spectra with SG smoothing

The width of the window and degree of the fitted polynomial function are two parameters which control the smoothing degree. Bigger window size gives stronger smoothing. And higher polynomial degree calculates more complex curves which could be fitted to the data.

3.2.5 Derivative

The derivative removes the baseline offsets, because the derivative of a constant is zero. Besides, it could be a high-pass filter which could narrow and sharp the absorption peaks. The resolution could

be increased and the baseline shifting could be removed. However, it could decrease the S/N too. Generally, there are two ways to calculate derivative.

3.2.5.1 Direct derivative transformation

This is the simplest method to do the derivative, the equations are:

1st derivative: $a_k = \frac{a_{k+g} - a_{k-g}}{g}$ Equation 3.9

2nd derivative: $a_k = \frac{a_{k+g} - 2a_k + a_{k-g}}{g^2}$ Equation 3.10

Where a_k is the pre-processed data matrix, k is the wavelength number and the g is the gap size.

3.2.5.2 Norris gap derivative

Before derivative, Prof. Norris applied the moving average first to the raw spectrum. The moving window size are 7 points, and the gap size are 3 points. By this way, the noise from the transform could be reduced. For example, the Norris 1st derivative could be explained as:

$$a_k = \bar{a}_k = \frac{\sum_{i=-3}^{+3} x_{k+i}}{7}$$ Equation 3.11

$$a_w = \frac{a_{w+3} - a_{w-3}}{3}$$ Equation 3.12

Where a_k is the pre-processed data matrix, k is the center point, w is the wavelength number.

3.2.5.3 Savitzky-Golay derivative (SG derivative)

Usually, the derivative method needs to be calculated with polynomial smoothing, because it may have a lower offset. The SG derivative means that the SG smoothing is used before derivative. By this way, the noise introduced by derivative could be lower. Fig. 3.6 shows the difference, the preprocessed spectra have more peaks and the baseline has been corrected.

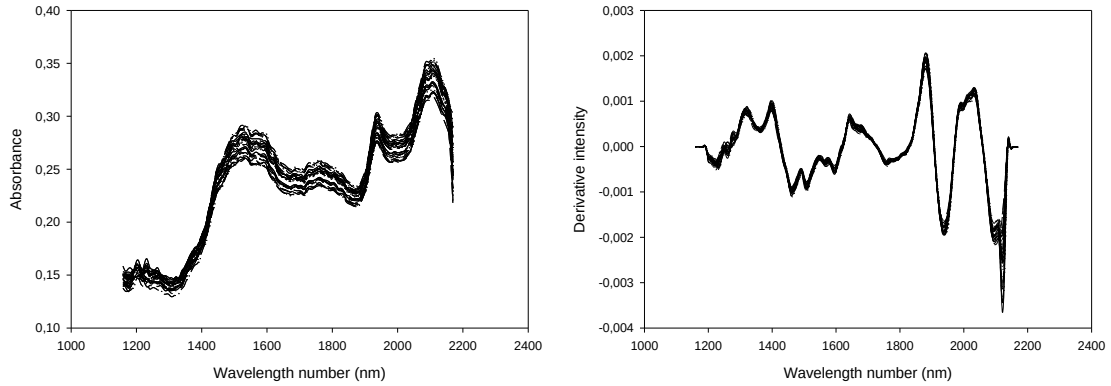

(a) (b)

Fig. 3.6 (a) is the raw spectra and (b) is the pre-processed spectra with SG 1st derivative

3.2.6 Standard Normal Variate transformation (SNV)

In the solid samples, the diffused reflection light of NIR is affected by the irregular particle shapes. Particles with a small size distribution tend to get larger baseline offsets in the spectra. And the path length also changes the peaks in the spectrum. In order to reduce these effects, sample wise SNV is used. It can be explained as:

$$\bar{a}_i = \frac{\sum_{j=1}^{n} a_{ij}}{n} \qquad \text{Equation 3.13}$$

$$S_i = \sqrt{\frac{\sum_{j=1}^{n} (a_{ij} - \bar{a}_i)^2}{n-1}} \qquad \text{Equation 3.14}$$

$$a_{ij}^{*} = \frac{a_{ij} - \bar{a}_i}{S_i} \qquad \text{Equation 3.15}$$

Where a_{ij}^{*} is the pre-processed data matrix, S_i is the standard deviation of spectral data, $\bar{a}_i$ is the average spectral vector and n is the wavelength number.

The average spectral vector is a mean of the variables in a single spectrum, not a mean of several spectra. Fig. 3.7 shows the difference, the baseline shift which is caused by the particle size or optical path has been corrected.

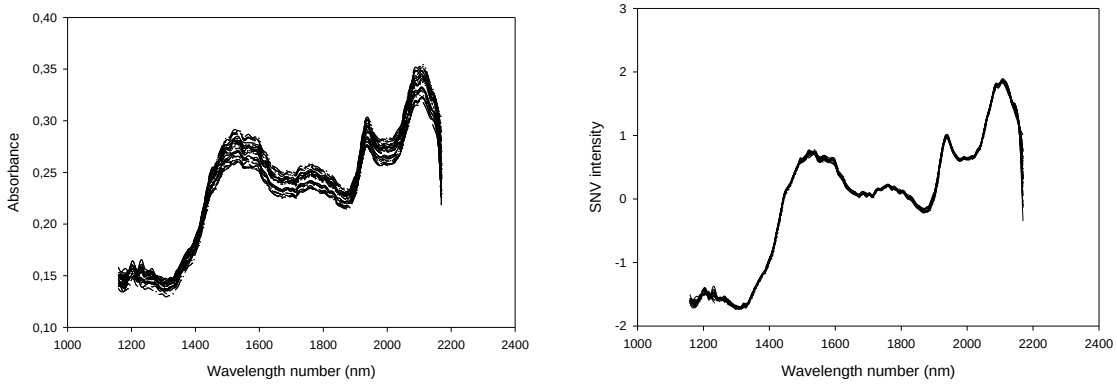

(a) (b)

Fig. 3.7 (a) is the raw spectra and (b) is pre-processed spectra with SNV.

3.2.7 Normalization

There are several algorithms to calculate the normalization, and the vector normalization is the most common one. It can be calculated as:

$$\bar{a}_j = \frac{\sum_{i=1}^{n} a_{ij}}{n} \qquad \text{Equation 16}$$

$$a_{ij}^{*} = \frac{a_{ij} - \bar{a}_j}{\sqrt{\sum_{i=1}^{n} a_{ij}^2}} \qquad \text{Equation 17}$$

Where a_{ij}^{*} is the pre-processed data matrix and $\bar{a}_j$ is the average spectral vector of calibration sample. It is fit for the noise which is caused by the optical path difference. Fig. 3.8 shows the difference, in the preprocessed spectra, the baseline shifting between each spectrum has been reduced.

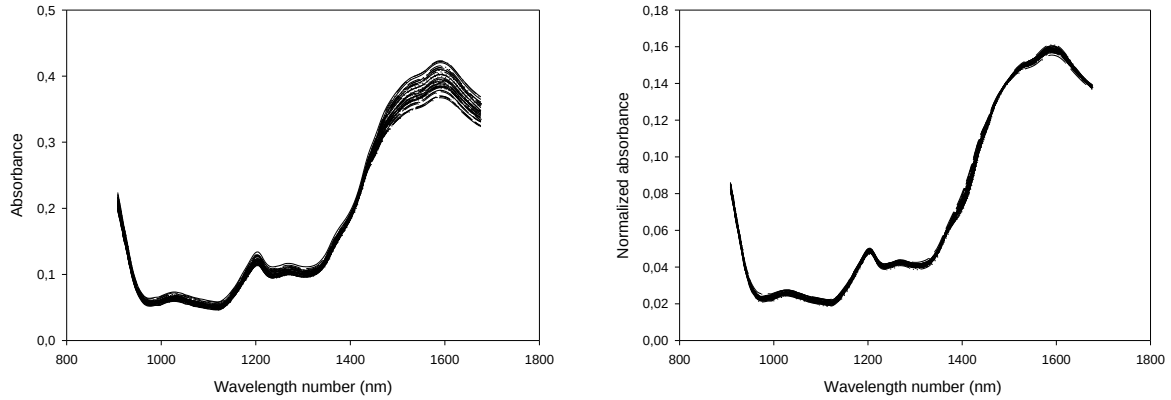

(a) (b)

Fig. 3.8 (a) is the original spectra and (b) is the spectra after vector normalization.

3.2.8 Multiplicative scattering correction (MSC)

The function of MSC is similar to SNV, but the calculation is different. Instead of the mean and standard deviation of the spectrum vector, the MSC uses a reference which is the linear fit spectrum of each original spectrum. Usually, the reference spectrum is the mean spectrum of calibration spectra. The MSC equation is:

$$a_r = \beta_0 + \beta_1 a_i \qquad \text{Equation 3.18}$$

Where a_r is the reference spectrum, β_0 and β_1 are least-squares coefficients, and a_i is an original spectrum. β_0 and β_1 are firstly estimated and then used to calculate the MSC-corrected spectrum a_i^*.

$$a_i^* = \beta_0 + \beta_1 a_i \qquad \text{Equation 3.19}$$

Fig. 3.9 shows the difference, in the preprocessed spectra, the baseline shifting of spectra has been reduced.

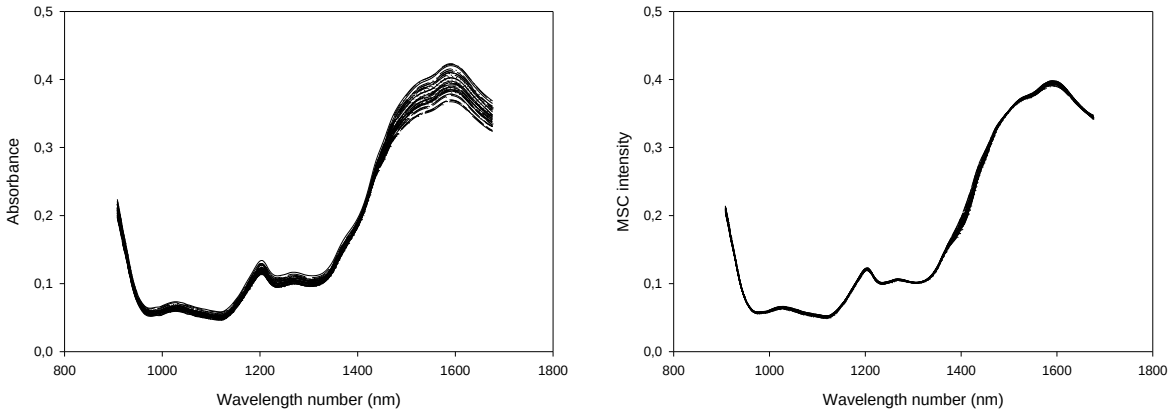

(a) (b)

Fig. 3.9 (a) is the original spectra and (b) is the spectra after MSC.

3.2.9 Fourier transform (FT)

FT is a method which could compress and smooth data by filtering high-frequency noise or reducing low-frequency baseline shifting.

For m discrete spectral data (x_0, x_1 … x_{m-1}) which have the same wavelength interval, their FT equation:

$$x_{k,\ FT} = \frac{1}{m}\sum_{j=0}^{m-1} \exp(\frac{-2i\pi kj}{m}) \qquad \text{Equation 3.20}$$

Where k=0,1…m-1 and $i = \sqrt{-1}$.

And the inverse transformation equation:

$$x_j = \sum_{k=0}^{m-1} x_k \exp(\frac{-2i\pi j}{m}) \qquad \text{Equation 3.21}$$

Where j=0,1…m-1 and $i = \sqrt{-1}$.

Also the spectrum $x_{k,\ FT}$ could be explained as:

$$x_{k,\ FT} = R_k + iL_k \qquad \text{Equation 3.22}$$

$$R_k = \frac{1}{m}\sum_{j=0}^{m-1} x_j \cos(\frac{2\pi kj}{m}) \quad \text{Equation 3.23}$$

$$L_k = -\frac{1}{m}\sum_{j=1}^{m-1} x_j \sin(\frac{2\pi kj}{m}) \quad \text{Equation 3.24}$$

But, it might not be optimal choice if the dominant frequency components vary through the spectrum.

3.2.10 Wavelet transform(WT)

The WT method includes both position and frequency information. So, comparing to FT, it describes not only the frenquncy infromation of spectra, but also the position information. Its core is the ‘ mother wavelet ’ which could have dilation and translation. Once the mother wavelet function is selected, then it is ‘stretched ’ to fit different x axis scales. Thus, it could carry out local analysis[97], [98].

The equation of mother wavelet is :

$$\Psi_{a,b}(t) = \frac{1}{\sqrt{|a|}}\Psi\left(\frac{t-b}{a}\right) \quad \text{Equation 3.25}$$

Where $\Psi_{a,b}(t)$ is the mother wavelet, a is the scale parameter, b is the translation parameter.

The aim of WT is to project the spectral signal x(t) onto the $\Psi_{a,b}(t)$, and we can get the WT coefficient. According to a threshold, the coefficint is reduced. By this way, the noise is filtered and the spectra are smoothed.

3.3 Chemometrics data analysis

The data analysis is a key application in chemometrics. It combines the mathematical and statistical methods with the chemical or physical information collected by analytical instrument to evaluate the underlying parameters or properties. The chemometrics data methods have two types, the qualitative and quantitative. The quantitative methods are carried out with calibration models which could predict the mathematical relationship between the underlying parameters or properties and the variables measured by the analytical instrument. And the qualitative methods could be used when a) an outlier -

or fault - detection system is needed, b) reference data is not precise enough for a quantitative model, c) X and Y variables are quite nonlinear and complex[94].

Some data analysis methods don´t need a calibration model, but the calibration is a very important item in chemometrics data analysis. The univariate calibration is the most traditional and still widely used method of calibration. It correlates a single Y variable to a single X variable. However, there are several driving forces for the development of multivariate calibration, and the NIRS is the major influence. Different from univariate calibration, the multivariate calibration contents several variables in the experimental data. For example, the calibration of NIR spectra and concentration correlates many spectral variables with the concentration. The calculation of the multivariate calibration is complex but the application of computers solved the problem with large quantities of data. In following part, some classical qualitative and quantitative data analysis methods are introduced.

3.3.1 Qualitative methods

The qualitative methods also named pattern recognition, has two parts: supervised and unsupervised classifications. Supervised classification has already defined the class numbers and the standards of classification with calibration set. But the unsupervised classification does not have any information about the class numbers or the standards of classification[94].

For the supervised classification, it can be divided into modeling and discriminant methods. Modelling method has unique volume and bound for each class in the pattern space. The bound could be calculated by correlation coefficients or distances. However, discriminant method separates the pattern space into many regions whose bounds are shared. An unknown sample is classified as a specific class. Fig. 3.10 is the plot of pattern recognition methods

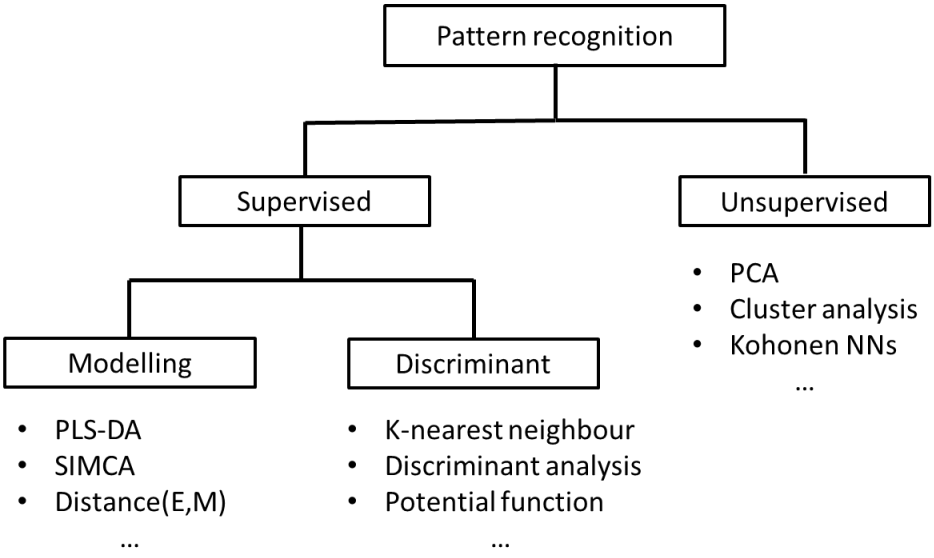

Fig.3.10 the classification of pattern recognition

3.3.1.1 Principal Components Analysis (PCA)

Data compression reduces the original data into a new data set which uses fewer variables and still expresses most of the original information. PCA is a kind of linear data compression method. It is considered to be one of the foundations in chemometrics.

PCA compresses the original data matrix (M*N) into a simpler data matrix which uses fewer number of variables A<<M. And A is named the Principal Components (PCs). The equation is:

$$X = t_1 p_1^T + t_2 p_2^T + \cdots + t_f p_f^T + E \qquad \text{Equation 3.26}$$

Where t is the score of the A principal components, p is the loading vector of the A principal components, E is the residual and f is the number of PCs. Fig. 3.11 shows PCA result plot, (a) plot shows the 2D distribution of samples, PC 1 vs PC 2, (b) plot shows the loading value with PC 1, (c) plot shows the loading value with PC 2.

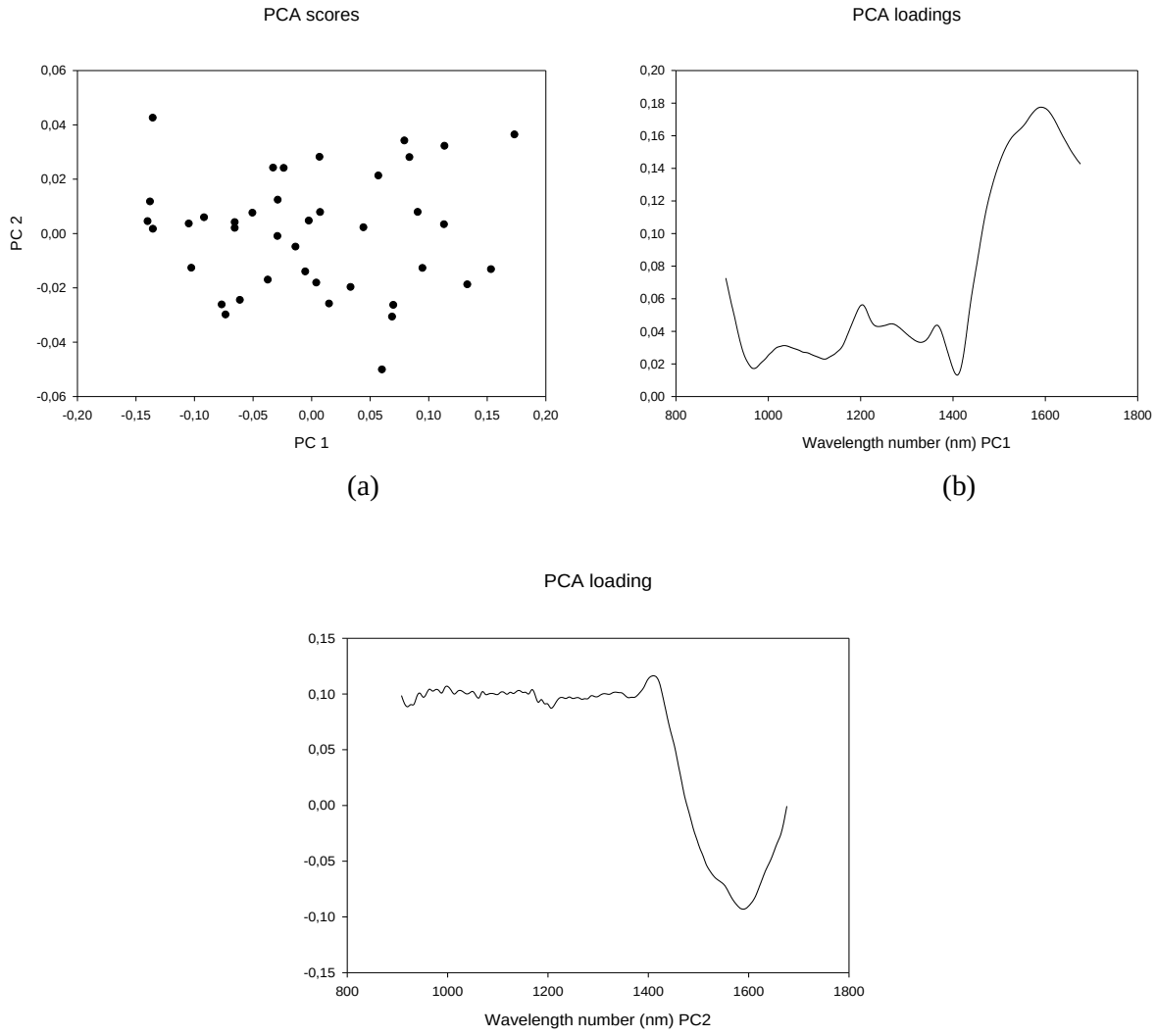

Fig. 3.11 (a) is the PCA scores plot and the (b), (c) are the loadings plots.

The loadings of each PC are orthogonal and normalized. Also, the scores of each PC are orthogonal. Therefore, any two vectors are completely uncorrelated. They could be defined as:

$$p_i^T p_j = 0 \, , i \neq j \qquad \text{Equation 3.27}$$

OR

$$p_i^T p_j = 1 \, , i = j \qquad \text{Equation 3.28}$$

$$t_i^T t_j = 0 \, , i \neq j \qquad \text{Equation 3.29}$$

OR

$$\frac{t^T t}{N-1} = diag(\lambda) \qquad \text{Equation 3.30}$$

Where λ is the eigenvalue of PC and reflects the amount of variance explained by each PC.

The E is mainly generated by the noise and could be calculated by the equation:

$$E = X - \left(t_1 p_1^T + t_2 p_2^T + \cdots + t_f p_f^T\right) \qquad \text{Equation 3.31}$$

The larger the number of PCs (f) is, the more original data is explained, and the lower the E becomes. But, the E is not the smaller the better. A too small E may signify that too much noise has been introduced into the PCA model (overfitting). Fig. 3.12 shows the plot of explained X variance, 2 LVs have explained 90 % of X variance and there is a sharp change of the slope.

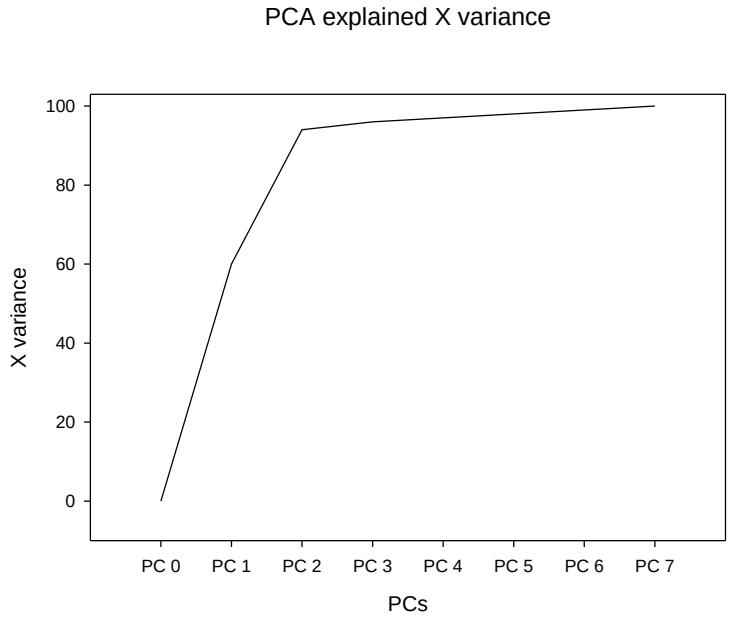

Fig. 3.12 is the percentage of the explained original data variance in a PCA model

In order to perform the PCA as a pattern recognition method, the unknown sample x_p have to be projected onto the space of the PCA model:

$$\hat{t}_P = x_p p \qquad \text{Equation 3.32}$$

Where $\hat{t}_P$ is a set of PCA scores and the P are the PCA loadings.

Then the unknown sample ($\hat{x}_P$) can be calculated by PCA model:

$$\hat{x}_P = \hat{t}_P P^t \quad \text{Equation 3.33}$$

And the residual of the unknown sample $\hat{e}_P$ is:

$$\hat{e}_P = x_p - \hat{x}_P \quad \text{Equation 3.34}$$

Residual is the portion which the PCA model can´t explain.

Finally, some metrics could be used to define a space which helps us identify unknown samples. For example, the Hotelling T^2 statistic and the Q residual statistic are defined as:

$$T^2_{samp} = \hat{t}_P \times diag(\lambda) \times \hat{t}^t_p \quad \text{Equation 3.35}$$

$$Q_{samp} = \hat{e}_P \times \hat{e}^t_p \quad \text{Equation 3.36}$$

The unknown sample can be assessed by these two quality metrics with a selected confidence limit.

3.3.1.2 Cluster analysis

Cluster analysis is a set of unsupervised pattern recognition methods. In the cluster analysis, the similarity between samples is related to the similarity coefficient and the distance. A small distance or a high similarity coefficient indicates that the similarity is high. The common distances are the Euclidean distance and the Mahalanobis distance which have been discussed before. The common similarity coefficients include cosine similarity and correlation coefficient.

The equation of cosine similarity is:

$$\cos\alpha_{ij} = \frac{\sum_{k=1}^{m} x_{ik}x_{jk}}{\sqrt{\sum_{k=1}^{m} x_{ik}^2 \sum_{k=1}^{m} x_{jk}^2}}$$ Equation 3.37

Where $\cos\alpha_{ij}$ is the cosine similarity between sample i and j, m is the variable number and x_{ik} is the *k*th characteristic variable of the sample i. When two samples are completely the same, $\cos\alpha_{ij}$=1, and when two samples are completely different, $\cos\alpha_{ij}$=0.

The equation of correlation coefficient is:

$$R_{ij} = \frac{\sum_{k=1}^{m}(x_{ik}-\bar{x}_i)(x_{jk}-\bar{x}_j)}{\sqrt{\sum_{k=1}^{m}(x_{ik}-\bar{x}_i)^2 \sum_{k=1}^{m}(x_{jk}-\bar{x}_j)^2}}$$ Equation 3.38

Where R_{ij} is the correlation coefficient between sample i and j, m is the variable number and $\bar{x}_i$ is the mean value of all characteristic variable of the sample i. When R_{ij} is close to ± 1, the similarity of two samples is high.

Hierarchical cluster analysis is the most used cluster analysis in practice. Firstly, each sample is defined as a single class and the distance between samples is calculated. Then, the nearest two classes are combined together. This combination process will continue until all the samples belong to a single class. Finally, the dendrogram is plotted like Fig. 3.13. From left to right, there are seven levels in the dendrogram and all samples combined into a single class.

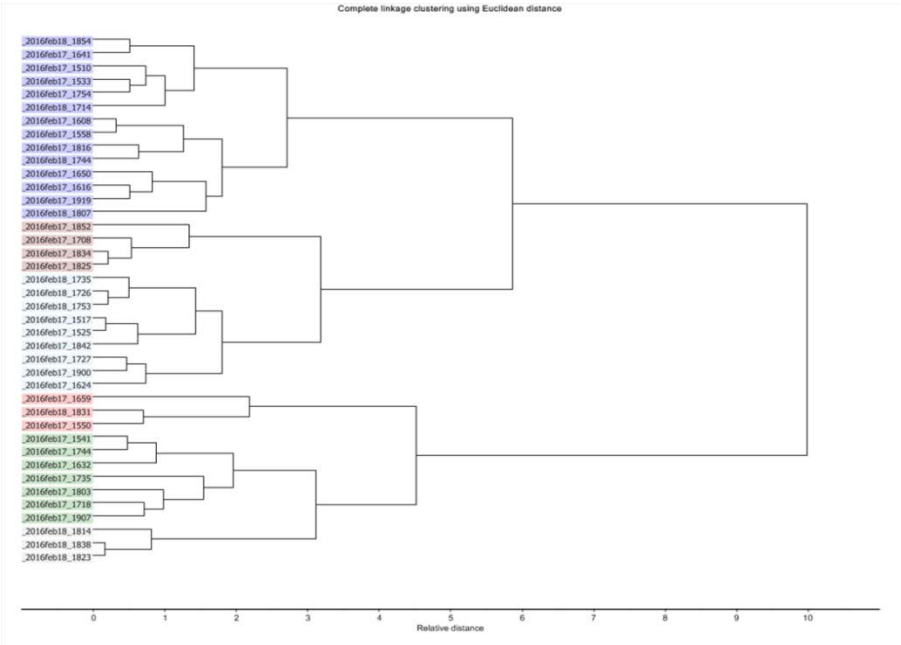

Fig. 3.13 Dendrogram of hierarchical cluster analysis

The distance between clusters could be calculated in several ways, such as single linkage, complete linkage and average linkage. Fig. 3.14 shows the three ways

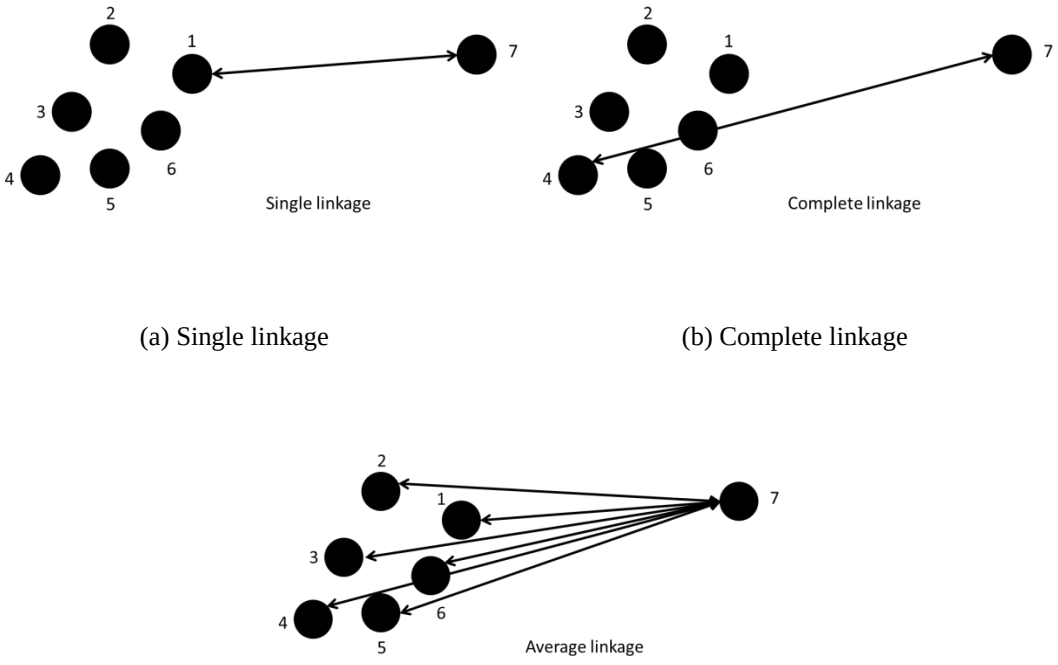

(a) Single linkage

(b) Complete linkage

(c) Average linkage

Fig. 3.14 Three ways to calculate the distance between cluster and sample

Single linkage uses the nearest distance between sample 1 and 7 as the cluster distance. Complete linkage uses the longest distance between sample 4 and 7 as the cluster distance. And the average linkage uses the average distance between samples in the cluster and sample 7 as the cluster distance. Two clusters which have the shortest distance are combined as a new class. Different calculation method may offer different dendrogram, so the operator needs to evaluate the result according to the properties of samples.

3.3.1.3 Soft Independent Modeling of Class Analogy (SIMCA)

SIMCA is a supervised pattern recognition based on PCA. Firstly, each class has a unique PCA model which is calculated by samples of a single class[99]. The equation is:

$$X_k = T_k P_k^t + E_k \qquad \text{Equation 3.39}$$

Where X_k is the spectral matrix (n*m), n is sample number, m is the wavelength number, T_k is score matrix (n*f), f is the best principle components, P_k is the loading matrix (m*f), E_k is the residuals matrix (n*m).

Every class could have its own confidence levels for the Hotelling T^2 and Q values. After that, the unknown sample is introduced into each PCA model. According to the Hotelling T^2 and Q values of the unknown sample and the former confidence levels, the classification can be done.

The SIMCA is suitable for the nonlinear class responses and also could handle the sample which belongs to several classes or to no class at all.

3.3.1.4 Distance

Typically, there are two distance methods which are mostly used in a qualitative model, the Euclidean distance[100] and the Mahalanobis distance[101]. Both of them can be used to access the relationship of samples. A shorter distance means a lager similarity.

In a p dimensions space, the Euclidean distance is:

$$D_{ij} = \sqrt{\left[\sum_{k=1}^{p}\left(x_{ik} - x_{jk}\right)\right]^2} \qquad \text{Equation 3.40}$$

Where I and j= 1, 2…, n.

The Mahalanobis distance is:

$$D_{ij} = \sqrt{(X_i - X_j)S^{-1}(X_i - X_j)^T} \qquad \text{Equation 3.41}$$

Where X_i is the vector of x variables whose dimension is 1*p. S is the covariance matrix of the x variables or PCs whose dimension is p*p.

Comparing to Euclidean distance, the Mahalanobis distance considers the interactions between each dimension when PCs are not used to define the space. Besides, the Mahalanobis distance is scale-invariant. Generally, the Mahalanobis distance is the weighted Euclidean distance.

3.3.1.5 K - Nearest Neighbor (KNN)

KNN is the easiest pattern recognition method based on distance function. The Mahalanobis distance is the typical distance in KNN.

Instead of only comparing the distance between mean values of classes and an unknown sample, KNN calculates the distance between every calibration sample and the unknown sample. Then k closest calibration samples are chosen, and the unknown sample belongs to the class which contains the highest proportion of closest calibration samples.

For example, if there are two classes, KNN could be defined as:

$$S = \sum_{i=1}^{n} \frac{S_i}{D_i} \qquad \text{Equation 3.42}$$

Where S_i is +1 when the i calibration sample belongs to class 1 and S_i is -1 when the calibration sample belongs to class 2. The D_i is the distance between the unknown sample and the i calibration sample.

If the S is a positive number, the unknown sample will be in the 1st class. And if the S is a negative number, the unknown sample will be in the 2nd class.

The KNN could deal with samples which have highly nonlinear separation structures.

3.3.2 Quantitative method

The quantitative methods have three types: the direct method, the inverse method and the learning/searching method. The direct and inverse methods are belonging to the linear regression methods and the other one is a nonlinear regression method[94]. Fig. 3.15 is the plot of quantitative methods

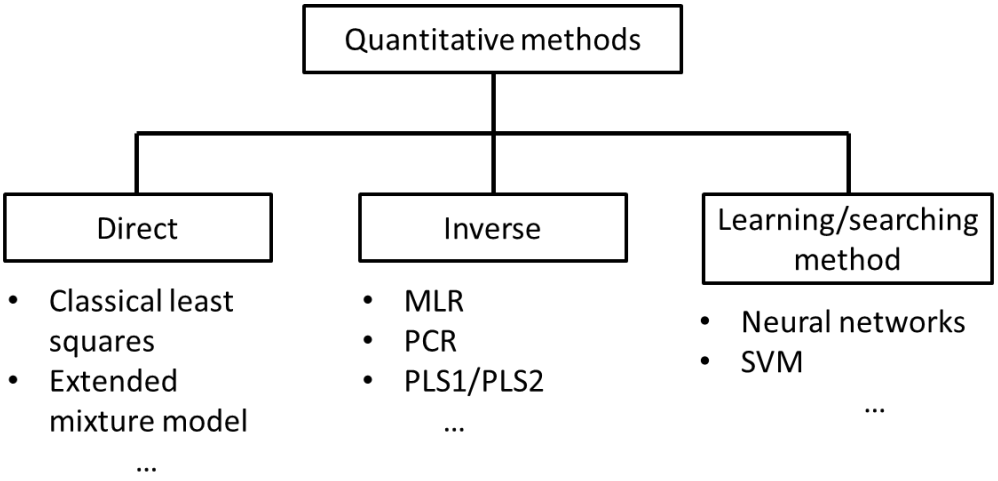

Fig.3.15 The classification of quantitative methods in chemometrics

The direct method could be explained as:

$$X = CS^T + E_x \qquad \text{Equation 3.43}$$

Where X is the spectral matrix, C is the reference value, for example concentration, S is a matrix of basis vectors and E_x is the residual of x variables.

And the inverse method is defined as:

$$C = XB + E_c \qquad \text{Equation 3.44}$$

Where E_c is the residual of reference value and B is the regression coefficient.

The direct method expresses the X as a function of C, but the inverse method expresses the C as a function of X. The inverse method has achieved a great success in the process analysis technology. Especially, the Partial Least Square Regression (PLSR) becomes a standard method in NIRS.

3.3.2.1 Multiple Linear Regression (MLR)

The MLR is a quantitative NIR method which is popular in the early time. Its equation is:

$$C = XB + E \qquad \text{Equation 3.45}$$

$$B = (X^T X)^{-1} X^T C$$ Equation 3.46

Where C is the reference value, X is the spectral matrix, B is the regression coefficient and E is the residual.

But there are some disadvantages for MLR. Because of the function dimension, the wavelength number can´t be more than the sample number in the calibration set. And the collinearity in X matrix is a common problem.

Thus, the MLR is suitable for the simple system which has a very good linearity and uses few wavelength numbers.

3.3.2.2 Classical Least Squares (CLS)

The CLS is a typical direct linear regression method. According to Beer – Lambert Law, its equation is:

$$X = CK + E$$ Equation 3.47

$$K = (C^T C)^{-1} C^T X$$ Equation 3.48

Where C is the reference value, X is the spectral matrix, K is the pure component spectra and E is the residual.

Both experimentally measured spectra and estimated spectra could be used to calculate K. In PAT, the estimated standard spectra are better than the experimentally measured spectra.

The CLS could analyze all components at one time, but only the concentration properties can be determined.

3.3.2.3 Principal Components Regression (PCR)

PCR uses PCA to compress the data matrix and chooses the compressed PCs to calculate a multiple linear regression model. The MLR model includes the PCA scores (T) and loadings (P). Its function is:

$$C = TB + E$$ Equation 3.49

$$B = (T^t T)^{-1} T^t C$$ Equation 3.50

For a sample spectrum X,

$$C_{pred} = tB$$ Equation 3.51

$$t = X_{pred} P$$ Equation 3.52

By PCR, the collinearity of variables could be overcome. And it also reduced the influence of noise. It is fit for a complex system but the calculation speed is slower than MLR.

Like PCA, the determination of the number of PCs is important for the model. There are several ways to choose the PCs, and the common one in NIRS is cross validation. Predicted REsidual Sum of Squares (PRESS) is the criterion:

$$PRESS = \sum_{i=1}^{n} (y_i - \hat{y}_i)^2$$ Equation 3.53

Where n is the sample number and y_i is the reference and $\hat{y}_i$ is the predicted value.

3.3.2.4 Partial Least Squares (PLS)

The PLS method is similar with PCR. Besides the compression of spectral matrix (X), the PLS method compresses the reference matrix (Y) too. Therefore, the compressed variables obtained in PLS are called Latent Variables (LVs) which are selected by leave-one-out cross validation usually. It is different from PCs in PCA[102], [103].

Firstly, the X and Y matrix are compressed:

$$X = TP + E$$ Equation 3.54

$$Y = UQ + F$$ Equation 3.55

Where T and U are scores matrix, P and Q are loadings matrix, E and F are residuals.

Secondly, the linear regression of T and U:

$$U = TB \quad \text{Equation 3.56}$$

$$B = (T^t T)^{-1} T^t Y \quad \text{Equation 3.57}$$

In the prediction step,

$$Y_{pred} = U_{pred} Q = T_{pred} BQ \quad \text{Equation 3.58}$$

The T_{pred} is compressed from the X_{pred}.

Practically, the compression and regression steps are carried out at the same time. By this way, the information of Y matrix is introduced into the compression of X matrix. Thus, the PLS method can be a quantitative regression.

The PLS regression has two forms, the PLS1and the PLS2. The PLS1 could only be calculated with one reference value, and PLS2 can be calculated with more than one reference value. However, the PLS2 uses the same T and P matrix for each reference data, so it could not be the best choice for every reference data. Especially when the two reference value have a large difference in the range of concentration. Meanwhile, the PLS1 method uses the best T and P matrix for only one reference data, so the prediction result could be better.

Nowadays, the PLS regression is widely applied in NIRS research.

3.3.2.5 Support Vector Machine (SVM)

Initially, SVM was used for the pattern recognition. But now, the SVM regression becomes a good method to deal with nonlinear quantitative problems. The principle idea is to transfer a nonlinear relationship into a linear relationship in a higher dimension space[104], [105]. The nonlinear calculation needs a kernel function K (x_i, x_j) to replace the $x_i^T x_j$ of the regression function:

$$f(x)=\sum_{i=1}^{n}(a_i^* - a_i)K(x_i, x_j) + b \quad \text{Equation 3.59}$$

Where a_i^* and a_i are the Lagrange multiplier, a_i^* is the optimal solution, $0 \leq a_i \leq C$ and C is penalty factor.

The SVM only needs few calibration samples and the choice of the penalty factor C is an important process for SVM regression.

In this thesis, preprocessing methods such as mean centering, smoothing, 1st or 2nd derivative and SNV have been used. All quantitative models were calculated with PLS regression and the library was calculated with supervised distance method.

3.4 Wavelength selection

Whole wavelength range calibration could provide all the chemical and physical information of sample, even the affects caused by the instrument or operation may be included in the spectrum. However, the model quality may decrease if all these information is used. The wavelength selection not only simplfies the the model, but also reduce the uninformative or nonlinear variables.

3.4.1 Correlation coefficient method

The correlation coefficient method correlates the change of absorbance of each wavelegth with the change of reference value. The larger the correlation coefficient (r) is, the more useful the wavelength is to explain relation with the variable of interest. Its equation is:

$$r = \frac{\sum_{i=1}^{n}(x_i-\bar{x})(y_i-\bar{y})}{\sqrt{\sum_{i=1}^{n}(x_i-\bar{x})^2 \sum_{i=1}^{n}(y_i-\bar{y})^2}} \quad \text{Equation 3.60}$$

$$\bar{x} = \frac{\sum_{i=1}^{n} x_i}{n} \quad \text{Equation 3.61}$$

$$\bar{y} = \frac{\sum_{i=1}^{n} y_i}{n} \quad \text{Equation 3.62}$$

Where x is the absorbance, y is the reference value and n is calibration set number.

The r is from -1 to 1. When the r is 1, it means that these two variables have full positive linear correlation. When the r is 0, it means there is no correlation between them.

3.4.2 Competitive Adaptive Reweighted Sampling (CARS)

CARS is a method combines Monte-Carlo sampling and PLS[106]. First, calibration set is selected by Monte-Carlo sampleing and the PLS model is calculated. Sencond, the wavelengths which have low regression coefficients are removed by exponentially decreasing function. The retention rate of wavelengths is calculated by:

$$r_i = ae^{-ki} \quad \text{Equation 3.63}$$

$$a = (\frac{m}{2})^{\frac{1}{i-1}} \quad \text{Equation 3.64}$$

$$k = \frac{ln\frac{m}{2}}{i-1} \quad \text{Equation 3.65}$$

Where r_i is the retention, i is the sampling time and m is the whole wavelength number.

Finally, the wavelengths which have high regression coefficients are kept. The PLS models are calculated with them, and the one has the lowest Root Mean Square Error of Cross-Validation (RMSECV) is adopt as the best wavelength range.

3.4.3 Interval PLS (IPLS)

IPLS divides the the spectral range into several zones which have the same width. Then, PLS models are calculated with each zone, and those have low RMSECV is kept. These zones could be combined in order to get the best wavelength range[107].

3.5 Outliers

An outlier is a sample that is not well described by the model.

It could have three types[94]:

- An x - sample outlier, based on spectra of sample.
- An x - variable outlier, based on the behavior of a single x variable comparing to the other x variables.

- A y - sample outlier, based on the reference value of sample.

An outlier is not an incorrect sample or variable. The outlier should be detected and accessed firstly, and then removed if appropriate. The most obvious outlier could be detected by plotting the spectra of all samples. Spectra which are highly different from others may be outliers. Y-sample outliers could be detected by the similar method. X-sample outlier and x-variable outliers could be detected by PCA using scores, loadings, and x residuals. The Hotelling T^2 statistic and the Q residual statistic are two methods to find out the extreme samples which locate within or outside of the model space. Their equations are:

$$T_m^2 = \hat{p}_m diag(\lambda) \hat{p}_m^t \qquad \text{Equation 3.66}$$

Where p_m are the PCA loadings of the *m*th variable for all A PCs.

$$Q_m = \hat{e}_m \hat{e}_m^t \qquad \text{Equation 3.67}$$

where e_m are the PCA residuals for variable m over all N samples.

Samples which are outside 95% confidence limits of the T^2 and Q values may be outliers.

3.6 Validation

In order to have a high quality model, a validation is necessary to be carried out. There are some parameters, such as r, paired t – test, correlation coefficient, bias, explained Y variance which explains the total variation described by models with different numbers of components, the Root Mean Square Errors of Calibration (RMSEC) and Prediction (RMSEP):

$$\mathrm{RMSE} = \sqrt{\frac{\sum_{i=1}^{n}\left(y_i^{pred} - y_i^{ref}\right)^2}{n}} \qquad \text{Equation 3.68}$$

Where n is the number of samples, Y_{ref} is the reference and Y_{pred} is the value estimated by the NIR method.

Besides, the EMA, the Pharmaceutical Analytical Sciences Group, ICH and Pharmacopoeias have published some items which should be validated for a NIRS model: linearity, range, accuracy, robustness, repeatability, intermediate precision. For the NIRS models, the accuracy means the systematic errors between the reference value and the prediction value and the intermediate precision means the repeatability of the prediction value between different days and operators. In the experiment chapters, these items were explained in detail.

Reference

[1] F. and D. Administration, “Classification of Products as Drugs and Devices & Additional Product Classification Issues: Guidance for Industry and FDA Staff,” no. June, pp. 1–12, 2011.

[2] J. Windheuser and J. Cooper, “The pharmaceutics of coating tablets by compression,” *J. Am. Pharm. Assoc.*, vol. 45, no. 8, pp. 542–545, 2006.

[3] H. EAGLE, R. FLEISCHMAN, and M. LEVY, “‘Continuous’ vs. ‘discontinuous’ therapy with penicillin; the effect of the interval between injections on therapeutic efficacy.,” *N. Engl. J. Med.*, vol. 248, no. 12, pp. 481–8, 1953.

[4] K. Park, “Controlled drug delivery systems: Past forward and future back,” *J. Control. Release*, vol. 190, pp. 3–8, 2014.

[5] S. Uchiyama, “Liquid formulation for antibody drugs,” *Biochim. Biophys. Acta - Proteins Proteomics*, vol. 1844, no. 11, pp. 2041–2052, 2014.

[6] M. Y. Yang, J. G. Y. Chan, and H. K. Chan, “Pulmonary drug delivery by powder aerosols,” *Journal of Controlled Release*, vol. 193. pp. 228–240, 2014.

[7] A. Paudel, Z. A. Worku, J. Meeus, S. Guns, and G. Van Den Mooter, “Manufacturing of solid dispersions of poorly water soluble drugs by spray drying: Formulation and process considerations,” *International Journal of Pharmaceutics*, vol. 453, no. 1. pp. 253–284, 2013.

[8] C. N. Nguyen, J. M. Christensen, and J. W. Ayres, “Formulation of sustained-release verapamil HCl and diltiazem HCl semisolid matrix capsules.,” *Pharm. Dev. Technol.*, vol. 13, no. 2, pp. 115–25, 2008.

[9] J. Prescott and R. Barnum, “On powder flowability,” *Pharm. Technol.*, vol. 24, no. October, pp. 60–84, 2000.

[10] R. G. Holdich, “Crushing and classification,” in *Fundamentals of Particle Technology*, Midland Information Technology & Publishing, 2002, p. Chapter 11.

[11] D. W. Fuerstenau, J. J. Lutch, and A. De, “The effect of ball size on the energy efficiency of hybrid high-pressure roll mill/ball mill grinding,” in *Powder Technology*, 1999, vol. 105, no. 1–3, pp. 199–204.

[12] V. Deniz, “A new size distribution model by t-family curves for comminution of limestones in an impact crusher,” *Adv. Powder Technol.*, vol. 22, no. 6, pp. 761–765, 2011.

[13] P. B. Rajendran Nair, “Breakage parameters and the operating variables of a circular fluid energy mill. Part I. Breakage distribution parameter,” *Powder Technol.*, vol. 106, no. 1–2, pp. 45–53, 1999.

[14] S. Teng, P. Wang, L. Zhu, M. W. Young, and C. G. Gogos, “Experimental and numerical analysis of a lab-scale fluid energy mill,” *Powder Technol.*, vol. 195, no. 1, pp. 31–39, 2009.

[15] Q. Q. Zhao and G. Schurr, “Effect of motive gases on fine grinding in a fluid energy mill,” *Powder Technol.*, vol. 122, no. 2–3, pp. 129–135, 2002.

[16] Y. Gao, F. J. Muzzio, and M. G. Ierapetritou, “Scale-up strategy for continuous powder blending process,” *Powder Technol.*, vol. 235, pp. 55–69, 2013.

[17] A. S. L. Mendez, G. de Carli, and C. V. Garcia, “Evaluation of powder mixing operation during batch production: Application to operational qualification procedure in the pharmaceutical industry,” *Powder Technol.*, vol. 198, no. 2, pp. 310–313, 2010.

[18] P. M. Portillo, M. G. Ierapetritou, and F. J. Muzzio, “Characterization of continuous convective powder mixing processes,” *Powder Technol.*, vol. 182, no. 3, pp. 368–378, 2008.

[19] Z. T. Chowhan and E. E. Linn, “Mixing of pharmaceutical solids. I. Effect of particle size on mixing in cylindrical shear and V-shaped tumbling mixers,” *Powder Technol.*, vol. 24, no. 2, pp. 237–244, 1979.

[20] L. T. Fan, S. J. Chen, and C. A. Watson, “ANNUAL REVIEW Solids Mixing,” *Ind. Eng. Chem.*, vol. 62, no. 7, pp. 53–69, Jul. 1970.

[21] Y. Suzuki, T. Kato, Y. Kikkawa, T. Suzuki, N. Wakiyama, and K. Terada, “Scale-up and blender change model for the pharmaceutical lubricated mixing process,” *Powder Technol.*, vol. 280, pp. 113–118, 2015.

[22] K. Niranjan, D. L. O. Smith, C. D. Rielly, J. A. Lindley, and V. R. Phillips, “Mixing Processes for Agricultural and Food Materials: Part 5, Review of Mixer Types,” *J. Agric. Eng. Res.*, vol. 59, no. 3, pp. 145–161, 1994.

[23] H. G. Kristensen and T. Schaefer, “Granulation: a review on pharmaceutical wet-granulation,” *Drug Dev. Ind. Pharm.*, vol. 13, no. 4–5, pp. 803–872, 1987.

[24] K. P. Hapgood and J. D. Litster, “Wet Granulation Processes,” in *Chemical Engineering in the Pharmaceutical Industry: R&D to Manufacturing*, 2010, pp. 757–780.

[25] R. Agrawal and Y. Naveen, “Pharmaceutical Processing – A Review on Wet Granulation

Technology," *Int. J. Pharm. Front. Res.*, vol. 1, no. June, pp. 65–83, 2011.

[26] E. I. Keleb, A. Vermeire, C. Vervaet, and J. P. Remon, "Continuous twin screw extrusion for the wet granulation of lactose," *Int. J. Pharm.*, vol. 239, no. 1–2, pp. 69–80, 2002.

[27] G. M. Walker, "Granulation," *Handb. Powder Technol.*, vol. 11, pp. 219–254, 2007.

[28] T. M. Chitu, D. Oulahna, and M. Hemati, "Wet granulation in laboratory-scale high shear mixers: Effect of chopper presence, design and impeller speed," *Powder Technol.*, vol. 206, no. 1–2, pp. 34–43, 2011.

[29] A. Faure, P. York, and R. C. Rowe, "Process control and scale-up of pharmaceutical wet granulation processes: A review," *European Journal of Pharmaceutics and Biopharmaceutics*, vol. 52, no. 3. pp. 269–277, 2001.

[30] K. Christoph Link and E.-U. Schlünder, "Fluidized bed spray granulation," *Chem. Eng. Process. Process Intensif.*, vol. 36, no. 6, pp. 443–457, 1997.

[31] Z. H. Loh, D. Z. L. Er, L. W. Chan, C. V Liew, and P. W. S. Heng, "Spray granulation for drug formulation.," *Expert Opin. Drug Deliv.*, vol. 8, no. 12, pp. 1645–61, 2011.

[32] B. Kovacic, F. Vrecer, and O. Planinsek, "Spherical crystallization of drugs," *Acta Pharm*, vol. 62, pp. 1–14, 2012.

[33] S. Khoddam, A. Farhoumand, and P. D. Hodgson, "Axi-symmetric forward spiral extrusion, a kinematic and experimental study," *Mater. Sci. Eng. A*, vol. 528, no. 3, pp. 1023–1029, 2011.

[34] J. Thiry, F. Krier, and B. Evrard, "A review of pharmaceutical extrusion: Critical process parameters and scaling-up," *Int. J. Pharm.*, vol. 479, no. 1, pp. 227–240, 2015.

[35] G. E. Peck, J. L. P. Soh, and K. R. Morris, *Dry Granulation*, vol. 1:Unit Ope. 2008.

[36] M. G. Herting and P. Kleinebudde, "Roll compaction/dry granulation: Effect of raw material particle size on granule and tablet properties," *Int. J. Pharm.*, vol. 338, no. 1–2, pp. 110–118, 2007.

[37] R. W. Miller, A. Gupta, and K. R. Morris, "Roller compaction scale-up," *Drugs Pharm. Sci.*, vol. 157, no. Pharmaceutical Process Scale-Up (2nd Edition), pp. 237–266, 2006.

[38] M. K. Iqubal, P. K. Singh, M. Shuaib, A. Iqubal, and M. Singh, "Recent Advances in Direct Compression Technique for Pharmaceutical Tablet Formulation," *Int. J. Pharm. Res. Dev.*, vol. 6, no. 1, pp. 49–57, 2014.

[39] A. H. Gerhardt, “Fundamentals of Tablet Compression,” *J. GXP compliance*, vol. 14, no. 1, pp. 70–79, 2010.

[40] D. Natoli, M. Levin, L. Tsygan, and L. Liu, “Development, Optimization, and Scale-up of Process Parameters: Tablet Compression,” in *Developing Solid Oral Dosage Forms*, 2009, pp. 725–759.

[41] N. K. Bejugam, S. K. Mutyam, and G. N. Shankar, “Tablet formulation of an active pharmaceutical ingredient with a sticking and filming problem: direct compression and dry granulation evaluations,” *Drug Dev. Ind. Pharm.*, vol. 41, no. 2, pp. 333–341, 2015.

[42] J. Berggren, G. Frenning, and G. Alderborn, “Compression behaviour and tablet-forming ability of spray-dried amorphous composite particles,” *Eur. J. Pharm. Sci.*, vol. 22, no. 2–3, pp. 191–200, 2004.

[43] G. K. Dokala and C. Pallavi, “Direct Compression - An Overview,” *Int. J. Res. Pharm. Biomed. Sci.*, vol. 4, no. 1, pp. 155–158, 2013.

[44] U. S. D. of H. and H. S. FDA, “Guidance for Industry PAT — A Framework for Innovative Pharmaceutical Development, Manufacuring, and Quality Assurance,” *FDA Off. Doc.*, no. September, p. 16, 2004.

[45] ICH Expert Working Group, “Good Manufacturing Practice Guide for Active Pharmaceutical Ingredients Q7,” *ICH Harmon. Trpartite Guidel.*, no. November, p. 49, 2000.

[46] B. Trivedi, “Quality by design (QbD) in pharmaceuticals,” *International Journal of Pharmacy and Pharmaceutical Sciences*, vol. 4, no. 1. pp. 17–29, 2012.

[47] R. W. Bondi and J. K. Drennen, *Quality by Design and the Importance of PAT in QbD*, vol. 10, no. C. 2011.

[48] F. J. Muzzio, P. Robinson, C. Wightman, and Dean Brone, “Sampling practices in powder blending,” *International Journal of Pharmaceutics*, vol. 155, no. 2. pp. 153–178, 1997.

[49] K. P. Hapgood, S. M. lveson, J. D. Litster, and L. X. Liu, “Granulation,” *Handb. Powder Technol.*, vol. 11, pp. 897–977, 2007.

[50] D. C. Hinz, “Process analytical technologies in the pharmaceutical industry: The FDA’s PAT initiative,” *Analytical and Bioanalytical Chemistry*, vol. 384, no. 5. pp. 1036–1042, 2006.

[51] ICH, “ICH Q8(R2) Pharmaceutical Development,” 2009.

[52] L. Gronholdt, A. Martensen, and K. Kristensen, “The relationship between customer

satisfaction and loyalty: Cross-industry differences," *Total Qual. Manag.*, vol. 11, no. 4–6, pp. 509–514, 2000.

[53] J. Trienekens and P. Zuurbier, "Quality and safety standards in the food industry, developments and challenges," *Int. J. Prod. Econ.*, vol. 113, no. 1, pp. 107–122, 2008.

[54] A. Gunasekaran, J. Sarkis, C. J. Corbett, A. C. L. Yeung, J. Trienekens, and P. Zuurbier, "Quality and safety standards in the food industry, developments and challenges," *Int. J. Prod. Econ.*, vol. 113, no. 1, pp. 107–122, 2008.

[55] D. a. Garvin, "Competing on the eight dimensions of quality.," *Harv. Bus. Rev.*, vol. 65, no. 87603, pp. 101–109, 1987.

[56] D. A. Garvin, "Managing Quality - The strategic and competitive edge," in *Management Review , Vol . 13 , No . 4 (Oct ., 1988), pp . 656-657 Published by : Academy of Management*, vol. 13, no. 4, 1988, pp. 656–657.

[57] L. Fulponi, "Private voluntary standards in the food system: The perspective of major food retailers in OECD countries," *Food Policy*, vol. 31, no. 1, pp. 1–13, 2006.

[58] a. Hammoudi, R. Hoffmann, and Y. Surry, "Food safety standards and agri-food supply chains: an introductory overview," *Eur. Rev. Agric. Econ.*, vol. 36, no. 4, pp. 469–478, 2010.

[59] E. N. Sawyer, W. A. Kerr, and J. E. Hobbs, "Consumer preferences and the international harmonization of organic standards," *Food Policy*, vol. 33, no. 6, pp. 607–615, 2008.

[60] B.-H. Cho and N. H. Hooker, "Comparing food safety standards," *Food Control*, vol. 20, pp. 40–47, 2009.

[61] D.-W. Sun, A. Subramanian, and L. Rodriguez-Saona, *Infrared Spectroscopy for Food Quality Analysis and Control*. 2009.

[62] S. S. Nielsen, *Food Analysis Fourth Edition*. 2014.

[63] J. A. Vasconcellos, *Quality assurance for the food industry : a practical approach*. CRC Press, 2004.

[64] S. A. H. Lim, J. Antony, and S. Albliwi, "Statistical Process Control (SPC) in the food industry – A systematic review and future research agenda," *Trends Food Sci. Technol.*, vol. 37, no. 2, pp. 137–151, 2014.

[65] F. van den Berg, C. B. Lyndgaard, K. M. Sørensen, and S. B. Engelsen, "Process Analytical Technology in the food industry," *Trends Food Sci. Technol.*, vol. 31, no. 1, pp. 27–35, 2013.

[66] M. J. McGrath, J. F. O'Connor, and S. Cummins, "Implementing a process control strategy for the food processing industry," *J. Food Eng.*, vol. 35, no. 3, pp. 313–321, 1998.

[67] T. A. Haley and S. J. Mulvaney, "Advanced process control techniques for the food industry," *Trends Food Sci. Technol.*, vol. 6, no. 4, pp. 103–110, 1995.

[68] G. Saravacos and Z. Maroulis, *Food Process Engineering Operations.*, no. 7. 2011.

[69] J. Casals, L. Pascual, J. Cañizares, J. Cebolla-Cornejo, F. Casañas, and F. Nuez, "Genetic basis of long shelf life and variability into Penjar tomato," *Genet. Resour. Crop Evol.*, vol. 59, no. 2, pp. 219–229, 2012.

[70] J. Casals, L. Bosch, F. Casañas, J. Cebolla, and F. Nuez, "Montgrí, a cultivar within the montserrat tomato type," *HortScience*, vol. 45, no. 12, pp. 1885–1886, 2010.

[71] T. Hermann, M.; Pentek, "Desingn principles for industrie 4.0 scenarios: a literature review," no. 01, p. 15, 2015.

[72] J. Lee, H. A. Kao, and S. Yang, "Service innovation and smart analytics for Industry 4.0 and big data environment," *Procedia CIRP*, vol. 16, pp. 3–8, 2014.

[73] J. Lee, B. Bagheri, and H. A. Kao, "A Cyber-Physical Systems architecture for Industry 4.0-based manufacturing systems," *Manuf. Lett.*, vol. 3, pp. 18–23, 2015.

[74] H. Lasi, P. Fettke, H. G. Kemper, T. Feld, and M. Hoffmann, "Industry 4.0," *Bus. Inf. Syst. Eng.*, vol. 6, no. 4, pp. 239–242, 2014.

[75] European Commission, "What is Horizon 2020? - Horizon 2020 - European Commission," *Horizon 2020*, 2016. [Online]. Available: https://ec.europa.eu/programmes/horizon2020/en/what-horizon-2020.

[76] P. C. Evans and M. Annunziata, "Industrial Internet: Pushing the Boundaries of Minds and Machines," *Gen. Electr.*, p. 37, 2012.

[77] ASTM E1655-05, "Standard Practices for Infrared Multivariate Quantitative Analysis," *ASTM Int.*, vol. 05, no. Reapproved 2012, p. 29, 2012.

[78] A. Bittner, R. Marbach, and H. M. Heise, "Multivariate calibration for protein, cholesterol and triglycerides in human plasma using short-wave near infrared spectrometry," *J Mol Struct*, vol. 349, pp. 341–344, 1995.

[79] A. U. Vanarasea, M. Alcalàb, J. I. J. Rozoc, F. J. Muzzioa, and R. J. Romañachc, "Real-time monitoring of drug concentration in a continuous powder mixing process using NIR

spectroscopy," *Chem. Eng. Sci.*, vol. 65, 2012.

[80] M. Blanco and I. Villarroya, "NIR spectroscopy: a rapid-response analytical tool," *TrAC Trends Anal. Chem.*, vol. 21, no. 4, pp. 240–250, 2002.

[81] T. Davies, "The history of near infrared spectroscopic analysis: Past, present and future 'From sleeping technique to the morning star of spectroscopy,'" *Analusis*, vol. 26, pp. 17–19, 1998.

[82] D. L. Wetzel, "Near-infrared reflectance analysis," *Anal. Chem.*, vol. 55, no. 12, p. 1165A–1176A, Oct. 1983.

[83] J. G. Rosas, M. Blanco, J. M. González, and M. Alcalà, "Real-time determination of critical quality attributes using near-infrared spectroscopy: A contribution for Process Analytical Technology (PAT)," *Talanta*, vol. 97, pp. 163–170, 2012.

[84] M. Alcalà, J. León, J. Ropero, M. Blanco, and R. J. Romañach, "Analysis of low content drug tablets by transmission near infrared spectroscopy: Selection of calibration ranges according to multivariate detection and quantitation limits of PLS models," *J. Pharm. Sci.*, vol. 97, no. 12, pp. 5318–5327, Dec. 2008.

[85] M. Alcalà, J. Ropero, R. Vázquez, and R. J. Romañach, "Deconvolution of Chemical Physical Information from Intact Tablets NIR Spectra: Two-Three-Way Multivariate Calibration Strategies for Drug Quantitation," *J. Pharm. Sci.*, vol. 98, no. 8, pp. 2747–2758, Aug. 2009.

[86] M. Alcalà, M. Blanco, M. Bautista, and J. M. González, "On-line monitoring of a granulation process by NIR spectroscopy," *J. Pharm. Sci.*, vol. 99, no. 1, pp. 336–345, Jan. 2010.

[87] J. M. Amigo, J. Cruz, M. Bautista, S. Maspoch, J. Coello, and M. Blanco, "Study of pharmaceutical samples by NIR chemical-image and multivariate analysis," *TrAC Trends Anal. Chem.*, vol. 27, no. 8, pp. 696–713, 2008.

[88] M. Blanco, M. Alcalá, and M. Bautista, "Pharmaceutical gel analysis by NIR spectroscopy: Determination of the active principle and low concentration of preservatives," *Eur. J. Pharm. Sci.*, vol. 33, no. 4, pp. 409–414, 2008.

[89] M. Blanco, M. Alcalá, J. M. González, and E. Torras, "A process analytical technology approach based on near infrared spectroscopy: Tablet hardness, content uniformity, and dissolution test measurements of intact tablets," *J. Pharm. Sci.*, vol. 95, no. 10, pp. 2137–2144, Oct. 2006.

[90] M. Alcalà, M. Blanco, D. Moyano, N. Broad, N. O'Brien, D. Friedrich, F. Pfeifer, and H. Siesler, "Qualitative and quantitative pharmaceutical analysis with a novel handheld miniature

near-infrared spectrometer," *J. Near Infrared Spectrosc.*, vol. 21, no. 6, pp. 445– 457, 2013.

[91] P. Williams and K. Norris, *Near Infrared Technology in the Agricultural and Food Industries*. 2001.

[92] H. W. Siesler, Y. Ozaki, and S. Kawata, *Near-infrared spectroscopy. Principles, instruments, applications*, vol. 16, no. 12. 2002.

[93] M. Blanco, M. Alcalà, J. C. Menezes, P. M. Felizardo, A. Garrido, P. Dolores, E. Zamora, C. Pasquini, and R. J. Romañach, *Near-infrared Spectroscopy in Laboratory and Process Analysis*. 2012.

[94] K. A. Bakeev, *Process analytical technology : spectroscopic tools and implementation strategies for the chemical and pharmaceutical industries*. Wiley, 2010.

[95] M. Maeder and Y.-M. Neuhold, "Practical data analysis in chemistry," *Data Handl. Sci. Technol.*, no. 26, p. 326 S., 2007.

[96] E. Pharmacopoeia, "5.21. Chemometric Methods," 2016, pp. 5641–5658.

[97] B. Walczak, *Wavelets in chemistry*. Elsevier Science B.V, 2000.

[98] F. Ehrentreich, "Wavelet transform applications in analytical chemistry," *Anal. Bioanal. Chem.*, vol. 372, no. 1, pp. 115–121, 2002.

[99] A. Candolfi, R. De Maesschalck, D. L. Massart, P. A. Hailey, and A. C. E. Harrington, "Identification of pharmaceutical excipients using NIR spectroscopy and SIMCA," *J. Pharm. Biomed. Anal.*, vol. 19, no. 6, pp. 923–935, 1999.

[100] J. C. Gower, "Euclidean distance geometry," *Math. Sci.*, vol. 7, no. 1, pp. 1–14, 1982.

[101] R. De Maesschalck, D. Jouan-Rimbaud, and D. L. Massart, "The Mahalanobis distance," *Chemometrics and Intelligent Laboratory Systems*, vol. 50, no. 1. pp. 1–18, 2000.

[102] a Höskuldsson and A. Hoskuldsson, "PLS Regression Methods," *J. Chemom.*, vol. 2, no. July, pp. 211–228, 1988.

[103] S. Wold, M. Sjöström, and L. Eriksson, "PLS-regression: A basic tool of chemometrics," in *Chemometrics and Intelligent Laboratory Systems*, 2001, vol. 58, no. 2, pp. 109–130.

[104] R. G. Brereton and G. R. Lloyd, "Support vector machines for classification and regression.," *Analyst*, vol. 135, no. 2, pp. 230–267, 2010.

[105] C. C. J. C. Burges, "A Tutorial on Support Vector Machines for Pattern Recognition," *Data*

Min. Knowl. Discov., vol. 2, no. 2, pp. 121–167, 1998.

[106] H. Li, Y. Liang, Q. Xu, and D. Cao, "Key wavelengths screening using competitive adaptive reweighted sampling method for multivariate calibration," *Anal. Chim. Acta*, vol. 648, no. 1, pp. 77–84, 2009.

[107] J. H. Jiang, R. James, B. H. W. Siesler, and Y. Ozaki, "Wavelength interval selection in multicomponent spectral analysis by moving window partial least-squares regression with applications to mid-infrared and near-infrared spectroscopic data," *Anal. Chem.*, vol. 74, no. 14, pp. 3555–3565, 2002.

Chapter 4

Objectives

4. Objectives

The main objective of this thesis is to apply NIRS as a tool of industry 4.0 in the pharmaceutical and food industries. The smart factory is a trend of development in the information age. Human beings could receive a lot of assistance from the smart tools which make works be done in a better and efficient way. The physical and mental requirements that limit the employment of workers would be decreased. Technology-intensive industries, such as pharmaceutical and modern food industries, are pioneers who have the advantages to enjoy the smart factory. In detail, the smart factory could monitor the manufacturing process and control the product quality in real time automatically. Though this method, the high quality product could be manufactured in a simple way. Nowadays, the product quality is a key factor that determines the market share. In order to assure a high quality both in the process and final product, several institutions have published some guidelines. QbD and PAT were two guidelines used in this thesis. NIRS was taken as the tool to realize these concepts in the pharmaceutical industry. Besides, a study about food quality improvement was carried out with NIRS too.

The following are detail objectives of this thesis,

- To analyze the solid pharmaceutical manufacturing process with MicroNIR..
- To identify pharmaceutical formulations in retail stores with MicroNIR.
- To analyze the food quality with NIRS, both in chemical and sensory aspects.
- To investigate the combination of chemometrics and NIRS.
- To study the virtualization of manufacturing process by NIRS.
- To study the real-time analysis by NIRS.
- To investigate new solutions to deal with problems in pharmaceutical and food industries.

Chapter 5

Determination of API concentration in powder with portable MicroNIR

5. Determination of API concentration in powder with portable MicroNIR

NIRS is an analytical technique which improves the application of PAT in pharmaceutical industry. Nowadays the development of NIRS instruments is focusing on portability and miniaturization, which makes this technique become more practical for real time analysis. In this study, a portable MicroNIR with the dimension (diameter x height) 45 x 42mm was used to determine the concentration of API in powder. Samples were prepared with a concentration range from 70 to 104 mg/g. A quantitative PLS model was constructed and fully validated by linearity, range, accuracy, repeatability, and intermediate precision according to the guidelines of the ICH . Finally, the RMSEC is 0.20 mg/g and the RMSEP is 0.87 mg/g, which means this MicroNIR has a good performance for the determination of API concentration in powder.

Key words: Portability and miniaturization of NIRS instruments, Determination of concentration of API in powder, Pharmaceutical industry

5.1 Introduction

PAT [1] is a practical technique. In order to apply PAT into the pharmaceutical industry, we need to develop some practical analytical methodologies which are fit to it. A way to fulfill this idea is to develop the method which can monitor the different steps during the production process and provide accurate analytical results in a simple and fast way. NIRS is one of the analytical techniques which could meet these requirements mentioned above. Compare to some classic analysis methods, the NIRS is rapid, non – destructive and cheap. From 1940s, the companies began to develop NIRS instrument. But it was combined with UV/Vis spectroscopy and only was their extension. This kind of instrument was lack of a special design for NIRS, so its signal to noise ratio was not good and it was not stable. [2-6] In 1970s, the first special diffuse reflectance equipment of NIRS came out. After that, studies and applications with NIRS became active increasingly and different kinds of instruments have been developed, such as fixed wavelength filter system, grating dispersion system, fast fourier transform system, and acousto-optic tunable filter system.

Recently a number of successful qualitative and quantitative applications of NIRS in the pharmaceutical industry have been reported [7-10]. Its analytical power has been demonstrated clearly. And more and more applications ask the instrument to be portable and miniaturized. As we know, the drug production line must be very stable and any change of it needs to be well validated. And the validation of a new production line will cost a lot of time and money. Therefore, the factory

wants to keep the existing production line untouched or change it as little as possible. In order to reach this aim, the portable MicroNIR was designed. It is tiny and could communicate with a computer by USB interface. So it can be equipped in the pharmaceutical machines without a complicated change to them, which is important for the stability of the production line. What´s more, the micro NIR does not have movable components which would be very easy to be worn by the vibration of pharmaceutical machines.

The production process of tablets is a typical solid pharmaceutical process which is composed by several operation units, such as blending, granulation, tableting. NIRS can be applied to determine the API during granulation process. The most used method in pharmaceutical factories to determine the concentration of API in production process is High Performance Liquid Chromatography (HPLC) method [11, 12]. But the HPLC can´t fully meet the requirement of PAT due to the long analysis time and the complexity of sample preparation. Therefore, the MicroNIR was adopted to overcome these problems.

In this work, we developed and validated a quantitative method to determine the content of API in powder. Spectra of samples were acquired by the MicroNIR and a quantitative PLS model of API was constructed. The predictive ability of the model was fully validated according to the guidelines of ICH and EMA [13, 14]. The result shows us that the MicroNIR has a good performance in analyzing the granulation process.

5.2 Experiment

5.2.1 Instrument and performance verification

5.2.1.1 Parameters of MicroNIR

NIR spectra were recorded with the reflectance mode of the portable MicroNIR™ 2200 Spectrometer (VIAVI SOLUTIONS INC., USA) which was managed by the software IRSE Vision 1.5.3.0 from JDSU. The dimension of this instrument is (diameter x height) 45 x 42mm, weight<60g and the active sampling area is 2 x 4 mm. Its light source and spectroscopic system are fixed, so movements of this instrument will not affect the quality of spectrum. What´s more, it can be powered (<500mA@5V) by USB 2.0 interface, so the power consumption is low. All these features mentioned above make the Micro NIR a portable instrument. Its operating environment is from –20 to 40°C, noncondensing. So it can bear the cruel analysis environment in the factory which affects the quality of spectrum seriously.

5.2.1.2 Instrument noise analysis

Before starting to acquire the spectrum of API, we carried out the noise analysis of the Micro NIR. It included noise of 7 standard references which have spanned the near-infrared light diffuse reflectance property (R2%, R20%, R40%, R80%, R99%) and the noise of duration time (450mins).

For the noise of different standard references, firstly, the MicroNIR was warmed up for 30mins. Then, two spectra of every standard reference were acquired with the following parameter, integration time was100 μs, number of scans were 10000, scan range was 1158.8-2169.4 nm, and background spectrum was acquired with R02%. For the noise of duration time, firstly, the MicroNIR was warmed up for 30 mins. Then, two spectra at different duration time were acquired with the following parameter, integration time 100 μs number of scans 10000, scan range 1158.8-2169.4 nm, and the background spectrum was acquired with R99%. Finally, noise spectrum was calculated from the two spectra of each standard reference. Peak to peak deviation (max to min), bias (average of the noise deviation), and standard deviation of the noise were calculated to evaluate the instrument noise.

5.2.2 Sample preparation

Laboratory samples were weighted by the analytical balance. 26 laboratory samples were prepared in two parts, one was API and the other part was the mixture of excipients. After that, these two parts were mixed and the API spanned a concentration range from 70 to 104 mg/g. Such a range corresponded to ±30 % of the nominal API content and was wide enough to carry out a validation of the proposed model. The placebo was a mixture of lactose and starch, and these two ingredients were both prepared within ±5 % (w/w) around the nominal content in the formulation. In this way, the potential correlation between the samples could be reduced. What´s more, some production samples were added into the prediction set.

5.2.3 NIR spectra acquisition

For every sample, 3 spectra were acquired and the reference spectra were renewed when the sample was changed. The distance between the powder and the window of MicroNIR was fixed at 3mm and a special accessory was used for this purpose. The scan number was 10000 and the integration time was 100μs. Spectral region was from 1158.8 nm to 2153.1 nm. Geometric resolution of the spectrometer was 8.15 nm per pixel. And the 99% reference was used as background.

5.2.4 Data analysis

The multivariate models were calculated with Unscrambler X (Trondheim, Norway).The calculation of validation was carried out by Excel 2010 (Microsoft, USA).

Raw spectra were smoothed by Median Filter smoothing with 7-points segment size. 1st and 2nd derivative spectra were obtained by using the Savitzky–Golay algorithm with a 3-points or 5-points moving window and a second-order polynomial. PLS1 calibration models were constructed with full cross-validation, using the leave-one-out method. The quality of the models was assessed in terms of the RMSEC and RMSEP, defined as:

$$\mathrm{RMSE} = \sqrt{\frac{\sum_{i=1}^{n}\left(y_i^{pred} - y_i^{ref}\right)^2}{n}} \qquad \text{Equation 5.1}$$

Where n is the number of samples, Y_{ref} is the concentration of certirizine provided by the reference method and Y_{pred} is the value estimated by the NIR method.

5.3 Results and discussion

5.3.1 Noise spectra analysis

Peak to peak deviation (P-P) was calculated by the Y value of maximum peak minus the Y value of minimum peak in one noise spectrum. The minimum P-P among these seven samples was 0.01, the average P-P deviation was 0.08, and the maximum was 0.11. The difference between the largest and smallest P-P value in the noise spectrum was on the scale of 10^{-2}. Bias was the average of the Y value in one noise spectrum. The minimum among these seven samples was 0.001, the average bias was 0.010 and the maximum was 0.02628. The bias value of all points in the noise spectrum was on the scale of 10^{-3}. It was in the acceptable range of +/- 0.050. Standard deviation (SD) of the noise was also calculated by the Y value in one noise spectrum, the minimum was 0.002, the average was 0,009 and the maximum was 0.024. The SD across the full spectral region is on the scale of 10^{-3}. The results of this analysis showed us that the instrument noise caused by different samples was acceptable.

Table 5.1shows the P-P, bias and SD. Fig.5.1 is noise spectrum of the instrument with seven samples.

Table 5.1 Instrument noise

Sample	P-P	Minimum	Wavelength(nm)	Maximum	Wavelength(nm)	Bias	SD
R02	0.03	-0.018	1289.20	0.013	1281.05	0.001	0.004
R10	0.04	-0.010	1281.05	0.033	1264.75	0.008	0.005
R20	0.03	-0.021	1232.15	0.014	1281.05	0.005	0.004
R40	0.11	-0.088	1232.15	0.026	2169.40	0.026	0.016
R80	0.07	-0.037	2169.40	0.037	1232.15	0.010	0.008
R99	0.26	-0.191	2169.40	0.066	1232.15	0.016	0.024
WSR	0.01	-0.005	2169.40	0.006	1175.10	0.001	0.002

In Fig. 5.1, we can find that the noise value of the instrument is quite low and each wavelength has similar signal intensity, only the signal intensity of last two wavelength points is higher than the others sometimes. So it´s better to check the last two data points when we calculate models.

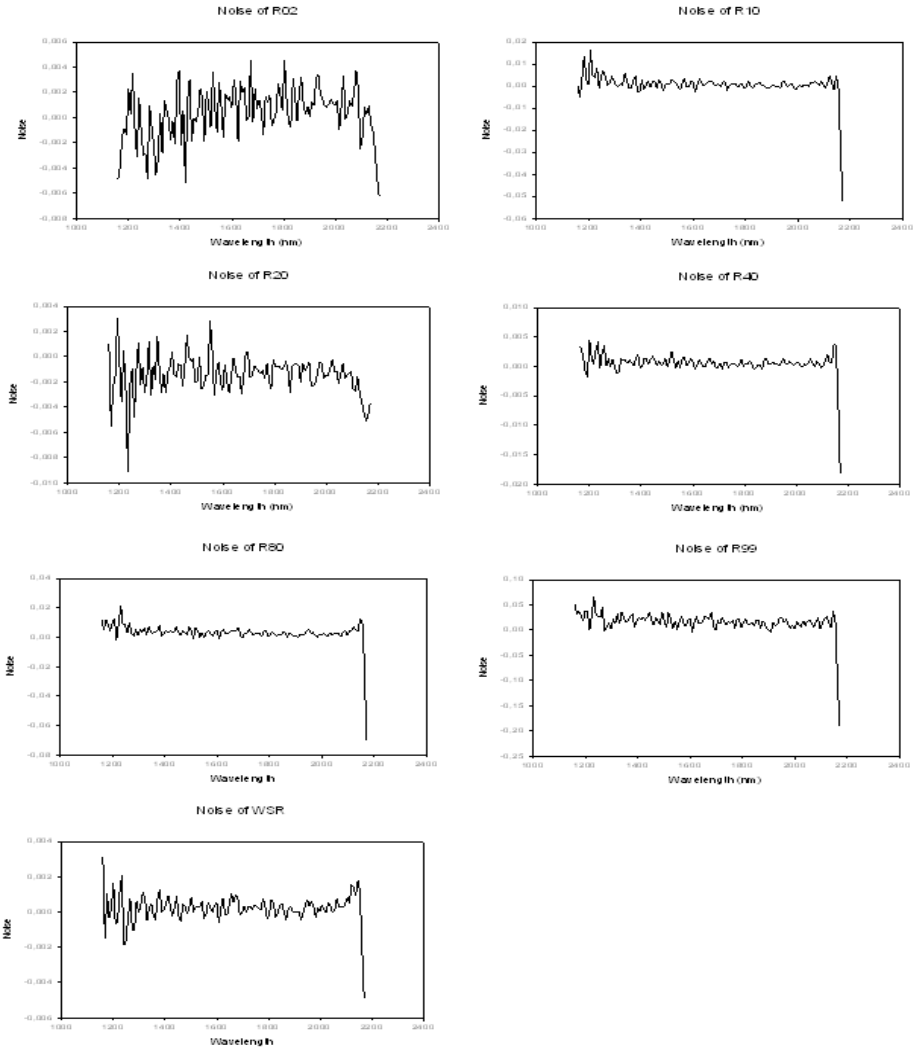

Fig 5.1 Instrument noise spectra of 7 samples

5.3.2 Noise of duration time

The noise of duration time is an important character which can represent the stability of the instrument. Table 5.2 shows the P-P, bias and SD of noise within different duration time. The bias value and SD value were on the scale of 10^{-3}-10^{-4}. The duration time which lasted for 450mins did not affect the noise. And the bias was in the acceptable range of +/- 0.050.

Table 5.2 Noise of duration time

Time(min)	P-P	Minimum	Wavelength(nm)	Maximum	Wavelength(nm)	Bias	SD
1	0.051	-0.038	2169.40	0.013	1232.15	0.0031	0.004
5	0.056	-0.042	2169.40	0.014	1232.15	0.0021	0.005
10	0.078	-0.064	2169.40	0.014	1232.15	0.0016	0.006
15	0.041	-0.035	2169.40	0.006	1158.80	0.0013	0.004
20	0.026	-0.005	1207.70	0.021	2169.40	-0.0014	0.002
25	0.051	-0.005	1166.95	0.046	2169.40	-0.0008	0.004
30	0.005	-0.004	1158.80	0.001	1313.65	-0.0005	0.001
60	0.006	-0.003	1191.40	0.004	1207.70	0.0010	0.001
90	0.061	-0.007	1175.10	0.054	2169.40	-0.0008	0.005
120	0.006	0.000	1305.50	0.005	1207.70	0.0011	0.001
150	0.025	-0.003	1158.80	0.023	2169.40	0.0011	0.002
180	0.010	-0.002	2153.10	0.008	2169.40	-0.0005	0.001
260	0.005	-0.003	1183.25	0.002	1272.90	0.0001	0.001
310	0.020	-0.001	1867.85	0.019	2169.40	0.0005	0.002
340	0.022	-0.001	1232.15	0.021	2169.40	0.0016	0.002
400	0.026	-0.004	1281.05	0.022	2169.40	-0.0004	0.002
430	0.021	-0.005	2153.10	0.016	2169.40	-0.0004	0.002
450	0.022	-0.004	1158.80	0.018	2169.40	-0.0001	0.002

100μs/10000scans R99%

5.3.3 Calibration

Calibration models were calculated with the data of laboratory samples. From the raw spectra, see Fig. 5.2, we found that there was noise in them and the spectral variation of API was not notable enough for a quantitative calibration model. Therefore, several pretreatment methods were applied when we

calculated the models such as median filter smoothing, Savitzky–Golay smoothing and 1st, 2nd derivatives. The prediction set included both laboratory and production samples.

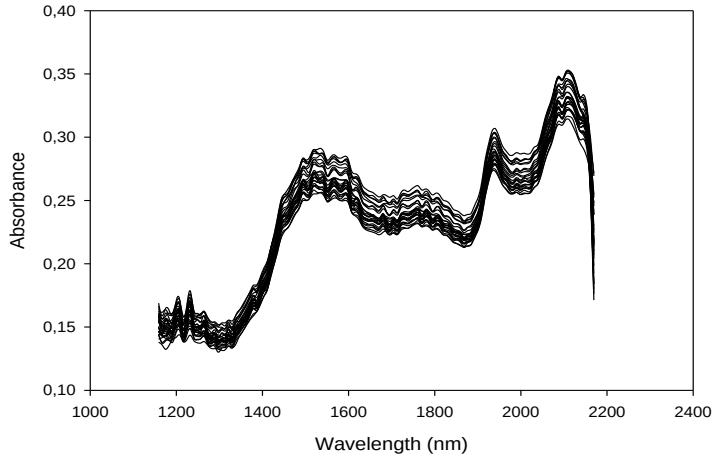

Fig.5.2 Raw spectra of API without pretreatment

The total laboratory powder set, which consisted of 26 samples, was split into two subsets. One was calibration set which included 17 samples and the other one was prediction set that consisted of 9 samples. The calibration set was selected by a scatter plot of PCs score, PC1 versus PC2 scores. It was obtained by the PCA with the smoothing and second derivative data matrix over the wavelength range from 1158.8 nm to 2153.1 nm. The samples were chosen in such a way, so that the API variabilities were encompassed in the model as much as possible. All other samples were included in the prediction set. Fig.5.3 shows the result of PCA plot. From the plot, we can find out that the prediction samples were included inside the calibration set.

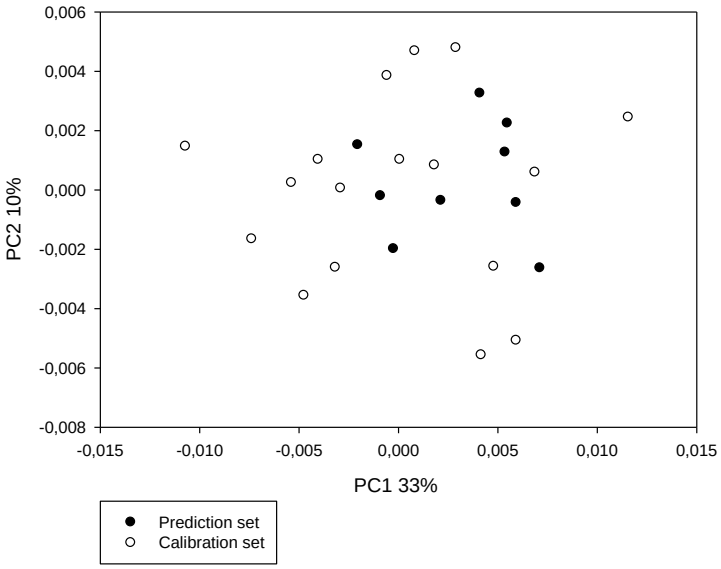

Fig. 5.3 PCA plot of the total 26 laboratory powder samples

Quantitative models were calculated with the pretreatments of median filter smoothing with 7-points segment size, first and second derivative spectra over the whole wavelength range. Table 5.3 shows the parameters of different multivariate models. With median filter smoothing + second derivative (order 2, 3 points) pretreatment, the value of Y-explained reached 95%, the RMSEC and RMSEP were low respectively. So it was chosen as the final quantitative model for determining the concentration of API.

Table 5.3 Statistics for the multivariate models developed with laboratory powder samples and production samples

Spectral pretreatment	Calibration			Prediction
		Y-explained	RMSEC	RMSEP
	PLS factors	(%)	(mg/g)	(mg/g)
Median Filter + SG 1D,Order 2, 3 points	1	60.66	0.64	0.77
	2	79.41	0.46	1.02
	3	95.34	0.22	1.07
	4	99.2	0.09	1.14
Median Filter + SG 1D,Order 2, 5 points	1	50.97	0.71	0.72
	2	71.56	0.54	0.97
	3	96.63	0.19	1.53
	4	99.02	0.1	1.62
Median Filter + SG 2D,Order 2, 3 points	1	41.37	0.78	0.97
	2	82.18	0.43	0.82
	3	96.32	0.2	0.87
	4	98.81	0.11	0.89
Median Filter + SG 2D,Order 2, 5 points	1	50.03	0.72	0.92
	2	69.41	0.56	0.85
	3	89.12	0.37	1.09
	4	97.37	0.17	1.30

With the selected pretreatment, parameters of models with different factors were summarized in Table 5.4. The model was constructed with 3 PLS factors, which resulted in a high correlation of calibration, a high explained value of Y-variance and a low error of prediction. Besides, a larger number of factors raised the error of prediction, which suggests that the model was over fitted.

Finally, the quantitative calibration was calculated with 17 samples, the optimal PCs were 3 LVs. And it´s slope was 0.96, the correlation was 0.98 and the RMSEC was 0.20 mg/g.

Table 5.4 Parameters of the quantitative model with various factors

PLS factors	Explained calibration value of Y-variance(%)	Correlation	RMSEP (mg/g)
1	41.37	0.643	0.97
2	82.18	0.907	0.82
3	96.32	0.981	0.87
4	98.81	0.994	0.89
5	99.68	0.998	0.90
6	99.93	0.999	0.90

5.3.4 Validation

Before applying the new analytical methods to pharmaceutical industry, they must be validated. The NIR method which was used to determine the content of API was validated in accordance with the ICH guidelines and EMA by assessing its linearity, accuracy, and precision (repeatability and intermediate precision).

5.3.4.1 Linearity and range

Linearity is evaluated by a signal versus concentration plot usually. However, multivariate calibration cannot obtain this plot because of their regression methods, so a NIRS predicted value versus reference value was plotted in order to assess the linearity of models. If the regression line for the predicted value versus reference plot is a line with a slope which is close to 1, it means the model can meet the linearity requirement. Meanwhile, linearity was evaluated within the concentration range which the samples have spanned. The samples used needs to cover a range at least 80–120% around the nominal concentration of API. At least nine samples and five different concentration levels should be included around ±20% of the nominal value. In Table 5.5, the confidence interval (α=0.05) of slope of the regression line includes 1 and the intercept includes 0, so they met the requirement for linearity over the concentration ranges.

Table 5.5 Validation parameters for the API quantitation with the proposed NIR method

Linearity		Accuracy		Repeatability		Intermediate Precision	
n	17	n	11	n	1	n	1
Concentration range (mg/g)	70-104	Average of residual	-0.02	RSD (%)	0.8	Day	
Correlation	0.981	S.D	0.90			F experimental	1.31
Slope	0.963	t. experimental	-0.07			F crit	19.00
Intercept	0.014	t(10.0.05)	1.81			Analyst	
						F experimental	0.25
						F crit	18.51
						RSD (%)	1.2

5.3.4.2 Accuracy

The accuracy of the NIR method was evaluated by the error between the reference and NIR predicted values. And prediction samples need to span a range ±20% around the nominal value. Therefore, the prediction results obtained by the NIR method were compared with reference via a T-test for residuals. The test showed that there was no significant difference between the NIR method and the reference, because that the absolute value of $t_{experimental}$ was less than $t_{critical}$ (10, 0.05).

5.3.4.3 Precision

5.3.4.3.1 Repeatability

The repeatability of the NIR method with micro spectrometer was assessed by the way that the same analyst acquired the spectra of the same production sample six times on the same day. The relative standard deviation (RSD) is 0.8%.

5.3.4.3.2 Intermediate precision

The intermediate precision was carried out by two analyst, we acquired spectra of the same production sample on three different days. Then, a two-way (analyst and day) ANalysis Of VAriance (ANOVA) was calculated, the result revealed that the value of F experimental were 1.31 and 0.25 which were lower than F crit. And RSD was 1.2%.

5.4 Conclusion

In this research, a quantitative PLS model for API in powder was built with a MicroNIR. The good result of validation reveals that this new instrument has the ability to be a PAT monitor in the solid pharmaceutical industry. What's more, its advantages in size, price and tolerance of production environment can promote NIR to make a breakthrough in realizing the PAT concept in the pharmaceutical industry.

Acknowledgements

Thank you very much for the cooperation from the laboratory Menarini S.A (Spain) and the engineers of VIAVI SOLUTIONS INC. (USA).

Reference

[1] PAT – a framework for innovative pharmaceutical development, manufacturing, and quality assurance, http://www.fda.gov/cder/guidance 2004;

[2] M. Blanco, NIR spectroscopy: a rapid-response analytical tool. Trends Anal. Chem. 21 (2002) 240–250.

[3] Burns, Donald A., and Emil W. Ciurczak, eds. Handbook of near-infrared analysis. CRC press, 2007.

[4] McClure W F. Near-infrared spectroscopy. The giant is running strong [J]. Analytical Chemistry, 1994, 66(1): 43A-53A.

[5] Henry C M. Product Review: Near-IR gets the job done [J]. Analytical chemistry, 1999, 71(17): 625A-628A.

[6] Near-infrared spectroscopy: principles, instruments, applications [M]. John Wiley & Sons, 2008.

[7] A. Burggraeve, T. Monteyne, C. Vervaet, J.P. Remon, T.D. Beer, Process analytical tools for monitoring, understanding, and control of pharmaceutical fluidized bed granulation: a review. Eur. J. Pharm. Biopharm. 83 (2013), 2–15.

[8] E. Räsänen, N. Sandler, Near infrared spectroscopy in the development of solid dosage forms. J. Pharm. Pharmacol. 59 (2007), 147–159

[9] T. De Beer, A. Burggraeve, M. Fonteyne, L. Saerens, J.P. Remon, C. Vervaet, Near infrared and Raman spectroscopy for the in-process monitoring of pharmaceutical production processes. Int. J. Pharm. 417 (2011),32–47

[10] M. Blanco, R. Cueva-Mestanza, A. Peguero, NIR analysis of pharmaceutical samples without reference data: Improving the calibration. Talanta. 85 (2011), 2218–2225

[11] A. L. Suryan, V. K. Bhusari, K. S. Rasal, S. R. Dhaneshwar, Simultaneous Quantitation and Validation of Paracetamol,Phenylpropanolamine Hydrochloride and Cetirizine Hydrochloride by RP-HPLC in Bulk Drug and Formulation. Int. J. Pharm. Sci. Drug Res. 3(4) (2011), 303-308

[12] M.Ma, F.Feng, Y.L.Sheng, S.J.Cui, H.Liu, Development and evaluation of an efficient HPLC/MS/MS method for the simultaneous determination of pseudoephedrine and cetirizine in human plasma: Application to Phase-I pharmacokinetic study. J. Chromatogr. B. 846(1-2) (2007), 105-111.

[13] ICH Q2 (R1). Validation of analytical procedures: text and methodology, 1995.

[14] European Medicines Agency, Guideline on the use of Near Infrared Spectroscopy (NIRS) by the pharmaceutical industry and the data requirements for new submissions and variations, 2012.

Chapter 6

Determination of API concentration in granulation process with portable MicroNIR

6. Determination of API concentration in granulation process with portable MicroNIR

Recently, NIRS becomes more and more important for PAT. And the miniaturization of the instrument improves NIRS to be a very practical method for pharmaceutical industry. In this study, a MicroNIR with the dimension (diameter x height) 45 x 42mm was used to determine the concentration of API in granules. Both lab and production samples of API were collected to calculate a quantitative PLS model, so that the model could include both chemical and physical variability. The predictive ability was fully validated by linearity, range, accuracy, robustness, repeatability, intermediate precision of the model according to the guidelines of ICH. Finally, the RMSEC was 0.58 mg/g and the RMSEP was 0.81 mg/g, which means this MicroNIR has a good performance for the determination of API concentration in granulation process.

Key word: Miniaturization of near infrared spectrometer, Concentration of API in granule, Pharmaceutical industry

6.1 Introduction

As we know, the quality of drugs must be controlled strictly so that it can cure diseases which are hurting the human health. The FDA and ICH (Q8-Q11) [1, 2] have published some important guidelines about QbD and PAT since 2004. And 10 years later, these guidelines have already been widely accepted and used in the pharmaceutical industry all over the world. These guidelines are essential for the factories to get a high level both in yield and quality of their products. PAT can help us better understand the Critical Process Parameters (CPPs) and control CQAs from the raw material to the end product [3].

In the pharmaceutical industry, one of the most used analytical techniques for process analysis is HPLC. However, the HPLC method is destructive, time consuming, labor-intensive and produces chemical waste. [4]For these reasons, great interests in the development of simple, reliable alternative technique which can provide accurate, precise results with an increased throughput and less human intervention have been aroused. Recently, NIRS becomes more and more important for PAT, because it has a lot of advantages in meeting the requirements mentioned above [5]. And the NIRS application is developing rapidly in the pharmaceutical industry. From the view of the solid pharmaceutical industry, NIRS has a great advantage in rapid monitoring particle size, humidity, blend process, granulation, compression, coating thickness, porosity, stability testing, polymorphism and crystallization. [6-13]

The production process of tablet is a typical solid pharmaceutical process which is composed by several operation units, such as blending, granulation, tableting and so on. The concentration of API during granulation process is one of the CQAs. In the factory, the method that used to analyze the concentration of API in granulation process is the HPLC method. However, the HPLC can´t fully meet the requirement of PAT due to the long analysis time and the complexity of sample preparation. So we take NIRS as a tool to help them follow PAT guidelines.

In the market, there are several types of NIRS instruments, and generally they can be classified by the splitting system such as fixed wavelength filter, grating dispersion, fast fourier transform, and acousto-optic tunable filter. The grating dispersion system has a high signal to noise ratio and resolution, but there are some moveable components which are very easy to be worn so that it is not suitable for on line analysis. The fast fourier transform system also has a high resolution and scanning speed, now it is the mainstream configuration, but they have some moveable components and needs a stable working environment. The acousto-optic tunable filter uses fixed birefringent crystal, has a high scanning speed but the resolution is low and the price is expensive. The MicroNIR is a kind of fixed wavelength filter, but it is a LVF which is different from the traditional filter. The LVF is a bandpass filter coating that intentionally wedged in one direction, the wavelength transmitted through the filter will vary in a linear fashion in the direction of the wedge. Therefore, it can provide a spectral range from 600 -2200nm.What's more, the miniaturization and portability of the NIRS instrument are very important for on line application. The LVF is tiny and does not need to work with a large laser light source, so the size of the instrument will be reduced significantly. And the spectrum generated by the LVF can be transferred to a tablet computer by USB interface, so the instrument is portable. [14] All these advantages make the MicroNIR a very practical instrument for pharmaceutical industry.

In this research, the performance of this new instrument in solid pharmaceutical production process has been validated. A quantitative PLS model of API was calculated with both powder samples prepared in the lab and the granule samples from the factory. The predictive ability of the model was fully validated according to the guidelines of ICH and EMA [15, 16].

6.2 Materials and methods

6.2.1 Instrument

A new portable MicroNIR spectrometer was used to determine the concentrate ion of the API in granulation process. The MicroNIR spectrometer has a LVF coupled with a linear detector array which creates a splitting system that is capable of providing the spectral information. Spectral region of the instrument is from 1158.8 nm to 2169.4 nm. There is no movable component so it could work in an environment with vibration. The dimension of this instrument is (diameter x height) 45 x 42mm,

weight<60g and the active sampling area is 2 x 4 mm. Therefore, it can be equipped in the production line without a complicated change for pharmaceutical machines. Illumination source are two integrated vacuum tungsten lamps and the detector is 128-pixel uncooled InGaAs photodiode array. So the power consumption is very low. And it can be powered by USB (<500mA@5V). Host interface is USB 2.0, high speed (480Mb S-1). So it is portable. It´s operating environment is from –20 to 40°C, noncondensing. These characters make it become a very suitable instrument for process control in the strict pharmaceutical industry. The new portable MicroNIR not only can bear the analysis environment in the factory which affects the quality of spectrum seriously, but also can reduce the large cost for adjusting and validating the production line to NIR instruments.

6.2.2 Laboratory samples

Laboratory samples were prepared in two parts, one was API and the other one was placebo. All of them were weighted by an analytical balance accurately. In order to span a concentration range ±20% around the nominal API content according to the ICH guidelines, the API content of calibration set was divided into ten levels evenly. And the range was from 40 mg/g to 60 mg/g. There were six ingredients in the placebo, and the concentrations of them were changed slightly. At the end, the placebo was prepared in five concentration levels which were ±5% around the nominal value. After that, the API and placebo were mixed randomly, so that we can minimize the correlation between them and avoid spurious correlation among constituents.

6.2.3 Production samples

The pharmaceutical products studied were granulation samples from different batches supplied by the laboratory Menarini S.A (Spain). The concentration value of API was determined by the HPLC method which offered by the laboratory Menarini S.A (Spain).

6.2.4 NIR spectra acquisition

Near infrared spectra were recorded by the portable MicroNIR™ 2200 Spectrometer (VIAVI SOLUTIONS INC, USA). The scan number was 10000 and the integration time was 100 μs. Because all the samples were in white color, spectrum of 99% reference was taken as the background to remove the influence of system noise. Samples were placed in a quartz cup which was located on the top of the window of the MicroNIR. The distance between sample and window can affect the quality of spectrum. After testing, we found at 3 mm the spectrum noise is the lowest. So the distance between quartz cup and the instrument window was fixed at 3mm with an appropriate accessory.

Then, six spectra for every sample were acquired and the reference spectrum was renewed when each sample was changed. Finally, raw spectra of samples were averaged.

6.2.5 Data analysis

The multivariate models were calculated with Unscrambler X (Trondheim, Norway).The calculation of validation was carried out by Excel 2010 (Microsoft, USA).

The raw spectrum needs to be pretreated, because there was a lot of noise and useless information which could decrease the quality of calibration. The spectral pretreatments were tested with the gap-segment 1st derivative, median filter smoothing and the SNV. Models used to determine the concentration of API were calculated by PLS1, using the leave-one-out method for cross-validation. The optimal LVs number used was which can result in a minimum value for prediction residual and could make the PLS model explain more than 95% of the Y variance in calibration. The predictive ability of the calibration was evaluated by Root Mean Square Error (RMSE):

$$RMSE = \sqrt{\frac{\sum_{i=1}^{n}\left(y_i^{pred} - y_i^{ref}\right)^2}{n}} \qquad \text{Equation 6.1}$$

Where n is the number of samples, y^{ref} is the reference value and y^{pred} is the predicted value of calibration.

6.3 Results and discussion

6.3.1 Calibration set and validation set

Calibration set included both production and laboratory samples. This is because the production samples can include the usual variabilities (viz. differences between batches, granulation and dryness) of the pharmaceutical preparation from the production process. And laboratory samples could span the concentration range of calibration set to the threshold required in the ICH and EMA guidelines. Therefore, in total, production samples from 19 different batches and 30 laboratory samples were prepared for this research. All the samples were divided into two sets which were selected by the principal scores plot of PCA. One was calibration set, which had 25 samples, was used to calculate the models. And the other one was a validation set, which included 24 samples, was used to estimate the predictive ability of the quantitative models. In Table 6.1**,** it was the composition of each laboratory sample. In total, there were 30 laboratory samples.

Table 6.1 Concentration of laboratory samples

NO. Sample	Concentration API(mg/g)	NO. Placebo
1	40.08	4
2	40.42	2
3	40.03	3
4	42.48	1
5	42.50	3
6	42.54	5
7	45.02	2
8	44.99	4
9	44.96	1
10	47.54	3
11	47.71	5
12	47.58	2
13	50.15	1
14	50.13	2
15	49.97	3
16	50.05	4
17	50.01	5
18	50.00	4
19	52.61	5
20	52.49	1
21	52.60	2
22	55.04	1
23	55.07	3
24	55.00	4
25	57.60	5
26	57.58	2
27	57.55	1
28	60.08	5
29	59.99	4
30	59.96	3

6.3.2 Spectra pretreatment

Fig.6.1. shows the pure spectra for the API and the major excipients. We can see that there was some noise caused by the different particle size in the powder. The main absorption peak of API was from

1558 nm to 1851 nm. They were mainly caused by the 1st overtone absorbance of N-H hydrogen bond and C-H bond. At 1150-1501 nm and 1876-2161 nm, there were several high absorption peaks from other excipients. Besides, in the sample spectrum, there was baseline shifting, it was caused by the physical variability of the powder.

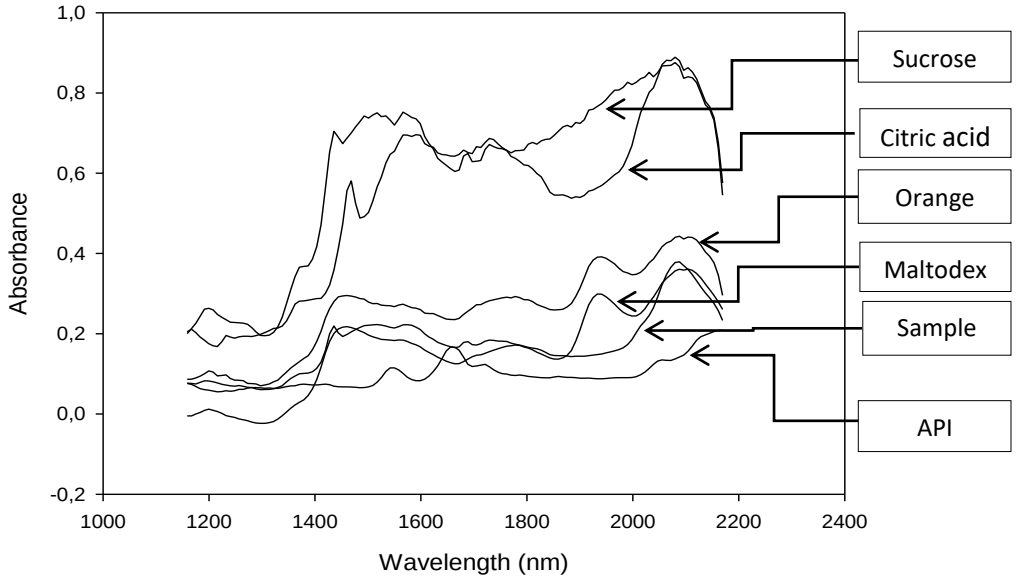

Fig.6.1 Raw spectrum of pure ingredients and sample

The granulated production samples could increase RMSE of calibration because of their physical variability. For this reason, SNV was applied to decrease the baseline shifting caused by different particle size, 1st derivative was to enlarge the absorbance signal of API, and median filter smoothing was adopted to remove the noise in spectrum. So the spectra were pretreated with median filter smoothing (segment size 3), followed by SNV and gap-segment 1st derivative (gap size 5, segment size 2). Fig.6.2. shows the spectra after pretreated. There were 3 bands in the spectra which show us an anomalistic separation, 1329-1411 nm, 1867-1957 nm and 1998-2071 nm. For this reason, we need to select special band to avoid the influence of this separation.

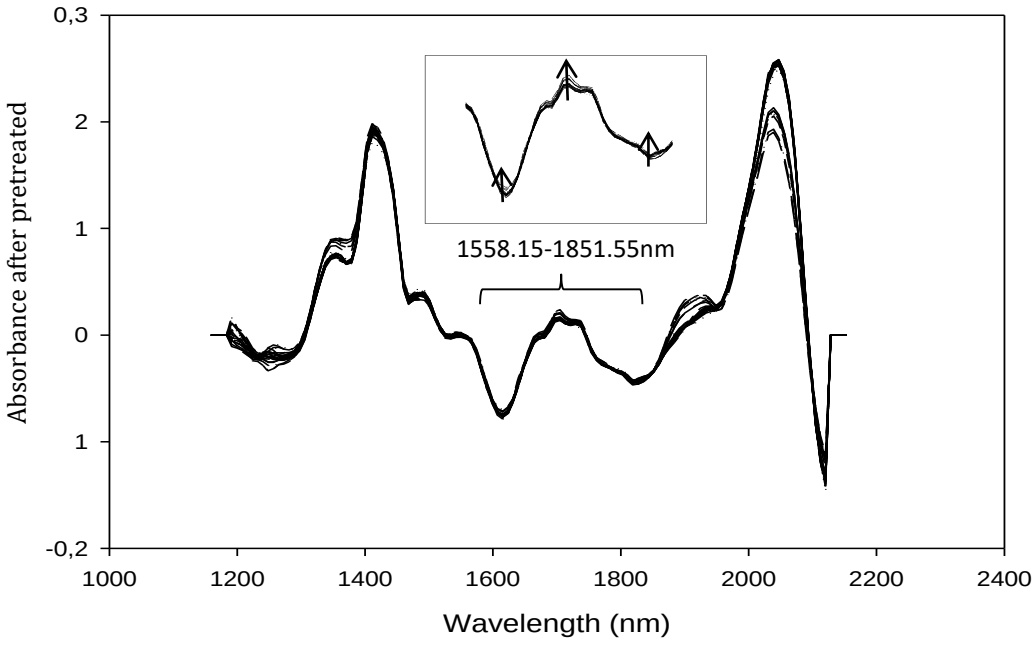

Fig. 6.2 Pretreated spectra of laboratory samples

6.3.3 Spectral band selection

Compare to the whole range, special band was selected to establish the quantitative PLS model. The whole spectral range could represent all the information from the sample, but sometimes some useless information will be included too. And if the intensity of absorbance of API is not strong enough, this useless information will affect the quality of calibration a lot. In Fig.6.2, it shows us that the main absorbance peak of API, which located round 1600-1700 nm, was the lowest among all the ingredients. So it was necessary to select a shorter range to remove the useless information. And a comparison of two models was made between the whole range and selected range. Band from1558 to 1851 nm contained the main absorption peak of API, so two models were established, one was within the whole range and the other one was from 1558.15-1851.55 nm. And Table 6.2 shows the comparison of the performance of these two models.

Table 6.2 Comparison of two models within different range

	Calibration		Prediction of lab samples		Prediction of production samples	
Whole range	RMSEC	1.175	RMSEP	8.245	RMSEP	5.170
	LVs	7	Average of residual	-2.156	Average of residual	-1.719
	Intercept	2.491	S.D	8.389	S.D	5.061
	Slope	0.950	t	-0.813	t	-1.271
			t(9.0.05)	2.262	t(13.0.05)	2.16
Selected range	RMSEC	0.584	RMSEP	1.077	RMSEP	0.810
	LVs	7	Average of residual	0.272	Average of residual	0.115
	Intercept	0.615	S.D	1.099	S.D	0.832
	Slope	0.988	t	0.783	t	0.517
			t(9.0.05)	2.262	t(13.0.05)	2.160

From Table 6.2, we can see the RMSEC, RMSEP in the model calculated with selected range were lower than the results with whole range. With the same LVs, the slope of second calibration was 0.988 which was higher than the first one and the intercept was lower.That means selected band was more suitable for calibration than the whole range.

6.3.4 Number of factors

In Table 6.3, they are the performance of models calculated with different PCs. The explained calibration value of Y-variance, RMSEC, and SEC were compared in order to choose the best number of LVs.

Table 6.3 Parameters of calibration according to 10 PCs

PCs	Explained calibration value of Y-variance (%)	RMSEC(mg/g)	SEC(mg/g)
1	37.6	4.161	4.240
2	54.9	3.536	3.604
3	67.6	2.999	3.056
4	80.9	2.300	2.344
5	89.0	1.750	1.783
6	93.7	1.323	1.348
7	98.8	0.584	0.595
8	99.3	0.456	0.465
9	99.4	0.413	0.421
10	99.4	0.394	0.401

The PLS model was built with 7 LVs (see Table 3). With 7 LVs, the explained calibration value of Y-variance reached 98.8 which is over the threshold of 95 and RMSEC was only 0.584.

Finally, the calibration PLS1 model of API was calculated with 27 samples, and the spectral range was from1558.150nm to 1851.55nm. Raw spectra were pretreated with median filter smoothing (segment size 3), followed by SNV and gap-segment 1st derivative (gap size 5, segment size 2), and PCs of the model were 7 LVs. The slope was 0.9877, correlation was 0.9938 and the RMSE of calibration was 0.58 which showed a high level of predictive ability.

6.3.5 Validation

According to a series of guidelines published by ICH and EMA, linearity, range, accuracy, robustness, repeatability, intermediate precision of the model need to be validated.

The samples of validation set also had two groups. One group was production samples from production line directly. Several batches of granules with different concentration were collected. And the other group was a series of powder samples prepared in the lab which cover the ±20% concentration range around the nominal API content.

Linearity and range

Linearity of the model was assessed by predicting 27 lab samples. These samples spanned ±20% around the nominal API content. A regression line of predicted value vs reference value was calculated. And the confidence interval (α=0.05) of slope includes 1 and the intercept includes 0.

Accuracy

The accuracy of the model was evaluated by the residual between the reference value and predicted value with 11 samples. What´s more prediction samples span a range±20% around the nominal value also. The prediction results were compared with reference value via a T-test for residuals. The average of residual was 0.282 which was very low. And the t-experimental was 0.897 which was lower than 2.228 of t (10, 0.05).The t test has shown that there was no significant difference between the predicted value and the reference value.

Repeatability

The repeatability of the model was assessed by the way that the same analyst acquired the spectra of the same production sample for six times on the same day. The relative standard deviation (RSD) of these 6 results should be low. The RSD of our model for repeatability is 1.62%.

Intermediate precision

The intermediate precision test was carried out by two analyst, we acquired spectra of the same production sample on three different days. Then, a two-way (analyst and day) ANOVA was calculated, the result revealed that the value of F experimental were lower than F crit. And RSD% was lower than 5%.

Robustness

Robustness was assessed by 13 production samples from different batches. The RMSE of the prediction was calculated. The residual of prediction was evaluated by a t-test, and t-experimental was 0.395 which was lower than 2.179 of t (12, 0.05).

In Table 6.4 shows the results of linearity, range, accuracy, repeatability, intermediate precision and robustness.

Table 6.4 Validation results

Linearity		**Accuracy**		**Repeatability**		**Intermediate Precision**		**Robustness**	
n	27	n	11	n	1	n	1	n	13
Concentration range (mg/g)	40.08-60.08	Average of residual	0.282	RSD (%)	1.62%	Day		RMSEP ($mg.g^{-1}$)	0.810
Intercept	0.615	S.D	1.043			F experimental	3.99	Average of residual	0.094
Slope	0.988	t	0.897			F crit	19.00	S.D	0.862
		t(10.0.05)	2.228			Analyst		t	0.395
						F experimental	0.15	t.(12.0.05)	2.179
						F crit	18.51		
						RSD (%)	2.93%		

6.4 Conclusion

In this research, a quantitative PLS model for granulation process was established with a portable MicroNIR. The good result of validation reveals that this new instrument has the ability to be a PAT monitor in the solid pharmaceutical industry. What's more, its advantages in size, price and tolerance of production environment can promote NIRS to make a breakthrough for realizing the PAT concept in the pharmaceutical industry.

Acknowledgements

Thank you very much for the cooperation from the laboratory Menarini S.A (Spain) and the engineers of VIAVI SOLUTIONS INC (USA).

References

1. U.S. Food and Drug Administration, Guidance for Industry.US Department of Health, 2004.

2. ICH, ICH Q8(R2) (Pharmaceutical Development), ICH Q9 (Quality Risk Management), ICH Q10 (Pharmaceutical Quality System) and ICH Q11 (Development and Manufacture of Drug Substances).

3. PAT—A Framework for Innovative Pharmaceutical Development, Manufacturing, and Quality Assurance". Available at: http://www.fda.gov/cder/guidance/6419fnl.pdf.

4. Blanco M, Bautista M, Alcalá M. Preparing calibration sets for use in pharmaceutical analysis by NIR spectroscopy [J]. Journal of pharmaceutical sciences, 2008, 97(3): 1236-1245.

5. Blanco M, Alcalá M, González J M, et al. A process analytical technology approach based on near infrared spectroscopy: tablet hardness, content uniformity, and dissolution test measurements of intact tablets [J]. Journal of pharmaceutical sciences, 2006, 95(10): 2137-2144.

6. Alcalà M, Blanco M, Bautista M, et al. On-line monitoring of a granulation process by NIR spectroscopy[J]. Journal of pharmaceutical sciences, 2010, 99(1): 336-345.

7. Martínez L, Peinado A, Liesum L, et al. Use of near-infrared spectroscopy to quantify drug content on a continuous blending process: Influence of mass flow and rotation speed variations[J]. European Journal of Pharmaceutics and Biopharmaceutics, 2013, 84(3): 606-615.

8. Knop K, Kleinebudde P. PAT-tools for process control in pharmaceutical film coating applications[J]. International journal of pharmaceutics, 2013, 457(2): 527-536.

9. Khorasani M, Amigo J M, Sonnergaard J, et al. Visualization and prediction of porosity in roller compacted ribbons with near-infrared chemical imaging (NIR-CI)[J]. Journal of pharmaceutical and biomedicalanalysis, 2015, 109: 11-17.

10. Schaefer C, Lecomte C, Clicq D, et al. On-line near infrared spectroscopy as a Process Analytical Technology (PAT) tool to control an industrial seeded API crystallization[J]. Journal of pharmaceutical and biomedical analysis, 2013, 83: 194-201.

11.Schönbichler S A, Bittner L K H, Weiss A K H, et al. Comparison of NIR chemical imaging with conventional NIR, Raman and ATR-IR spectroscopy for quantification of furosemide crystal polymorphs in ternary powder mixtures[J]. European Journal of Pharmaceutics and Biopharmaceutics, 2013, 84(3): 616-625.

12. Càrdenas V, Blanco M, Alcalà M. Strategies for Selecting the Calibration Set in Pharmaceutical Near Infrared Spectroscopy Analysis. A Comparative Study[J]. Journal of Pharmaceutical Innovation, 2014, 9(4): 272-281.

13. Wang P, Zhang H, Yang H, et al. Rapid determination of major bioactive isoflavonoid compounds during the extraction process of kudzu (Pueraria lobata) by near-infrared transmission spectroscopy[J]. Spectrochimica Acta Part A: Molecular and Biomolecular Spectroscopy, 2015, 137: 1403-1408.

14. Alcalà M, Blanco M, Moyano D, et al. Qualitative and quantitative pharmaceutical analysis with a novel handheld miniature near-infrared spectrometer[J]. Journal of Near Infrared Spectroscopy, 2013, 21(6): 445-457.

[15] ICH Q2 (R1). Validation of analytical procedures: text and methodology, 1995.

[16] European Medicines Agency, Guideline on the use of Near Infrared Spectroscopy (NIRS) by the pharmaceutical industry and the data requirements for new submissions and variations, 2012.

Chapter 7

Determination of segregation in solid pharmaceutical powder by the MicroNIR

7. Determination of the segregation in solid pharmaceutical powder by the MicroNIR

The real time concept, which is from the PAT, has introduced some methods to handle the segregation problem in pharmaceutical industry. The miniaturized and portable NIR spectrometer is a suitable tool to realize this concept. In this study, the MicroNIR whose dimension (diameter x height) is 45 x 42 mm was used to acquire spectra and calculate quantitative PLS1 models for monitoring the segregation in powder. Samples which were prepared in the lab and factory were used in this study. The selection of spectra improved the calibration quality, the correlation was 0.98, and the RMSEC was 1.32 mg/g. In the prediction, the RMSEP of lab and production samples was 0.89 mg/g and 1.52 mg/g. The result has shown that MicroNIR has a good performance in monitoring the segregation of pharmaceutical powder.

Key word: Real time analysis, MicroNIR, segregation

7.1 Introduction

The uniformity of materials in the pharmaceutical manufacturing process is a key factor. Several operation units such as the blending, granulation, drying and tableting are influenced by the uniformity of materials [1]-[3]. Segregation is one of the most important reasons which influence the uniformity. There are three items which would lead to the segregation in the manufacturing process. They are the material, the instrument and the operation. The powder properties of materials, such as particle size distribution, the particle shape, particle density, bulk density, humidity, flowability (angle of response, flow velocity, compressibility), adherence and cohesion are some reasons which has comprehensive effects on the uniformity of materials. The design of pharmaceutical instruments also is important. Their shape, size, structure, material and surface affect the uniformity significantly. The operation processes are the item which could be control by the operators directly and immediately, so there are Standard Operating Procedures (SOP) to assure the operations would produce a high quality product finally. Pharmaceutical factories have used several guidelines to help them with the improvement of the uniformity of the products [4]-[7].

The FDA and ICH (Q8-Q11) have published some important guidelines about QbD and PAT since 2004 [8]-[12]. These guidelines have suggested some methods to deal with the uniformity of materials in the pharmaceutical manufacturing process. The real time concept introduced by the PAT is a way to reach the uniformity. There are three levels of real time analysis, the real time monitor (RTM) of products CQAs, the real time assurance (RTA) of product quality and the real time release (RTR). In

order to realize the goal of real time, NIRS is taken into our account. NIRS is a technology which could transfer the chemical and physical information of an object into digital information without destructing the object. With the help of chemometrics, all the digital information could be analyzed and a final quantitative/qualitative decision could be made by the simulative model. It could help the virtualization of the product. What´s more, the real time capability is a main advantage for NIRS. Instead of hours or days, the NIRS only needs seconds or minutes to analyze samples in the whole process.

Miniaturized NIR instrument is a suitable choice for the pharmaceutical industry, because it is portable and the application doesn´t need a complex change of the production line for its application. As we know, GMP is the guideline which is widely used now in the pharmaceutical industry. It askes the production lines are fully validated and fixed. Therefore, it´s better to use a miniaturized NIR to carry out the RTM process.

The fine API powder has a much smaller particle size than the other raw excipients which may cause the segregation problem. Besides, the powder of API has heavy moisture absorption which makes it very sticky to the surface of container. It is hard to determine the end point of the operation because the process parameters change every batch. The traditional analytical methods have a time delay due to the sample preparation and analysis speed. Because of the delay, the quality can´t be improved in real time.

In this study, the MicroNIR was used to help pharmaceutical industry solve this problem. Quantitative PLS models were calculated to determine the content of API. The predictions of powder and granule have shown a good result that the MicroNIR is suitable for real time analysis of the product.

7.2 Materials and methods

7.2.1 Sample preparation

There are two kinds of samples were prepared, one is lab sample and the other one is production sample. The solid pharmaceutical sample includes aroma vainilla , sorbitol GDO 30-60, sorbitol P60G, saccharin and API. The nominal API concentration is 56.67 mg/g. 40 lab samples were prepared and their API concentration range varied from 45.33 to 67.99 mg/g which is around ±20% of the nominal value. 20 production samples were granules obtained directly from the production line. The API content of production samples was determined by the HPLC method. And the API concentration of lab samples was weighted by the analytical balance.

7.2.2 Spectra acquisition

MicroNIR (Viavi Solutions Inc., USA) was used to acquire the NIR spectra. The integration time was 13500 us and scan number was 50.

Powder samples were put in a flat watch glass without pressing. The watch glass filled with powder was placed on the top of the MicroNIR. In order to have all characters of the powder sample, for each sample, 20 spectra were acquired around the bottom of the watch glass. Every one hour, the background spectrum was renewed with the 99% reference. The operation temperature of the instrument was 50 degrees.

7.2.3 Data analysis

Models were calculated by the Unscrambler X. The useful wavelength range was selected by the correlation coefficient method. The correlation coefficient method correlates the change of absorbance of each wavelegth with the change of reference value. The larger the correlation coefficient (r) is, the more useful the wavelength is to explain relation with the variable of interest. Its equation is:

$$r = \frac{\sum_{i=1}^{n}(x_i-\bar{x})(y_i-\bar{y})}{\sqrt{\sum_{i=1}^{n}(x_i-\bar{x})^2 \sum_{i=1}^{n}(y_i-\bar{y})^2}} \quad \text{Equation 7.1}$$

Where x is the absorbance, y is the reference value and n is calibration set number.

The r is from -1 to 1. When the r is 1, it means that these two variables have full positive linear correlation. When the r is 0, it means there is no correlation between them.

Pretreatment method of raw spectra was selected from the derivative, smoothing and the SNV. PLS1 models were used to determine the concentration of API using the leave-one-out method for cross-validation. The optimal LVs number used was that could result in a minimum value for prediction residual and make the PLS1 model explain more than 95% of the Y variance in calibration. The predictive ability of the calibration was evaluated by RMSE:

$$RMSE = \sqrt{\frac{\sum_{i=1}^{n}\left(y_i^{pred}-y_i^{ref}\right)^2}{n}} \quad \text{Equation 7.2}$$

Where n is the number of samples, y^{ref} is the reference value and y^{pred} is the predicted value of calibration.

7.3 Results and discussion

7.3.1 The raw spectra

In total, there were 40 lab samples and 20 production samples, so 800 spectra of lab samples and 400 spectra of production samples were acquired. Fig.7.1 and Fig.7.2 are the average spectra of each sample.

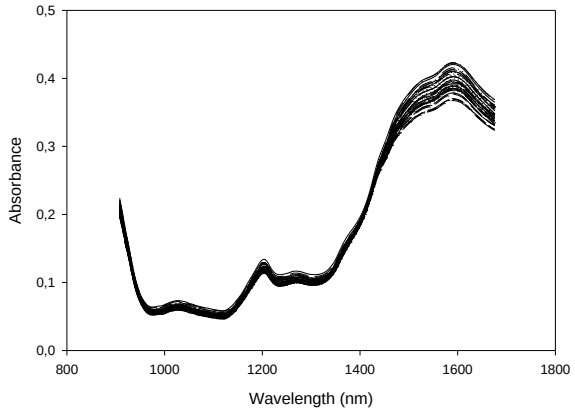

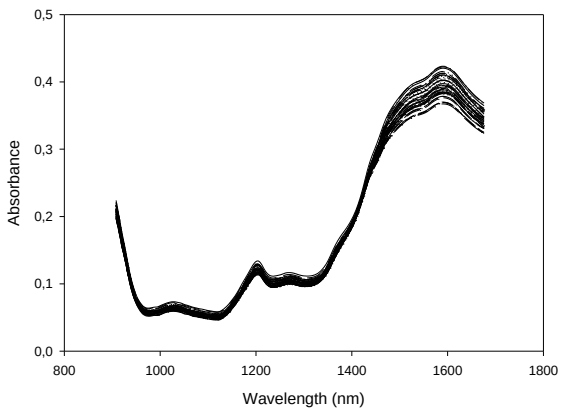

Fig.7.1 40 average spectra of lab samples ***Fig.7.2. 20 average spectra of production samples***

There are some peaks in the spectra but it is hard to find out which is the peak of the API. Therefore the data processing is needed.

7.3.2 Data processing

7.3.2.1 Spectral range

Comparing the spectra of samples with the spectrum of API, in Fig.7.3, we can find that the absorbance of API has contribution mainly in the ranges such as 900-950 nm and 1300-1500 nm..

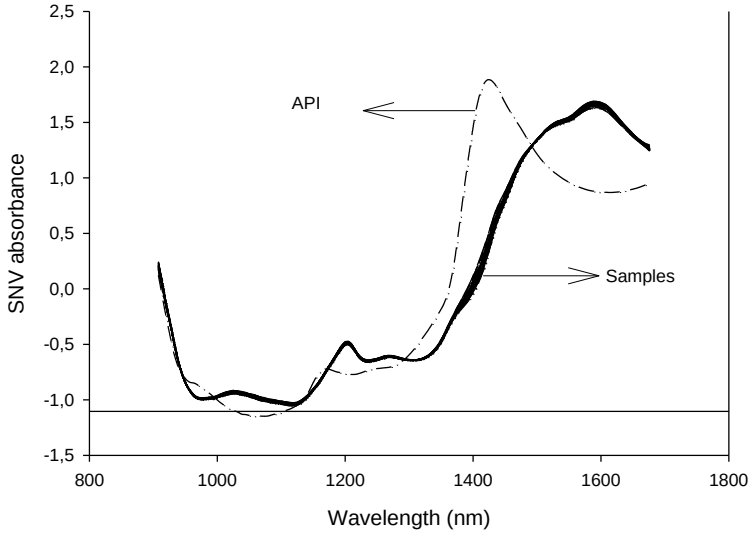

Fig.7.3. Average spectra of API and samples after SNV

In order to find out the best calibration spectral band, the correlation between concentration and wavelength numbers has been calculated. Fig.7.4 is the plot

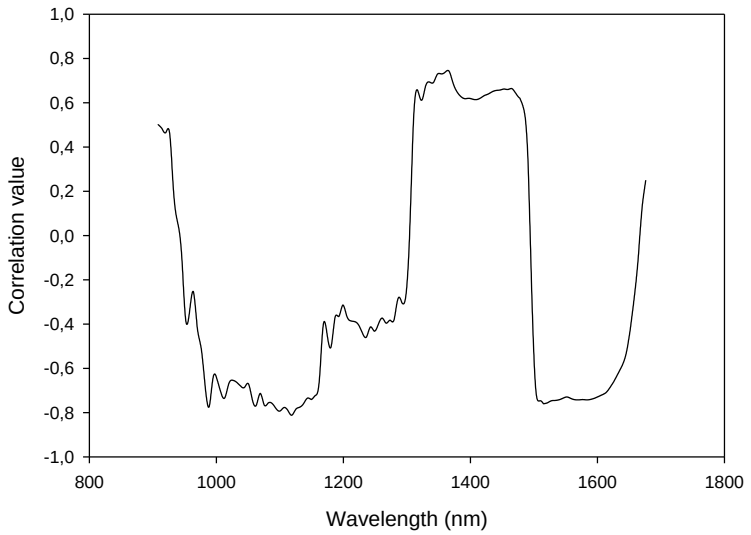

Fig.7.4. Correlation plot between concentration and wavelength (nm)

The positive correlated bands were around 900-950 nm and 1300-1500 nm which were caused by the main peak of API. Besides, there were some negative correlated bands which were around 980-1150 nm, 1200-1300 nm and 1500-1650 nm. Bands which have high correlation coefficient also have a high influence in the calibration model. Thus, the whole spectral range has been cut into five bands according to their correlation values. The combinations of these bands were tested and finally 908.10-1447.009 nm was chosen to calculate the quantitative model.

7.3.2.2 Selection of the pretreatment

All the samples were divided into calibration set and prediction set. 28 lab samples plus 4 production samples were selected as the calibration set. Concentration range of calibration sets spanned from 45.33 to 67.99 mg/g. 12 lab samples and 16 production samples were selected as the prediction set. Their concentration range was from 46.48-67.41 mg/g.

Several pretreatment have been applied to the raw spectra, and Table 7.1 shows the parameters of calibrations with different pretreatments

Table 7.1 Comparison of models preprocessed by different methods

Pretreatment	Factors	Explained calibration Y variance (%)	Calibration		Prediction
			Correlation	RMSEC (mg/g)	RMSEP (mg/g)
SNV	8	85,01	0,92	2,53	3,20
SG 1d+3 points	8	89,08	0,92	2,16	3,88
SG 1d+5 points	8	84,37	0,92	2,58	3,23
SG 1d+7 points	8	82,79	0,91	2,71	3,11
SNV+SG 1d+3 points	8	87,60	0,94	2,30	3,20
SNV+SG 1d+5 points	8	96,09	0,98	1,32	0,89
SNV+SG 1d+7 points	8	80,85	0,90	2,86	2,34

The quantitative model which was pretreated by SNV+ SG 1st derivative 5 points has shown a better quality. With 8 LVs, the explained Y of calibration was 96.09 %, correlation was 0.98, and the RMSEC was 1.32 mg/g. In the prediction, the RMESP was 0.89 mg/g which was the lowest value in Table.7.1. Therefore, the raw spectra were preprocessed with SNV+ SG 1st derivative 5 points.

7.3.3 Prediction performance

Following is the prediction performance of the model,

Table 7.2 Prediction performance of lab samples

Name	Reference(mg/g)	Predict(mg/g)	Residual(mg/g)
3	46,48	46,86	-0,37
10	50,57	50,91	-0,34
11	51,15	50,96	0,19
13	52,30	54,18	-1,88
17	54,61	54,70	-0,09
19	55,79	56,07	-0,28
20	56,37	56,86	-0,49
28	61,03	60,69	0,33
27	60,45	59,85	0,60
39	67,42	69,40	-1,99
25	59,28	59,33	-0,05
34	64,52	63,55	0,98
		Average	-0,28

		n	12
		s	0,88
t(11,0,05)	1,8	$t_{experiment}$	-1,11

For the lab samples, the RMSEP was 0.89 mg/g and t-experiment <t (11, 0.05), see table 7.2. And for the prediction of production samples, the RMSEP was 1.52 mg/g, see table 7.3, and t-experiment < t (15, 0.05).

Table 7.3 Prediction performance of production samples

Name	Reference	Predict	Residual
R5350794	54,72	55,35	-0,63
L5350802	56,18	57,01	-0,83
R5350789	57,84	55,21	2,63
L5350800	56,36	55,27	1,09
L5350801	56,27	53,66	2,61
L5350804	56,24	57,48	-1,24
L5684273	54,65	54,58	0,07
R5289263	55,61	56,23	-0,62
R5350785	56,53	55,67	0,86
R5350788	57,35	57,03	0,32
R5350790	52,65	55,85	-3,20
R5350791	55,90	57,47	-1,57
R5350799	56,10	55,17	0,93
R5902168	59,95	60,31	-0,36
R5902169	58,80	56,71	2,09
R5902170	55,44	54,81	0,63
		Average	0,17
		n	16
		s	1,56
t(15,0,05)	1,75	t	0,44

In order to have a good prediction result, the calibration set has to include as much sample information as possible. Fig.7.6 shows the relationship between calibration set and prediction set. This plot was calculated by PCA which used the 1st and 2nd principle components.

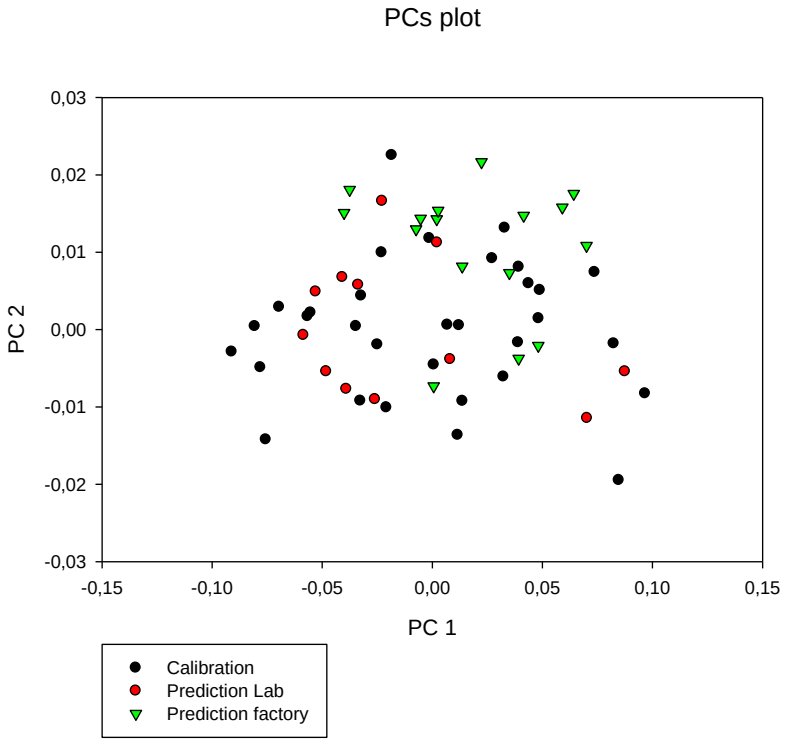

Fig.7.6. PCs plot of all sample sets

Two prediction sets, which were prepared in the lab and factory, both are located in the area of calibration set. Therefore, the calibration model has included variables which appeared in the prediction set.

7.4 Conclusion

In this study, the quantitative model of API was calculated with PLS1. The prediction results have shown that the model quality is high. The experiment design for the preparation of samples and selection of spectra has offered a new way to deal with the segregation in the solid pharmaceutical manufacturing process. The MicroNIR was used to acquire the spectra. It is portable and the size is small which is suitable to be installed in the factory for the on line analysis. The model performance shows that the MicroNIR can be the tool to solve the segregation problem in pharmaceutical industry.

Acknowledgements

Thank you very much for the cooperation from the laboratory Menarini S.A (Spain) and the engineers of VIAVI SOLUTIONS INC (USA).

Reference

[1] M. Blanco and M. Alcalá, "Content uniformity and tablet hardness testing of intact pharmaceutical tablets by near infrared spectroscopy: A contribution to process analytical technologies," in *Analytica Chimica Acta*, 2006, vol. 557, no. 1–2, pp. 353–359.

[2] C. Gendrin, Y. Roggo, and C. Collet, "Content uniformity of pharmaceutical solid dosage forms by near infrared hyperspectral imaging: A feasibility study," *Talanta*, vol. 73, no. 4, pp. 733–741, 2007.

[3] M. Alcalà, M. Blanco, M. Bautista, and J. M. González, "On-line monitoring of a granulation process by NIR spectroscopy," *J. Pharm. Sci.*, vol. 99, no. 1, pp. 336–345, Jan. 2010.

[4] X. He, X. Han, N. Ladyzhynsky, and R. Deanne, "Assessing powder segregation potential by near infrared (NIR) spectroscopy and correlating segregation tendency to tabletting performance," *Powder Technol.*, vol. 236, pp. 85–99, 2013.

[5] M. Wormsbecker, A. Adams, T. Pugsley, and C. Winters, "Segregation by size difference in a conical fluidized bed of pharmaceutical granulate," *Powder Technol.*, vol. 153, no. 1, pp. 72–80, 2005.

[6] L. Xie, H. Wu, M. Shen, L. L. Augsburger, R. C. Lyon, M. A. Khan, A. S. Hussain, and S. W. Hoag, "Quality-by-design (QbD): Effects of testing parameters and formulation variables on the segregation tendency of pharmaceutical powder measured by the ASTM D 6940-04 segregation tester," *J. Pharm. Sci.*, vol. 97, no. 10, pp. 4485–4497, 2008.

[7] L. R. Lawrence and J. K. Beddow, "Powder segregation during die filling," *Powder Technol.*, vol. 2, no. 5, pp. 253–259, 1969.

[8] ICH, "ICH Q8(R2) Pharmaceutical Development," 2009.

[9] ICH, "ICH Q9: Quality Risk Management," *CDER Advis. Comm. Pharm. Sci. Clin. Pharmacol.*, no. January, p. 23, 2006.

[10] Ich, "ICH Q10 Pharmaceutical Quality Systems," *EPT-The Electron. Newsl. Pharm. Tech. Jun*, no. May, p. 21, 2009.

[11] ICH, "ICH Q11 - Development and Manufacture of DSs," *Guideline*, no. May, p. 30, 2012.

[12] U. S. D. of H. and H. S. FDA, "Guidance for Industry PAT — A Framework for Innovative Pharmaceutical Development, Manufacuring, and Quality Assurance," *FDA Off. Doc.*, no. September, p. 16, 2004.